

2020-03-17

EVALUATING THE IMPACT OF CLIMATE CHANGE ON SEDIMENT YIELD IN GUMERO UPPER BLUE NILE RIVER

Ayenew, Chalachew

<http://hdl.handle.net/123456789/10483>

Downloaded from DSpace Repository, DSpace Institution's institutional repository



BAHIR DAR UNIVERSITY
BAHIR DAR INSTITUTE OF TECHNOLOGY
SCHOOL OF RESEARCH AND POSTGRADUATE STUDIES
FACULTY OF CIVIL AND WATER RESOURCES ENGINEERING

**EVALUATING THE IMPACT OF CLIMATE CHANGE ON SEDIMENT YIELD
IN GUMERO WATERSHED OF UPPER BLUE NILE RIVER BASIN, ETHIOPIA**

Chalachew Ayenew

Bahir Dar, Ethiopia
January 10, 2018

EVALUATING THE IMPACT OF CLIMATE CHANGE ON SEDIMENT YIELD IN
GUMERO UPPER BLUE NILE RIVER

Chalachew Ayenew Admassie

A thesis Submitted to the Faculty of Civil and Water Resource Engineering In partial
fulfillment of the requirements for the Degree of Master of Science Specialization in
engineering hydrology

Presented to the Faculty of Civil and Water Resource Engineering, Bahir Dar Institute of
Technology, Bahir Dar University

Advisor: Mamaru Ayalew (Ph.D.)

Co-Advisor: Anwar A. Adem (Ph.D. Candidate)

Bahir Dar, Ethiopia

January 10, 2018

DECLARATION

I, the undersigned, declare that the thesis comprises my own work. In compliance with internationally accepted practices, I have dually acknowledged and refereed all materials used in this work. I understand that non-adherence to the principles of academic honesty and integrity, misrepresentation/ fabrication of any idea/data/fact/source will constitute sufficient ground for disciplinary action by the university and can also evoke penal action from the sources which have not been properly cited or acknowledged.

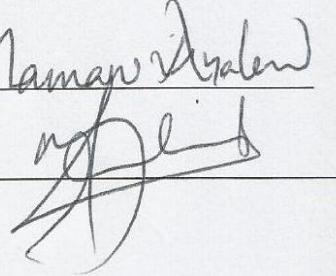
Name of the student: Chabelew Ayenew Signature 

Date of submission: 14/10/2010

Place: Bahir Dar

This thesis has been submitted for examination with my approval as a university advisor.

Advisor Name: Mariam Ayenew

Advisor's Signature: 

© 2018
Chalachew Ayenew Admassie
ALL RIGHTS RESERVED

Bahir Dar University
Bahir Dar Institute of Technology-
School of Research and Graduate Studies
Faculty of Civil and Water Resource Engineering
THESIS APPROVAL SHEET

Student:

Chalalew Arsenew  14/10/2020
Name Signature Date

The following graduate faculty members certify that this student has successfully presented the necessary written final thesis and oral presentation for partial fulfillment of the thesis requirements for the Degree of Master of Science in Engineering Hydrology

Approved By:

Advisor:
Naman Ayden  14/10/2020
Name Signature Date

External Examiner:
Abedle Kemal  14/10/2020
Name Signature Date

Internal Examiner:
Seif Admassu  14/10/2020
Name Signature Date

Chair Holder:
Fasikan Atanem  14/10/2020
Name Signature Date

Faculty Dean:
 14/10/2020
Name Signature Date

Endalamaw Arngie Tefera
Faculty Dean

To my Family

ACKNOWLEDGEMENT

First of all I would like to thank the Almighty God for his great help during the entire study of the course as well as the study period and every aspect of my life

My special thank s goes to Mamaru A, (Ph.D.) for giving me proper instruction .guidance and advice throughout this research works

I also give special thanks to all my instructors who helped me with great ideas criticism during various presentations from the beginning of the course up to the completion of the study.

Last but not least I would like to thank my family and my friend who have been always encouraging my academic understanding with prayer, normal inspiration and in several ways for the realization of the works.

ABSTRACT

Soil erosion and sedimentation which is partly impacted by climate change is one of the most important land degradation problems, as it removes soil rich nutrients and increases level of sedimentation in rivers and reducing reservoirs storage capacity. The main objective of this study was to evaluate the impact of climate change on sediment yield in Gumero watershed near Makesgnit. Gumero watershed is found in northeastern part of Lake Tana basin between the watersheds Arno-Garno and Megech with area of 116 km². In order to simulate the future discharge and sediment yield the PED-W model was calibrated with observed discharge and sediment data recorded in years (2014 and 2015) and validated with the year (2016). The future rainfall and temperature data was downscaled from two RCP 2.6 and RCP 8.5 emission scenario climate models of GCM dataset. The downscaled data was bias corrected the coarse resolution output of climate model to fine resolution using linear scaling bias correction method. Bias corrected future rainfall and potential evapotranspiration data under climate change effects with other landscape input parameter was applied in the calibrated PED-W model as input to simulate the future discharge and sediment yield. PED-W model was found good in predicting discharge with Nash-Sutcliffe Efficiency (NSE) of 0.71 and 0.69 for the calibration and validation periods, respectively. While an NSE of 0.56 was recorded in sediment modeling during the calibration periods. The result of this study showed that average mean annual temperature increase up to 0.94-5.37°C and precipitation will decrease up to 8.3-145.8 mm/year in the watershed for future three time periods under both emission scenarios. As a result the predicted average annual minimum discharge and sediment yield change will decrease up to 9.51mm/year (-1.1%) and 0.64 ton/ha/year (-7.2%) under 8.5 emission scenario of 2020s future time period and average annual maximum discharge and sediment yield change will decrease up to 402.95 mm/year (-34.2%) and 3.94 ton/ha/year (-44.3%) under 8.5 emission scenario of 2080s future time period respectively.

Key words: Climate change, sediment yield, PED-W model, GCM & RCP scenario

TABLE OF CONTENTS

ACKNOWLEDGEMENT	v
ABSTRACT	vi
LIST OF ABBREVIATIONS	x
LIST OF FIGURE.....	xi
LIST OF TABLE	XIV
1. INTRODUCTION	1
1.1 Back ground of the study	1
1.2 Statement of the problem	2
1.3 Objective	3
1.4 Specific objective	3
1.5 Research questions	3
1.6 Significance of the study.....	4
1.7 Scope of the study	4
1.8 Thesis Organization.....	4
2. LITERATURE REVIEW	5
2.1 Over view of climate change.....	5
2.1.1 Climate and Weather	5
2.2. Physical impacts of climate change	6
2.2.1. Impacts on water resources and hydrology	6
2.3 Projected future climate	6
2.3.1 Future global climate	6
2.3.2. Projected Climate Change in Ethiopia.....	7
2.4 Baseline climate scenario	8
2.5 Climate model	8
2.5.1 General Circulation Models (GCMs)	8
2.5.2 RCP scenario	8
2.6 Downscaling.....	9

2.6.1	Downscaling Methods	10
2.7	Bias correction.....	10
2.8	Previous climate studies in the Upper Blue Nile Basin	11
2.9	Hydrological model for climate change	12
3	MATERIALS AND METHODOLOGY	14
3.1	Description of the study area.....	14
3.1.1	Location	14
3.1.2	Topography.....	15
3.1.3	Climate.....	15
3.1.4	Hydrology	17
3.1.5	Soil.....	18
3.1.6	Slope	19
3.1.7	Land use land cover	21
3.2	General Research Method	22
3.2.1	Data collection methods	24
3.3	Data quality analysis	25
3.5	Data availability	30
3.6	Down scaling GCM of RCP Climate Scenario	31
3.6.1	Grid points selection.....	32
3.6.2	Bias Correction	33
3.7	Potential evapotranspiration.....	34
3.8	Trend test for meteorological data	34
3.9	PED-W water balance module	35
3.10	PED-W sediment module.....	35
3.11	PED-W model calibration and validation	36
3.12	Impact analysis	37
4	RESULT AND DISCUSSION	38
4.1	Climate change analysis	38

4.1.1 Baseline and observation data	38
4.2 Bias correction.....	42
4.3 Trend Test of Climate data.....	45
4.3.1. Mean annual observed baseline rainfall trend analysis	45
4.3.2 Mean annual observed baseline temperature trend analysis.....	47
4.3.3 Mean annual baseline rainfall trend analysis.....	48
4.3.4 Mean annual baseline temperature trend analysis	49
4.3.5 Mean annual projected rainfall trend analysis	50
4.3.6 Mean annual projected temperature trend analysis	53
4.4 PED-W model simulation	57
4.4.1 Sensitivity analysis	57
4.4.2 PED –W Model calibration	60
4.4.3 PED –W Model validation	63
4.7 Changes in future meteorological variables	65
4.7.1. Projected downscaled average mean temperature change.....	65
4.7.2. Projected downscaled average precipitation change	67
4.8 The impacts of future climate change on discharge	71
4.9 The impacts of future climate change on sediment yield.....	73
5. CONCLUSION AND RECOMMENDATION.....	77
5.1. Conclusion.....	77
5.2. Recommendation.....	78
REFERENCE.....	79
APEENDIX.....	86

LIST OF ABBREVIATIONS

CMIP5	Coupled Model Intercomparison Project phase
DEM	Digital Elevation Model
GCM	Global circulation model
GIS	Geographical Information System
IPCC	Inter-governmental pane on climate change
MoWIE	Ministry of Water Irrigation Electricity
NMAE	National Meteorological Agency Of Ethiopia
NS	Nash-Sutcliffe
PED-W	Parameter Efficient Distribution Watershed Model
R^2	Coefficient of determination
RCP	Representative Concentration Pathways
RMSE	Rot Mean Square Error
SDSM	Statistical downscaling Method
SRES	Special Report on Emission Scenarios
UBNRB	Upper Blue Nile River Basin

LIST OF FIGURE

Figure 1. The study area description.....	14
Figure 2. Topography of the study area	15
Figure 3. Annual average monthly maximum and minimum temperature of the watershed	16
Figure 4. Annual average monthly precipitation of the watershed from (1970-2005)	17
Figure 5. The study area stream flow characteristics.....	17
Figure 6. Soil type of the study area	18
Figure 7. The study area slope classification	20
Figure 8. Land use land cover map of Gumero watershed	21
Figure 9. Flow chart of general methodology of this study work.....	23
Figure 10. Non-dimensionless plot for homogeneity test.....	26
Figure 11. Double mass curve consistency checking of rainfall in the watershed	30
Figure 12. Grid point daily climate variable value representing and observed station.....	32
Figure 13. Projected average annual monthly rainfall distribution over 1970-2100 before biased correction	40
Figure 14. Projected average annual monthly maximum and minimum temperature distribution over 1970-2100 before biased correction	42
Figure 15. Projected average annual monthly rainfall distributions over 1970-2100 after biased correction	43
Figure 16. Projected average annual monthly maximum and minimum temperature distributions over 1970-2100 after biased correction	45
Figure 17. Mann-Kendall trend test of observed baseline average annual rainfall of the watershed	47
Figure 18. Mann-Kendall trend test of observed annual mean temperature for the watershed	48
Figure 19 . Mann-Kendall Trend test of baseline precipitation for the watershed.	49
Figure 20. Mann-Kendall Trend test of baseline average annual mean temperature for the watershed	50

Figure 21. Mann-Kendall Trend test of projected average annual precipitation of the watershed for 2020s (2011-2040).	51
Figure 22. Mann-Kendall trend test of projected average annual precipitation of the watershed for 2050s (2041-2070)	52
Figure 23. Mann-Kendall trend test of projected average annual precipitation of the watershed for 2080s (2071-2100)	53
Figure 24. Mann-Kendall Trends test of projected mean annual temperature for the watershed (2011-2040)	54
Figure 25. Mann-Kendall Trends test of projected mean annual temperature for the watershed (2041-2070)	55
Figure 26. Mann-Kendall Trends test of projected mean annual temperature for the watershed (2071-2100)	56
Figure 27. Water balance module sensitivity analysis Nash Sutcliffe Efficiency value ..	58
Figure 28 . Sediment module sensitivity analysis Nash Sutcliffe Efficiency	59
Figure 29. Coefficient of correlation (R^2) of Gumero daily discharge during calibration period (2014-2015)	61
Figure 30. Coefficient of correlation (R^2) of Gumero daily sediment yield during calibration period (2014-2015).	61
Figure 31. The daily predicted (dash line) and observed (solid line) discharge of Gumero during calibration period (2014-2015).	61
Figure 32. The daily predicted (solid line) and observed (dash line) sediment yield of Gumero during calibration period (2014-2015).	62
Figure 33. Coefficient of correlation (R^2) of Gumero daily discharge during validation period (2016).	64
Figure 34. The daily predicted (solid line) and observed (dash line) discharge of Gumero during validation period (2016)	64
Figure 35. Projected average annual monthly mean temperature change difference	66
Figure 36. Projected average annual monthly rainfall change difference	68
Figure 37. Projected average annual monthly mean flow change difference	72
Figure 38. Projected average annual monthly sediment yield change difference.....	74

LIST OF TABLE

Table 1. The study watershed soil classification	18
Table 2. Gumero watershed slope area classification.....	20
Table 3. Land use land cover change area coverage of the watershed	21
Table 4. Available RCP grid point selected for study area.....	31
Table 5. Grid point coefficient of correlation (R^2) without biases correction	38
Table 6. Annual observed baseline average rainfall statistics for Mann -Kendall trend test	46
Table 7. Mean annual observed baseline temperature statistics for Mann Kendall trend test.....	47
Table 8. Mean annual baseline rain fall statistics for Mann Kendall trend test.....	48
Table 9. Average annual baseline temperature statistics for Mann- Kendall trend test ...	49
Table 10. 2020s average annual rainfall Mann-Kendall trend test value	50
Table 11. 2050s average annual rainfall Mann-Kendall trend test value	51
Table 12. 2080s average annual rainfall Mann-Kendall trend test value	52
Table 13. 2020s average annual mean temperature Mann-Kendall trend test value	54
Table 14. 2050s average annual mean temperature Mann-Kendall trend test value	55
Table 15. 2080s average annual mean temperature Mann-Kendall trend test value	56
Table 16. Water balance module sensitive parameter (NSE) value	57
Table 17. Sediment module sensitive parameter analysis Nash Sutcliff Efficiency value	59
Table 18. Model calibration Statistical value	60
Table 19. Calibrated models parameters in Gumero watershed	62
Table 20. Model validation statistical value	63
Table 21. Average annual mean temperature change difference in (%).....	66
Table 22. Average annual mean rain fall changes differences in (mm)	69
Table 23. Average annual mean flow differences in (%)	73
Table 24. Average annual mean sediment yield change differences in (%).....	75
Table 25. Percentage change comparison of projected hydro-meteorological variable based on baseline period	76

1. INTRODUCTION

1.1 Back ground of the study

Climate change is a change in statistical descriptions of weather conditions (temperature, humidity, precipitation, atmospheric pressure, and wind) and their variations, averages and extremes at a particular location (Pell, 2011). However, the changes in weather from day to day, between seasons, and from one year to the next, do not represent climate change. The period for estimating climate change is over 30 years. Although rainfall patterns and seasonal temperature are common in climate expressions, the average surface temperature is a key global climate variable (Rafferty, 2011).

Changes in climate have been observed in the past, and more changes have been projected for the coming (Parry et al., 2007a). An increasing global temperature is expected to increase evapotranspiration and to cause precipitation changes (Meehl et al., 2012), which will significantly affect the hydrological regimes of many river systems. Many studies have shown that climate change could significantly affect stream flow, soil erosion rates and sediment flux (Zhu et al., 2008). Globally, temperature is increasing and the amount and distribution of rainfall is being altered (Gregory et al., 2002). According to (Sánchez et al., 2004), global average temperature was expected rise between 1.4 and 5.8°C by 2100 as result of with the doubling of the CO₂ concentration in the atmosphere. Sea level rise, change in precipitation pattern (up to ±20%), and change in other local climate conditions are expected to occur as a consequence of rising global temperature (Gregory et al., 2002). In many parts of the world climate is both changed and varying. Changes are from humid equatorial to seasonally-arid tropical regimes and vary because climate reveals differing extent of temporal and spatial unevenness (Mitchell et al., 2004).

Climate change is commonly projected at continental or global scale, the magnitude and type of impact at regional-scale catchment is not investigated in many parts of the world that also including Lake Tana in the Ethiopia (Abdo et al., 2009) and downscaled the temperature and precipitation to a watershed scale for the upper Blue Nile River basin for

the future periods and evaluated the climate change impact on the hydrology of the Blue Nile River at selected gauge stations. The impacts of climate changes on hydrology and sediment yield on the Lake Tana basin are not well researched. (Taye et al., 2011) studied climate change impacts on hydrological and sediment in upper blue Nile by using direct GCM outputs that has high uncertainty but did not focus on downscaling at watershed level in the local climate change. It is necessary to study the effect of climate change at the watershed scale in order to take the effect into account by the policy and decision makers when planning water resources and land management. The main objective of this study is to evaluating the impact of climate change on sediment yield for Gumero watershed in the Lake Tana basin using a hydrological model that is forced by the outcome from RCP emission scenarios. In this study RCP 2.6 and 8.5 emission scenario were used by downscaling the temperature and precipitation to a watershed scale for the Gumero watershed for the 2020 (2011-2040), 2050 (2041-2070) and 2080 (2071-2100) future time periods. The impact on the hydrology of the watershed was evaluated. The parameter efficient distributed (PED-W) model output based on the downscaled emission scenario biased corrected output data were used to evaluate the impacts of climate change on Sediment yield for Gumero watershed, in the Lake Tana Basin.

1.2 Statement of the problem

The environmental challenge on natural ecosystems, directly in many areas of the world are partly caused by global climate change (Chen et al., 2012). For instance, it has significant effects on the hydrological cycle because the distribution of water resources and sediment yield is very sensitive to climate change (Solomon, 2007). Global climate change has also the potential to impose additional pressures on water availability, sediment transportation, and water demand (Bates et al., 2008). Moreover climate change may further reinforce the vulnerability of agriculture by decreasing rainfall variability, evapotranspiration losses, and loss of soil structure, nutrient degradation, and soil salinity. These are very real and at times severe issues. The effects of climate change on soil erosion go beyond the loss of fertile land. It has led to increased pollution and sedimentation in streams and rivers, clogging these waterways and causing declines in fish and other species and degraded lands are also often less able to hold onto water,

which can worsen flooding. Climate change on Soil erosion and sedimentation by runoff is one of the most important land degradation problem and a critical environmental hazard in modern time, worldwide (Song et al., 2015). It is one of the most serious problems as it removes soil rich nutrients and increases natural level of sedimentation in rivers and, reducing reservoirs storage capacity. Hence Sediment is a particular concern in the UBNB, where some of the highest erosion rates in the world have been documented, greater than 500 tons/ha/year (Easton et al., 2010) and has the potential to impact the significant investments in hydropower and irrigation schemes. (Zelege and Hurni, 2001) estimates annual loss of 1.9 billion tons of soil from the Ethiopian Highlands; resulting in depletion of live storage in Nile basin reservoirs. Then evaluating the impact of climate change on erosion and sediment would provide basin managers with data to incorporate into reservoir operation and irrigation planning and provide information pertinent to addressing land degradation and agricultural productivity.

1.3 Objective

The overall objective of this study was evaluating the impact of climate change on sediment yield using RCP with PED-watershed model in case study of Gumero watershed on upper Blue Nile River Basin.

1.4 Specific objective

- To downscale RCP scenario into station level
- To calibrate and validate PED-W discharge and sediment modules using observed discharge and sediment data
- To evaluating the impact of climate change on sediment yield from base line period

1.5 Research questions

- What is the trend in meteorological variable in the river basin based on downscaled climate models?
- What are the possible impacts of climate change on sediment yield?

1.6 Significance of the study

Evaluating the impact of climate change on soil erosion and sediment yield would provide basin managers with data to incorporate into reservoir operation and irrigation planning and to provide information necessary to addressing land degradation and agricultural productivity. It will also supportive to evaluate the effectiveness of soil and water conservation measures implemented so far in the Gumero watershed and the result of this study will serves as a baseline for further research and ecosystem management.

1.7 Scope of the study

The regional climatic model output used in future projection for this study was a grid 50 km by 50 km with only 2.6 and 8.5 emission scenarios. In addition, in this study watershed Land cover land use change was not considered in future time projection.

1.8 Thesis Organization

This study has been organized in to five chapter. The first chapter deals with the background information of the study, statement of the problem which indicates the reason that initiate the researcher to conduct on this title ,objective of the study ,scope and significant of the study. The second chapter consists of the review of detail literatures about the study including definitions and summary of related and similar studies in the other parts of Lake Tana and Blue Nile Basin. The third chapter deals with materials and methodology of the study that contains description of the study area, detail methodology used to carry out the study including biased correction techniques for future climate data, trend test, data collection and quality assessment. The fourth chapter focuses on the result and discussion part of the study which contains the evaluation of climate change on sediment yield dynamics for future years. It also includes results and discussion sections of sensitivity analysis, calibration and validation of PED-W model and the overall relationships of the climate change impact on sediment yield of the watershed. The final chapter, chapter five includes conclusion and recommendations of the study.

2. LITERATURE REVIEW

2.1 Over view of climate change

2.1.1 Climate and Weather

Climate is usually defined as the “average weather” or more rigorously as the statistical description in terms of the mean and variability of relevant quantities over a period of time ranging from months to thousands or millions of years. The classical period is 30 years, as defined by the World Meteorological Organization (WMO, 2007). But weather are a short-term phenomenon, describing atmosphere, daily air temperature, pressure, humidity, wind speed, and participation (Parry et al., 2007b)

2.1.1 Climate change and Climate variability

A change in the state of the climate that can be identified by using Statistical tests or by changes in the mean or the variability of its properties, and that persists for an extended period, typically decades or longer. Climate change may be due to natural internal processes or external forcing or to persistent anthropogenic changes in the composition of the atmosphere or in land use (IPCC, 2007). According to IPCC (2007) Scientific Assessment Report, global average temperature would rise between 1.4 °C and 5.8°C by 2100 with the doubling of the CO₂ concentration in the atmosphere. Sea level rise, change in precipitation pattern (up to ±20%), and change in other local climate conditions are expected to occur as a consequence of rising global temperature (Cubasch et al., 2001). Variations in the mean state and other statistics (such as standard deviations, the occurrence of extremes, etc.) of the climate on all temporal and spatial scales beyond that of individual weather events (Fusel and Klein, 2000).

Climate projections

A response of the climate system to emission or concentration scenarios of greenhouse gases and radioactive forcing scenarios, based upon simulations by climate models (IPCC, 2013).

2.2. Physical impacts of climate change

2.2.1. Impacts on water resources and hydrology

Water is fundamental to human life and many other social, economic and industrial activities. It is required for agriculture, industry, ecosystems, energy, transportation, recreation and waste disposal (Wass and Leeks, 1999). The climate change over the next century is expected to severely impact water resources; arid and semi-arid areas are particularly more vulnerable to that change and are projected to suffer from water shortage due to precipitation reduction (Setegn et al., 2011). Therefore, any changes in water resources system could have a direct effect on the society, environment and economy. There are very complex relations between climates, hydrology and water resources. Climatic processes influence the hydrologic processes, vegetation, soils and water demands.(Vörösmarty et al., 2000). Water resources are influenced by various social, technical, environmental and economic factors. The process of water circulation in the hydrosphere through different paths and states is called hydrological cycle (Chow, 1988). Any changes in the climatic system or the energy balance in the atmosphere may alter the water balance of the hydrological cycle. Change in precipitation could have very important implications for hydrology and water resources (Olmos, 2001). Floods and droughts primarily occur as a result of too much or too little of precipitation. Changes in river flows from year to year have been found to be much more strongly related to precipitation changes than to temperature changes (IPCC, 2001). The patterns of changes in river flow are broadly similar to the change in annual precipitation. The real impacts of climate changes vary with catchment characteristics. Under climate change, many river systems show changes in the timing and magnitude of seasonal peak and low flows.

2.3 Projected future climate

2.3.1 Future global climate

The future climate change largely depends on the existing and expected level of influencing factors of climate change, e.g. level of greenhouse gas emissions. Future greenhouse gas emissions are mainly determined by the economic and technological

advancement, policy intervention, industrial development, type of energy sources etc. So, different scenarios have been developed to project the future climate change.

2.3.2. Projected Climate Change in Ethiopia

Over the coming decades climate change is projected to affect the lives of billions of people around the world. No region or country is invulnerable to its impacts; however, the extent of vulnerability differs widely. Developing countries are especially vulnerable, though every developing country will face additional challenges to attain the United Nations Millennium Development Goals by 2015 (UNMDG, 2007). Projected climate changes could not only have serious environmental, social and economic implications, but also implications for peace and security and migration. However, the specific impacts of climate change will depend on the climate variance and change it experiences as well as its geographical, social, cultural, economic and political situations. As a result, countries require a diversity of adaptation measures that reflect their unique circumstances (Zakieldeen, 2009). Future climate change cannot be adequately predicted without a sound understanding of the future expectation of the emission and concentration of greenhouse gases in the atmosphere, which will depend on socio-economic trends including population and economic growth, technological changes and energy demand (ASCHALEW, 2007). Under intermediate warming scenarios, most models project that by 2050 North Africa and the interior of Southern Africa will experience decreases in precipitation during the growing season that exceed one standard deviation of natural variability; in parts of equatorial East Africa, rainfall is predicted to increase in December–February and decrease in June–August (ASCHALEW, 2007). Climate change scenarios for Africa, based on results from several general circulation models using data collected by the IPCC data indicate that future warming across Africa ranging from 0.2°C per decade (low scenario) to more than 0.5°C per decade (high scenario). This warming is greatest over the interior of semi-arid margins of the Sahara and Central Southern Africa (ASCHALEW, 2007). According to NMA (2007), Climate projections for Ethiopia have been generated using the software MAGICC (Model for the Assessment of Greenhouse-gas Induced Climate Change)/(Regional and Global Climate Scenario Generator) coupled model (Version 4.1) for three periods centered on the years

2030, 2050 and 2080. For the IPCC emission scenario, the mean annual temperature will increase in the range of 0.9 -1.1 °C by 2030, in the range of 1.7 - 2.1 °C by 2050 and in the range of 2.7-3.4 °C by 2080 over Ethiopia compared to the 1961-1990 normal.

2.4 Baseline climate scenario

According to IPCC (1994) possible criteria for selecting the baseline period are representativeness for the present-day, recent average climate and sufficient duration to encompass a range of climatic variations. The baseline climate scenario represents current climate conditions, typically precipitation and temperature patterns. As in most climate change studies, this study uses daily precipitation and temperature from 1976 to 2005 to represent the current climate conditions of the study area.

2.5 Climate model

A numerical representation of the climate system based on the physical, chemical, and biological properties of its components, their interactions and feedback processes, and accounting for all or some of its known properties.

2.5.1 General Circulation Models (GCMs)

General Circulation Models (GCMs) are mathematical representations of atmospheric, oceanic, and continental processes and interactions. These models are limited by complexity and uncertainty as well as non-linear interactions among atmospheric and oceanic processes (Hillel and Rosenzweig, 2002).

2.5.2 RCP scenario

Representative Concentration Pathways (RCPs) assist in the development of GCM results that account for different combinations of economic, technological, demographic, policy and institutional futures (Moss et al., 2010) and are used to initiate climate model simulations for developing climate scenarios for use in a broad range of climate-change related research an assessment (IPCC ,2007). RCPs are used as inputs for modeling and are affected by concentrations of a variety of greenhouse gases, as well as land-use, air

pollution, changes in technology, population, energy production and a variety of additional factors (Van Vuuren et al., 2011). The international climate modeling community has adopted four RCPs through the Intergovernmental Panel on Climate Change (IPCC) (Sillmann et al., 2013). The RCP 8.5 scenario range which corresponds to a “non-climate policy” scenario translating into high severity climate change impacts, RCP 2.6, which is the future requiring strict climate policy to limit greenhouse gas emissions, translating into low severity impacts (Van Vuuren et al., 2011). Two middle scenarios, RCPs 4.5 and 6.0 were selected by the IPCC to be evenly spaced between RCPs 2.6 and 8.5. Together, these scenarios represent the range of radiative forcing’s available in the peer-reviewed literature at the time of their development in 2007. (Sillmann et al., 2013). The term “representative” indicates that that the RCPs represent a largest set of scenarios available in the literature. The term “concentration pathway” emphasizes that the RCPs are not finalized, fully integrated scenarios comprised of a complete set of socio-economic, emission and climate projections, but are rather “...internally consistent sets of projections of the components of radiative forcing that are used in subsequent phases.” Further, unlike the previous SRES scenarios, the term “concentration” emphasis the use of concentrations as the output of RCPs for use in climate models, rather than emissions (Van Vuuren et al., 2011). RCPs were adopted by the IPCC for generation of climate model results for the fifth IPCC Assessment Report (AR5). Previously, climate change scenarios published in the IPCC Special Report on Emission Scenarios (SRES) were applied by the climate modeling community to represent different future greenhouse gas emissions scenarios (IPCC, 2000). For the purposes of comparison, RCP 8.5 results in a future climate change scenario slightly more severe than the SRES A2 scenario. RCP 2.6 provides a scenario that would lead to lower climate change severity than all SRES scenarios (Stocker et al., 2013).

2.6 Downscaling

Downscaling is a technique for exploring the regional and local-scale response to global climate change as simulated by comparatively low-resolution global climate models (GCMs) (IPCC, 2001). Downscaling is commonly done either by using Regional Climate Downscaling (RCD) or Statistical Downscaling Methods (SDSM). RCD has been

increasingly used to address a variety of climate-change issues and have by now become an important method in climate change research (WMO, 2008).

2.6.1 Downscaling Methods

GCM's are coarse in resolution and are unable to resolve significant sub-grid scale features such as topography, clouds and land use (Grotch and MacCracken, 1991). Basically, there are two main approaches available for the downscaling of large spatial resolution GCM outputs to a finer spatial resolution, termed dynamical and statistical downscaling.

2.6.1.1 Dynamical downscaling

It is a higher resolution climate model or regional climate model is forced using a GCM. The statistical approach establishes empirical relationships between GCM-resolution climate variables and local climate.

2.6.1.2. Statistical downscaling

It is a tool for downscaling climate information from coarse spatial scales to finer scales. Statistical downscaling consists of identifying empirical links between large-scale patterns of climate elements (predictors) and local climate (predictands), and applying them to output from global or regional models. statistical downscaling is less technically demanding than regional modeling; it is thus possible to downscale from several GCMs and several different emissions scenarios relatively quickly and inexpensive; it is possible to tailor scenarios for specific localities, scales, and problems.

2.7 Bias correction

Bias is a term used to refer the process of adjusting the coarse resolution climate model data to the fine spatial scale data to allow local analyses of climate effects. The liner scaling method (Hay et al., 2000) is an ordinary bias correction method. The liner scaling method is often used to exclude or minimize the bias between observations and the model outputs. The liner scaling procedures rely on modifying the daily time step series of the climate variables such as precipitation and temperature for prediction period.

2.8 Previous climate studies in the Upper Blue Nile Basin

Numerous climate studies in the Upper Blue Nile Basin (UBNB) have been conducted over the last two decades (Cherie and Koch, 2013). However, the results of these investigations are often divergent and inconsistent. Although a better agreement among authors with regard to the prediction of the future temperature is observed over the UBNRB, conflicting results are often obtained for the GCM-predicted precipitations. Thus, almost all study results indicate a temperature increase from a range of 1.4°C to 2.6 °C depending on the type of GCMs in 2050s (Kim and Kaluarachchi, 2009) and 3.7°C to 4.7°C by 2080s (Beyene et al., 2009). As for the precipitation prediction over the UBNRB, the results of the various authors referenced above are more different. For example, (Conway et al., 1996) used 3 GCMs and predicted the change in precipitation ranges from -2 to 7% by the 2025s. (Yates and Strzepek, 1998) found that for a doubling of the carbon dioxide concentration the annual rainfall by 2060 will range from -9% to 55%. The results of (Conway, 2005) show no clear evidence, whether precipitation over the UBNRB region increase or decrease for both current and future periods. Later on the same author (Conway, 2005) applied 9 GCMs are obtained changes from -40% to 100% (Dec-Feb), 120% (June-August) for the 2080s period. (Beyene et al., 2010) used 11 GCMs and observed data from the predicted precipitation changes from -16 to 40% for the 2020s (2010-2039) and -24% to 26% for the 2080s (2070-2099). (Elshamy et al., 2009) considered 17 GCMs and found that the annual precipitation will change between -15% to +14% over the UBNRB, whereby out of the set of GCM's used, 10 GCMs predict a decrease and 7 GCMs an increase of the precipitation. The inconsistencies of the results of these studies in predicting future climate change in the UBNRB are due to various reasons:

- Number and type of the GCM
- Number and type of emission scenarios
- Length of both hydrological and metrological data
- Spatial and temporal resolutions of observed and grid data sets
- Downscaling biased corrected output data for simulation hydrology model
- Scale of study area

So, based on such differences, it is not clear which combination of input give a good insight for the understanding of future plausible climate conditions in the UBNRB. Even, the current hydrological and meteorological parameter values are different in most of the studies mentioned. Most of the previous studies used gridded data sets which are constructed based on the interpolation of a few climate stations distributed sparsely across Ethiopia. Due to the high spatial variability of the UBNRB, incorporating only a few stations may not be reasonable for such a large area. In order to fill the gap for inconsistency of studies detail investigation and evaluation of climate changes on mean and extreme state on hydrological variable on specific watershed needs to be done. Therefore this study will evaluate the impacts of climate change on sediment yield in Gumero watershed by considering the ways to include the reduction of uncertainty. This investigation focuses on the watershed level of downscale biased corrected output data for two RCP scenarios to detecting trends in annual temperature and precipitation for the Gumero watershed. For this study Mann-Kendall test was run at 5% significance level on time series.

2.9 Hydrological model for climate change

Hydrological models can be defined as mathematical formulations that determine the runoff signal that leaves a river basin from the rainfall signal received by the watershed (Beyene, 2001). Hydrological models provide a means of quantitative prediction of catchment runoff and sediment yield that may be required for efficient management of water resources systems and land. The physically based models are based on the understanding of the physics of the hydrological processes controlling the catchment response and describe these processes using physically based equations. These hydrological models are used as a means of extrapolating from those available measurements in both space and time, in particular into the future to assess the likely impact of future hydrological changes otherwise known as forecasting.

2.10 Climate change on sediment yield by (PED-W) Model

Parameter efficient distributed watershed (PED-W) model was the ideal choice for use in this study because of various reasons; it is a physically based model that requires specific information about climate condition, and land scape parameter which uses as inputs to simulate the physical processes associated with water and sediment movement. This enables to quantify the impact of scenarios (alternative input data) such as changes in climate on water quality and quantity and it uses readily available data, while more inputs can be used to simulate more specialized processes it is still able to operate on minimum data which is an advantage especially when working in areas with insufficient or unreliable data like the Gumero River. Second, the PED-W model is computationally efficient, able to run simulations of very large basins or management practices without consuming large amounts of time and expenses compared to lumped, conceptual or fully distributed, physically based models (Moges et al 2016). These qualities of the PED-W model will enable the quantification of long term impacts of climate changes, variations in rainfall and air temperature on the hydrology of the Gumero River basin.

3 MATERIALS AND METHODOLOGY

3.1 Description of the study area

3.1.1 Location

Gumero watershed, located in the northwestern Amhara region, Ethiopia, between 12° 24' and 12° 31' north and between 37° 33' and 37° 37' East (Fig. 1) and watershed has an area of 116 km². The main stream (Gumero River) is training into Lake Tana and originates in the north mountainous parts of the watershed. Gumero watershed could be representative of wider sectors of the northern highlands of Ethiopia because of its geological, geomorphological and climatic features similarity.

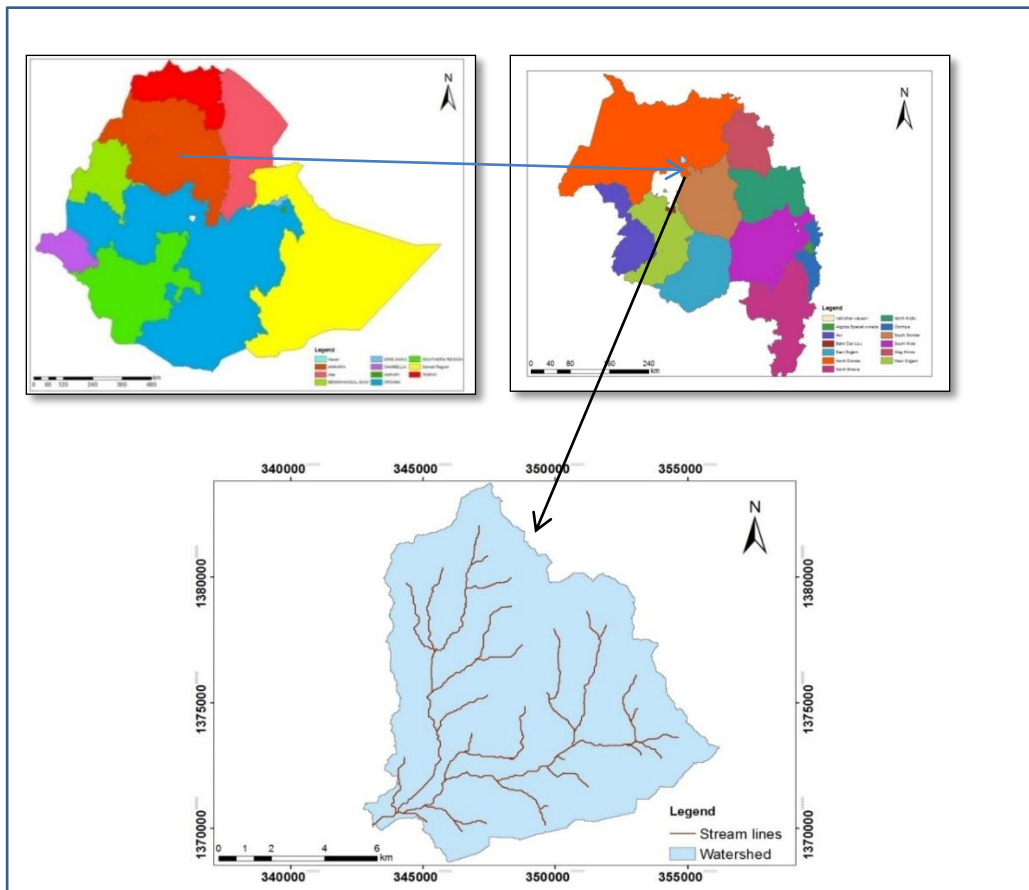


Figure 1. The study area description

3.1.2 Topography

The elevation of the study area is extends from 1,792 to 2,862 meters above mean see level. The maximum elevation of Gumero watershed is located in the North West and South West part of watershed .The minimum elevation of this watershed is located in the southeastern part of this watershed. Elevation map of watershed is shown below in the Figure 2

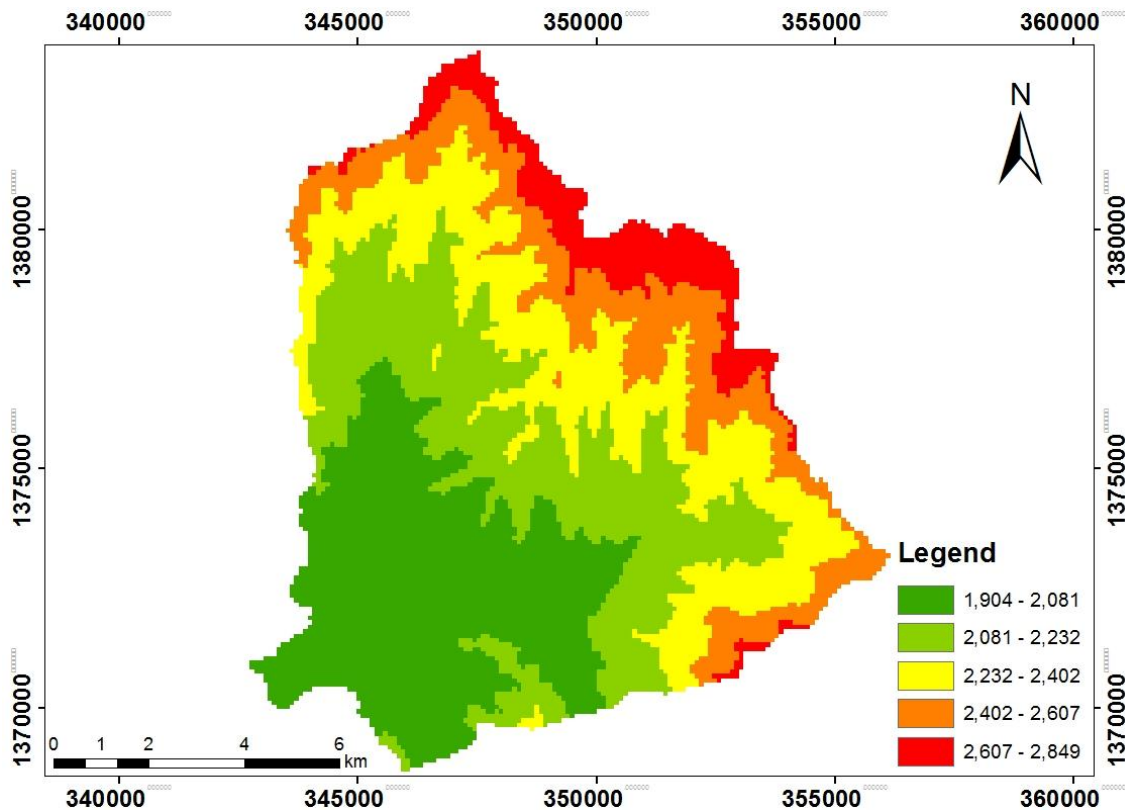


Figure 2. Topography of the study area

3.1.3 Climate

Average annual precipitation varies from 1,009.2 to 1120.32 mm and average minimum and maximum temperature is 13.9 °C to 26.9 °C respectively. The altitude of this watershed is varying from 1,792 to 2,862 meter due to agro climatic zone of Ethiopia. Gumero watershed is categorized into two climatic zones, Such as woynadega, and degas. Climatic zone indicates as altitude increase with decreasing temperature and increase precipitation. Temperature and rainfall are the most important elements in

characterizing the climatic condition of a given region maximum and minimum Temperature for each station from 1970-2005 can be seen in the figure 3 below.

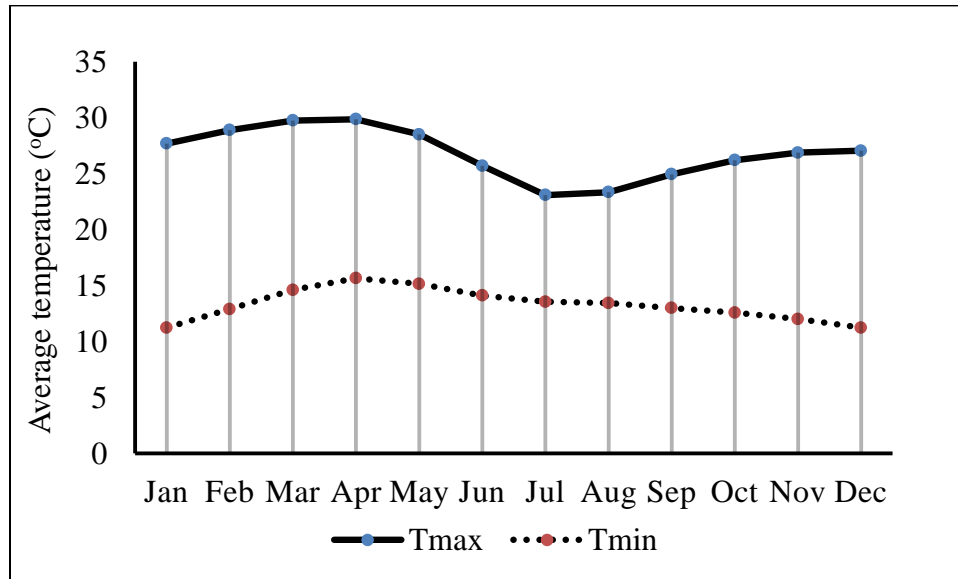


Figure 3. Annual average monthly maximum and minimum temperature of the watershed

The maximum and minimum mean annual precipitation of Gumero watershed was varying from 1009 mm to 1120 mm respectively. Average maximum and minimum monthly precipitation is varying from 304.8 mm and 1.85 mm respectively. Figure 4 shows mean maximum and minimum precipitations was record in July and March respectively.

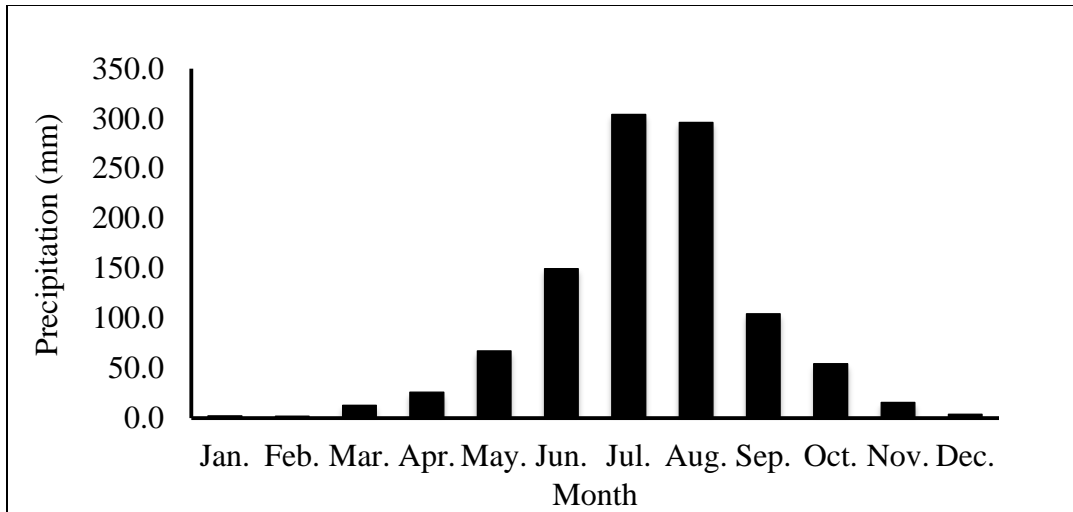


Figure 4. Annual average monthly precipitation of the watershed from (1970-2005)

3.1.4 Hydrology

Gumero river is draining from Gumero watershed where gauging station was found at the geographical location of latitude $12^{\circ}24'$ N and longitude $37^{\circ}33'$ E. The river discharge is highly dependent on seasonal rainfall variability. Hence highest river discharge is measured during main rainy season of the year, which starts from the beginning of June to end of September. An average annual discharge of the river was 507.7 mm/year.

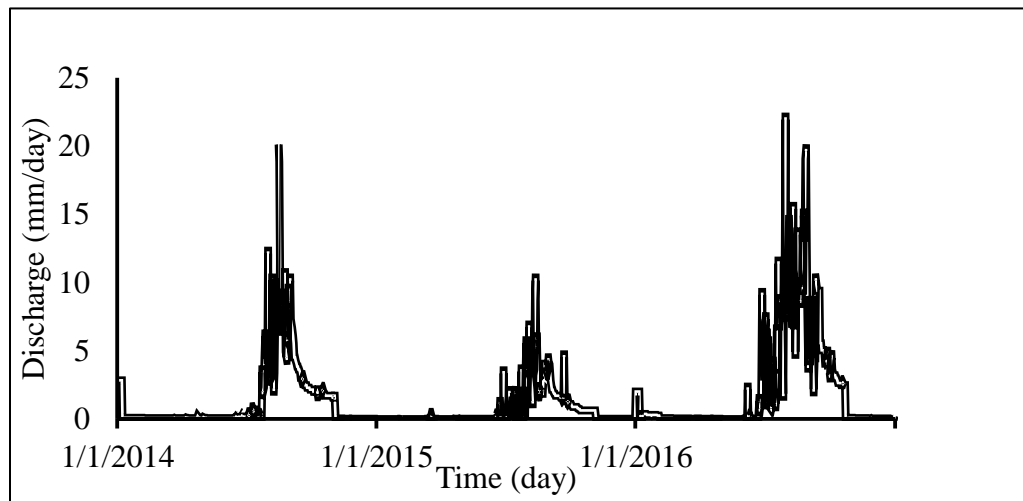


Figure 5. The study area stream flow characteristics

3.1.5 Soil

The soil of the study watershed area was derived from Abay basin shape file. Twenty-eight types of soil were identified. The Major types of soil found in the study watershed are DystricNitosols, HyperskeletalLeptosols, VerticLuvisols, ProfondicLuvisols, LepticLuvisols, HyperskeletalAlisols, VerticCambisols. From all types of soil DystricNitosols, is dominated in the study area as shown in the figure 6. and table 1 below.

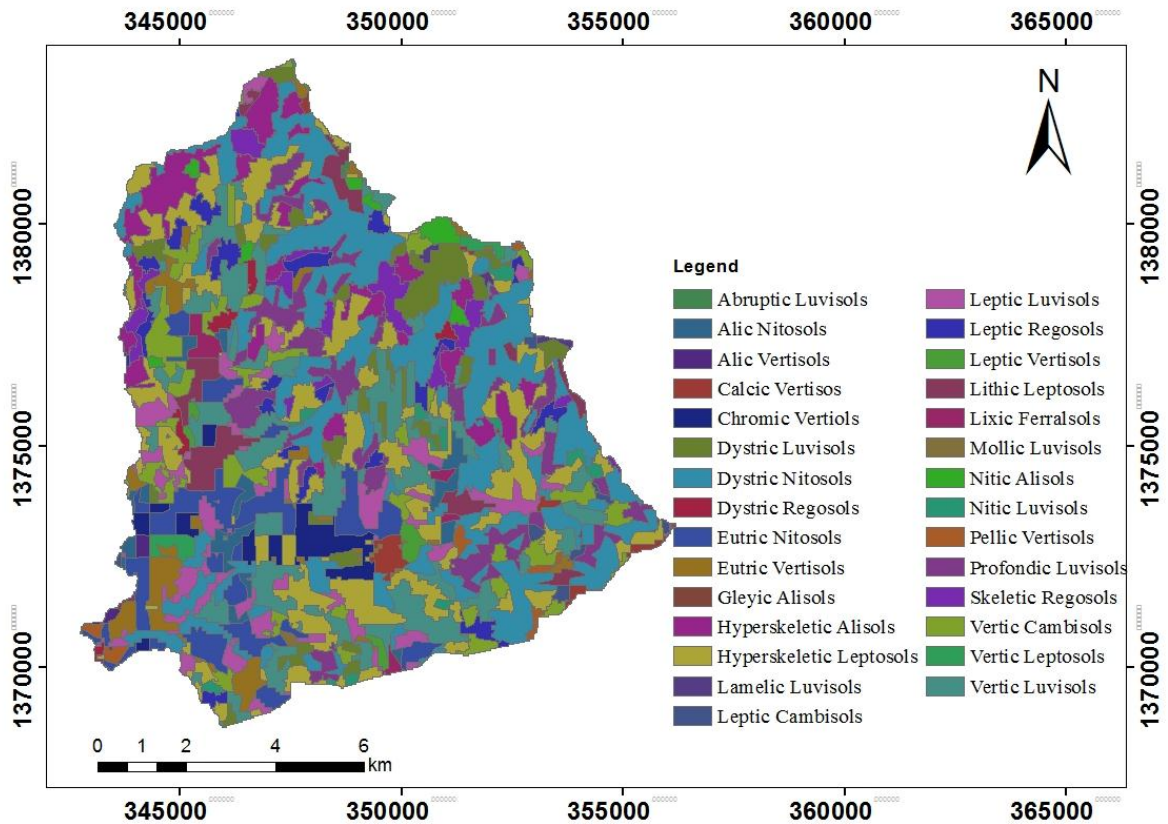


Figure 6. Soil type of the study area

Table 1. The study watershed soil classification

No	Soil type	Area(km ²)	Percent coverage
1	Alic Nitosols	2.16	1.86
2	Alic Vertisols	0.24	0.20
3	Calcic Vertisols	0.95	0.82

4	ChromicVertisols	2.59	2.23
5	DystricLuvisols	4.82	4.15
6	DystricNitosols	22.9	19.71
7	DystricRegosols	0.73	0.63
8	Eutric Nitosols	7.13	6.14
9	Eutric Vertisols	3.45	2.97
10	Gleyic Alisols	0.01	0.07
11	HyperskeletalAlisols	6.46	5.56
12	HyperskeletalLeptosols	15.98	13.75
13	Lamelic Luvisols	0.24	0.21
14	Leptic Cambisols	0.52	0.45
15	Leptic Luvisols	6.42	5.53
16	Leptic Regosols	3.36	2.89
17	Leptic Vertisols	0.65	0.56
18	Lithic Leptosols	3.30	2.84
19	Lixic Ferralsols	0.77	0.66
20	Mollic Luvisols	0.08	0.07
21	Nitic Alisols	1.03	0.89
22	Nitic Luvisols	1.03	0.88
23	Pellic Vertisols	0.69	0.59
24	Profondic Luvisols	7.75	6.67
25	Skeletal Regosols	2.98	2.56
26	Vertic Cambisols	6.06	5.22
27	Vertic Leptosols	0.69	0.59
28	Vertic Luvisols	13.04	11.22
Total area		116.14	

3.1.6 Slope

The slope of the study area was derived from Abay basin shape file. The average slope class based on (FAO, 1998) major slope classes by using ArcGIS 10.1 software to understand its topographical characteristics was done. On the slope map generated from

DEM under figure 7 indicates highest slope which consists 15-30%. Most of the area is having the slope ranging from 0 to 8%.

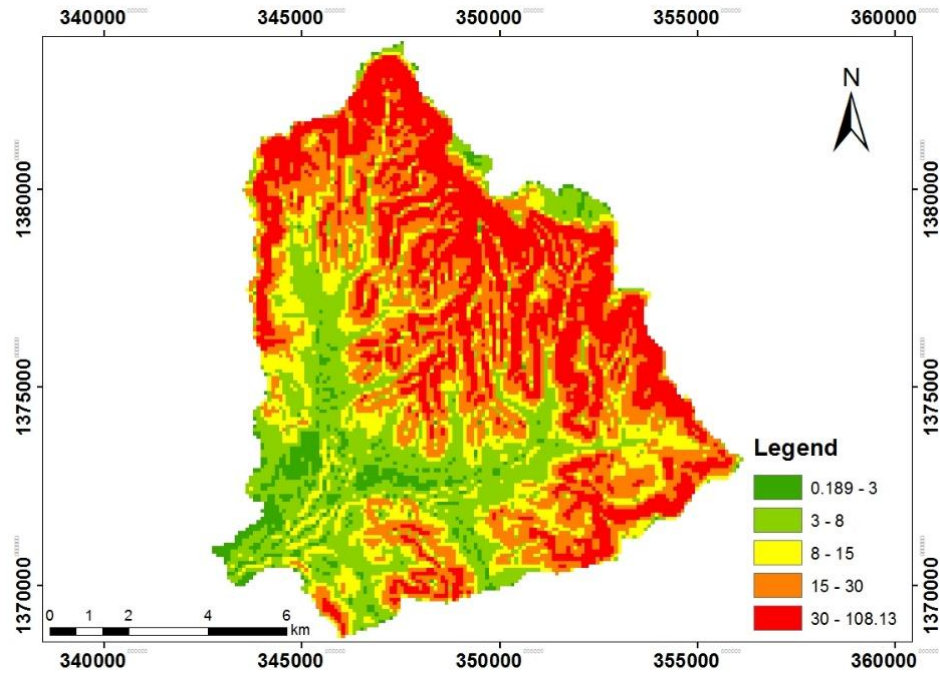


Figure 7. The study area slope classification

Table 2. Gumero watershed slope area classification

No	Slope	Area(km ²)	% coverage
0	0-3	4.78	4.11
1	8-Mar	21.61	18.60
2	15-Aug	23.14	19.92
3	15-30	31.07	26.75
4	30-50	27.13	23.35
5	>50	9.08	7.81
		116.14	

3.1.7 Land use land cover

The watershed land cover map was collected from Ministry of Water Irrigation and Electricity (MoWIE, 2014). The land use cover of the watershed consists 6 land use change types which described below in figure 8 and table 3.

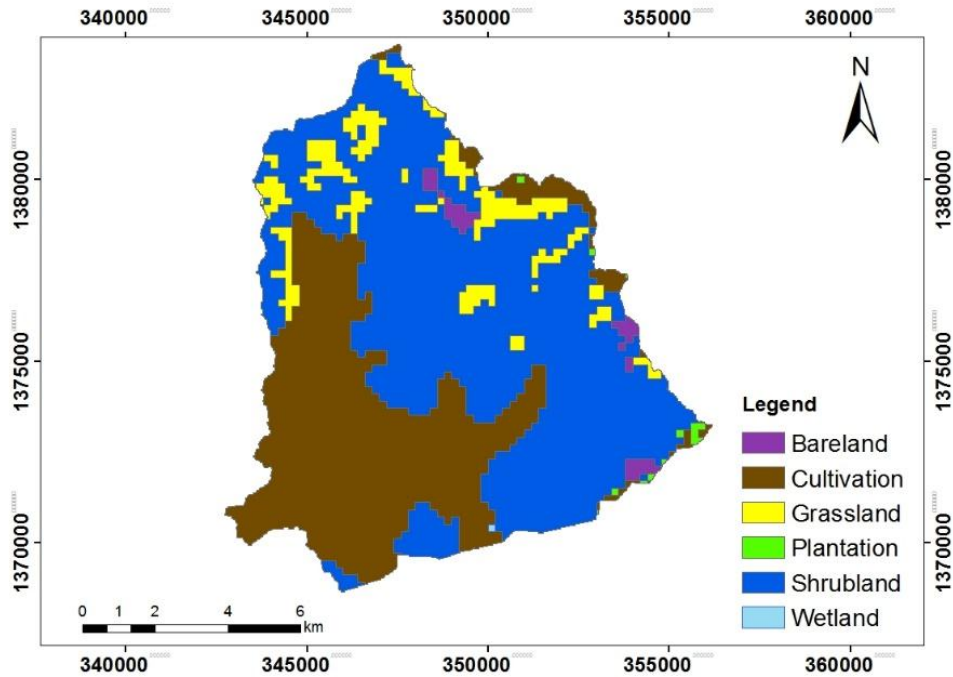


Figure 8. Land use land cover map of Gumero watershed

Table 3. Land use land cover change area coverage of the watershed

No	LCLU	Area(km ²)	% coverage
1	Bare land	15.08	1.28
2	Cultivated land	90.30	12.99
3	Grassland	7.92	6.82
4	Plantation	0.87	0.75
5	Shrub land	1.49	77.75
6	Wetland	0.07	0.06
	Total area	116.14	

3.2 General Research Method

The methodology includes: - collecting the observed hydro meteorological data from national meteorology agency of Ethiopia (NMAE) and Amhara Regional Agricultural Research Institute Gondar branch (ARARIGB); fill the missing data; data quality checking; select the type of RCP emission scenario. Based on watershed scale generate daily climate projection data from four grid point of RCP emission scenario of 2.6 and 8.5 by down scaling from CORDEX Africa CMIP5 dataset. Were one grid point emission scenario best fit selected by evaluating their historical run with the observed meteorological station based on coefficient of determination (R^2) and overlaying the grid point to watershed station by ArcGIS10.1? The selected data were bias corrected using linear scaling bias correction method. Calibrate and validate the parameter efficient distributed watershed hydrologic model (PED-W). Use the bias corrected projected climate data as an input to the calibrated and validated hydrological model to predict the sediment yield in the watershed for future three time period of 2020s (2011-2040), 2050s (2041-2070) and 2080s (2071-2100). Finally evaluate the impact of future climate change on sediment yield from the watershed based on baseline period.

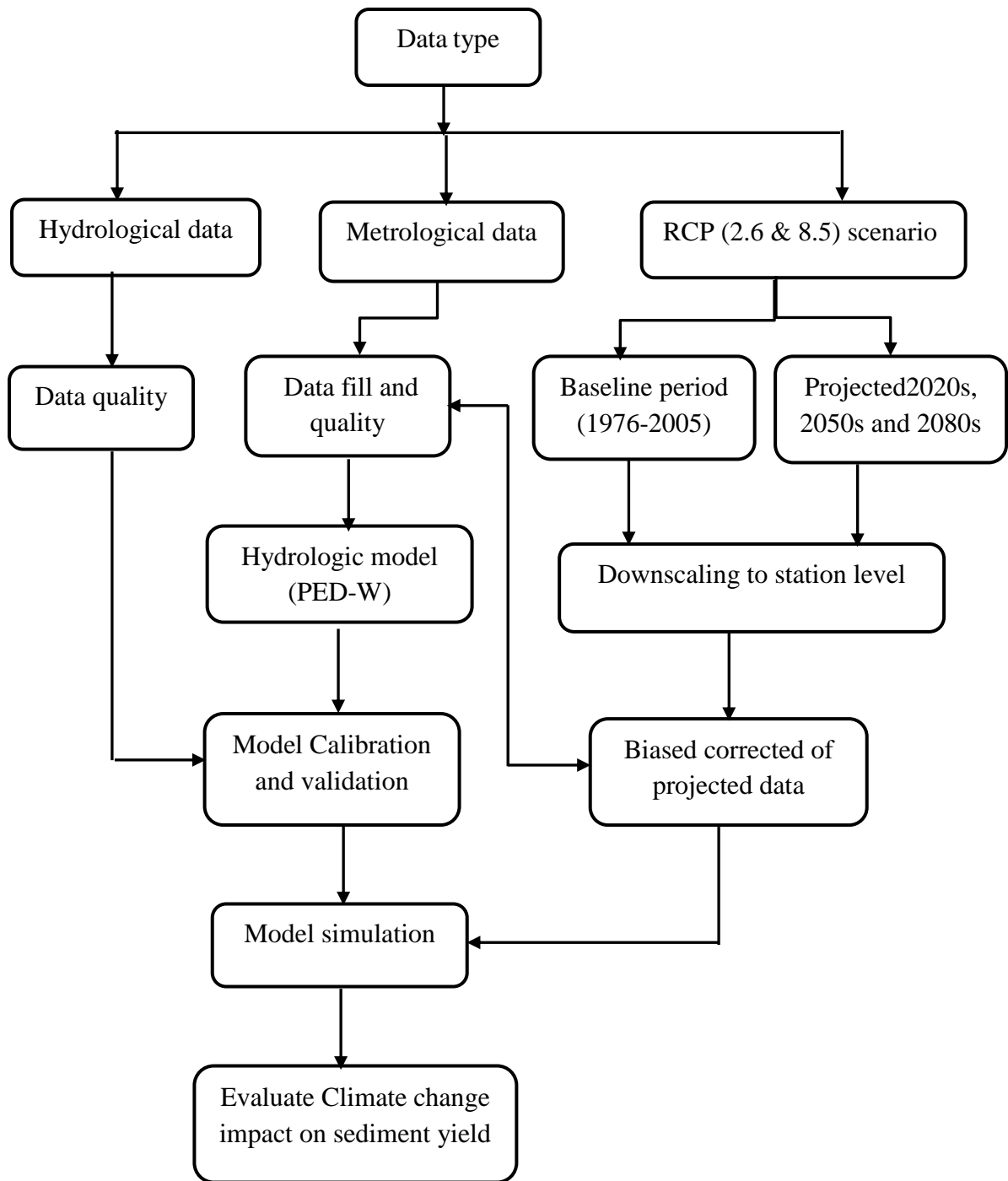


Figure 9. Flow chart of general methodology of this study work

3.2.1 Data collection methods

Data is the crucial input in hydrological modeling. Data preparation, analysis and formatting to suit the required model are important and have influences on the model output. The relevant time series data used in this study includes daily rainfall data, discharge, sediment yield, and temperature (minimum and maximum). The data was collected from the Ministry of Water Irrigation & electricity (MoWIE), Gondar Agriculture Research Institution, and National Meteorological Agency of Ethiopia and CORDEX Africa CMIP5 dataset. The National Meteorological Agency of Ethiopia (NMAE) allowed access and use of the data for this research. A considerable part of the research area is covered by makesegnit stations.

Precipitation

The PED-W model requires daily rainfall data as a major input. The data measured from meteorological stations found in and near to the watershed were considered. Makesegnit rainfall stations were considered for this study. The 30 (1976-2005) year's daily rainfall data for this station were obtained from the National Meteorological Agency Ethiopia Bahirdar branch.

Temperature

The daily maximum and minimum temperature data was used for biased correction the coarse resolution GCM model output in to fine resolution and for generating of potential evapotranspiration. The potential evapotranspiration was used as an input for PED-W model. The 30 (1976-2005) year's daily maximum and minimum temperature data for this station were obtained from the National Meteorological Agency Ethiopia, Bahirdar branch.

Discharge and sediment data

To calibrate and validate the hydrological model for the watershed observed Sediment yield and discharge data was essential. One of the primary goals of this research has to evaluate if any changes in the sediment yield due to climate change in Gumero

watershed. The observed Sediment yield and flow data was obtained from Gondar agriculture research institution. Depending on the extent of calibration and validation, sediment yield and discharge data was collected and arranged as per the PED-W model need.

Digital Elevation Model (DEM)

The Digital Elevation Model of 30m by 30m resolution of different type has been taken from Ministry of Water, Irrigation and Electricity GIS department. The DEM was imported to ArcGIS. ArcGIS has been used to process geospatial data which includes the Digital Elevation Model (DEM) and watershed delineation.

3.3 Data quality analysis

In Gumero watershed there is one raingage stations near to watershed which have 30 years of record used for this study. But, collected data has the errors/missing due to failure of measuring device or record. Before using the data for specific purpose, the error/missing of hydrological and meteorological data were systematically ignored and prepare input data to perform the objective of the study. The quality of the data determines to a great extent the hydrological model efficiency, a result conclusions that can be drawn from the modeling results. In hydrological model the input data should be stationary, consistent, and homogeneous (Dahmen et al, 1989). To determine whether the data meet these criteria, the hydrologist needs a simple but efficient screening statistical variability procedure. In this study, the main data quality analysis as presented as follow.

Estimation of missing data

Climate data contain error/missing due to failure of measuring device or recorder. Hence before using such kinds of data for research purpose checking is very important to remove missing/errors. The analysis has been extended to hydrological and metrological data to prepare inputs data for evaluating the impact of climate change on sediment yield using PED_W model. To compute the missing climate data of Gumero watershed, Gondar, Makesgnit and Ayekel station were used. The missing data was estimated using the inversely distance weighting proportion.

Homogeneity test

The data qualities with regard to possible temporal and spatial variations or errors should have to be investigated by checking homogeneity and consistency of selected stations. The purpose of this technical was to present and demonstrate the basic analysis of long-term hydrological and climate data quality or to check whether the data Homogenous (come from the same distribution) or non- homogenous (a change in the statistical properties of the time series). Its causes can either natural or man -made. These include alterations to land use, relocation of the observation station, and implementation of flow diversions. Non-dimensional plots are the widely used methods for checking homogeneity.

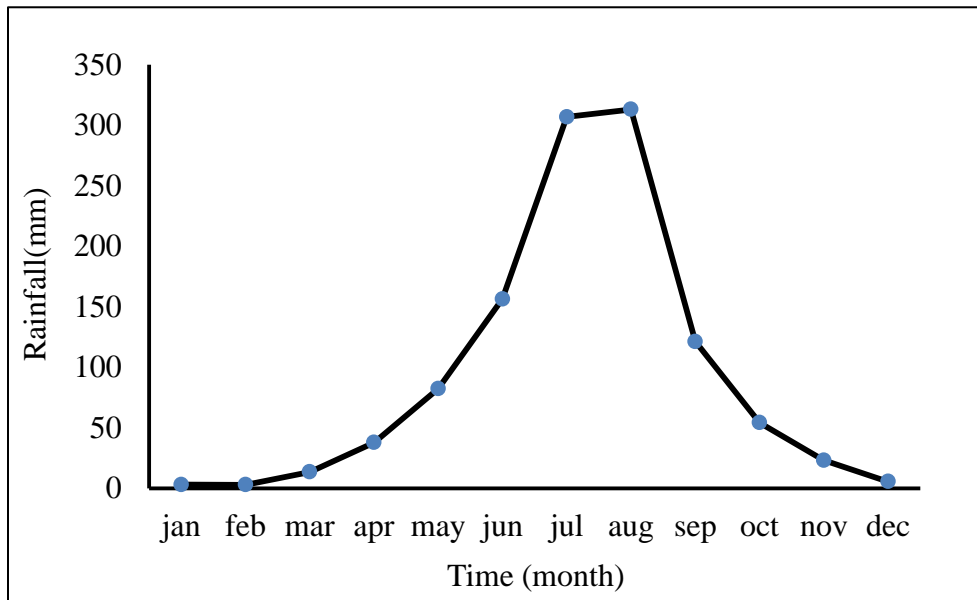


Figure 10. Non-dimensionless plot for homogeneity test

Figure 10 clearly show the homogeneous nature of the stations in study area, because they have one distinct climatic and rainfall pattern in a stations, the maximum rain falls between Jun to September.

Stationery Test

A time series of hydrological data should be stationary if its statistical properties (e.g. its mean, variance, and higher-order moments) are unaffected by the choice of time origin. By ‘unaffected’, illustrates that estimates of these properties agree within the range of expected. The main advantage of stationary test was to check the time independent of the data to reach with a good result conclusion about the objective of the study. Stationary of time series data was checked by using the Mann-Whitney (M-W) test. By using the program M-W test, the results of stationary within a given data set was tested by splitting it into two subsets of sizes p and q by setting hypothesis.

HO (Null hypothesis): The data is stationary

HA (Alternative hypothesis): The data is not stationary

The combined data set of size $N = p + q$ is ranked in increasing order. The Mann-Whitney (M-W) test considers the quantities V and W

$$V = R - \frac{(P(P+1))}{2} \quad 3.1$$

$$w = pq - V \quad 3.2$$

Where R is the sum of the ranks of the elements of the first sample (size p) in the combined series (size N), and V and W were calculated from R, p, and q. Similarly, W can be computed in eq 3.2 U is approximately normally distributed with mean and variance

$$\text{Var}(U) = \left[\frac{pq}{N(N-1)} \right] \left[\frac{N^3 - N}{12} - \sum T \right] \quad 3.3$$

$$T = \frac{(J^3 - J)}{12} \quad 3.4$$

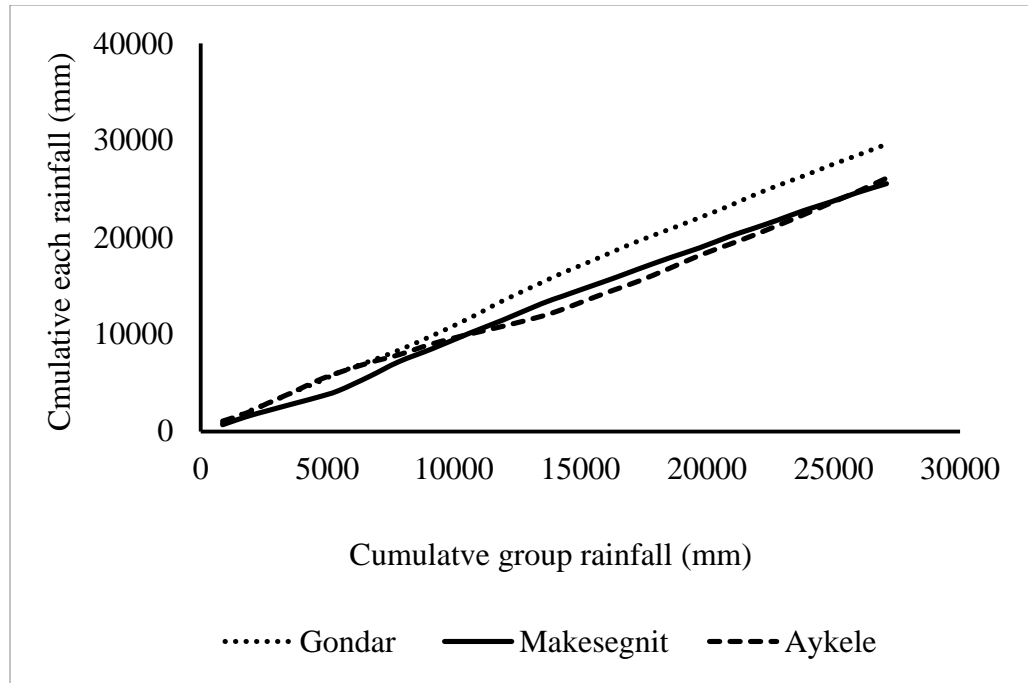
Where J is the number of observations tied at a given rank and T is summed over all groups of tied observations in both samples of size p and q.

$$U = \frac{(u - \bar{u})}{[\text{var}(U)]^{1/2}} \quad 3.5$$

Eq 3.5 statistical value was used to test the hypothesis of stationery at significance level $\alpha = 0.05$ by comparing it with the standard normal variate for that significance level. Since $|u| = |-0.83863| = 0.83863$ was less than $u_{0.025} = 1.960$, the two data sets were stationary at 5% significance level. Thus the alternative hypothesis was rejected the null hypothesis was accepted.

Consistency test

Consistency is the validity or reliability of hydro-meteorological data. The main advantage of Consistency test was to ignore the error of hydro-meteorological data in order to reduce the uncertainty to reach with a good result conclusion about the objective of the study. Double mass curve is a simple, visual and practical method, and widely used for checking the consistency of hydro-meteorological data. It is used to determine whether there is a need for corrections to the data to account for changes in data collection procedures or other local conditions. Such changes may result from a variety of things including changes in instrumentation, changes in observation procedures, or changes in gauge location or surrounding conditions. Double mass curve was carried out by using the annual rainfall of a station and the average rainfall of the group base station was arranged in reverse order.



The precipitation value at station beyond the period of change of regime was corrected by using the relation

$$P_{cx} = P_x \frac{M_c}{M_a} \quad 3.6$$

Where P_{cx} is Corrected precipitation at any time period, P_x is Original recorded precipitation at time period, M_c = Vertical height difference between beak regime and corrected and M_a = Vertical height difference between beak regime and the pervious

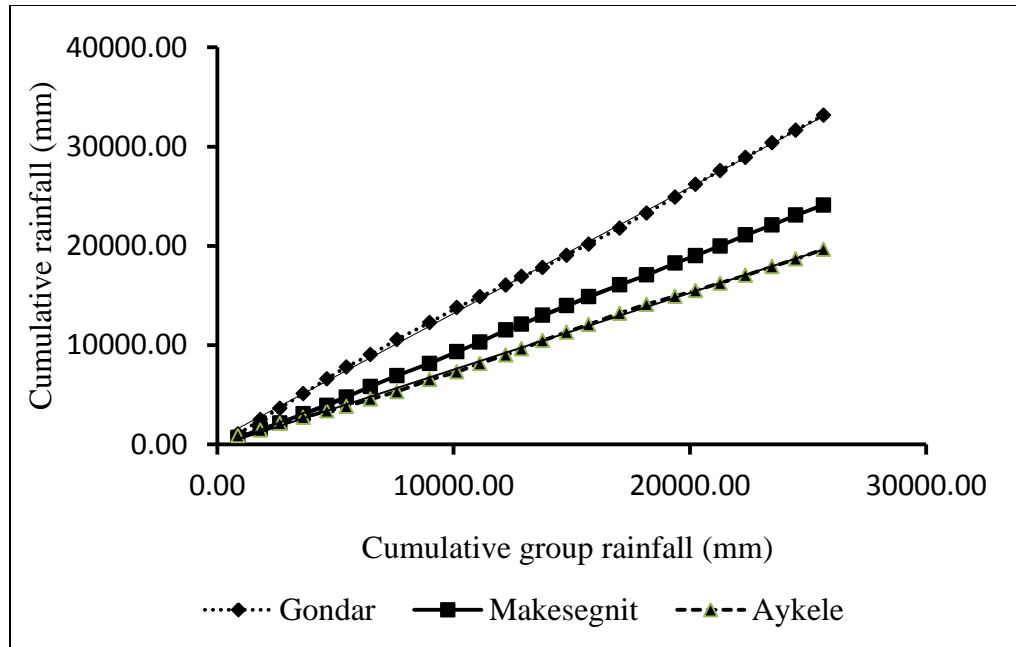


Figure 11. Double mass curve consistency checking of rainfall in the watershed

The above figure indicates the consistency of meteorological data for the stations.

3.5 Data availability

Until the beginning of the last decade, little was known about what data exist for with regards to Meteorological and hydrological, and what time periods they represent. Little was known about what may have been achieved in these areas for the desired periods of 1976-2005 to synchronize with the already cleaned data of pervious work. This time series data is essential for this research because for any useful comparison of conditions of the past and the future, a good presentation of the meteorological and hydrological data was needed. Initial assessment of the data archived by national agencies showed that continuous meteorological data for the watershed for 30 years periods was lacking quality and questionable with missing data. Available daily data from meteorological stations monitored solely by the metrological services of Makesegnit station needed some verification and quality checks. Meteorological data such as precipitation and temperature were collected from National meteorological service agency of Ethiopia (NMSE). These data have been used to correct the biases of RCP scenario output due to its limited spatial resolution using statistical downscaling method (liner scaling). Both

sediment yield and Discharge of the gauge station has been collected from Gondar research institute. This data was helpful to calibrate and validate the hydrologic model (PED-W) to simulate the future sediment yield.

3.6 Down scaling GCM of RCP Climate Scenario

The Representative Concentration Pathways (RCP) is the latest generation of scenarios that provide input to climate models. Scenarios have long been used by planners and decision makers to analyses situations in which outcomes are uncertain. There are 4 types of Representative concentration pathway emission scenarios but for this study only 2.6 and 8.5 RCP emission scenarios were selected. The baseline historical period (1976-2005) and the future time periods (2011-2100) emission scenario data was downloading from CORDEX Africa Climate Model Inter comparison Project Phase 5 (CMIP5) dataset ESGF Website (<http://www.csag.uct.ac.za/cordex-africa>).

Table 4. Available RCP grid point selected for study area

Grid point	Modeling group country	Atmospheric resolution
GP111222	Africa	0.44°
GP111223	Africa	0.44°
GP112222	Africa	0.44°
GP112223	Africa	0.44°

The RCP scenarios 2.6 and 8.5 are outlined in the (IPCC, 2013) fifth assessment report as part of twenties scenarios covering the total future emissions uncertainty. These scenarios have been employed in the CMIP5 CORDEX Africa to prepare CMIP5 multi-model datasets for future (Meehl et al., 2007). They represent “high” and “low” emission scenarios with regards to full range of emission forcing projected by the RCP scenarios. Future projections made regionally by RCP selected emission scenarios to analyze the uncertainty.

3.6.1 Grid points selection

The RCP grid point data have been classified based on their grid geographical location (Latitude and Longitude). Based on the watershed scale four grid point were down scaled from CORDEX Africa CMIP5 dataset that was shown from (table 4). Were one grid point emission scenario near to the observed station and best fit selected by evaluating their daily and monthly historical run with the observed meteorological station based on coefficient of determination (R^2) and overlaying the grid point to watershed station by ArcGIS 10.1? The selected data were bias corrected using linear scaling bias correction method to project the daily sediment yield in the watershed.

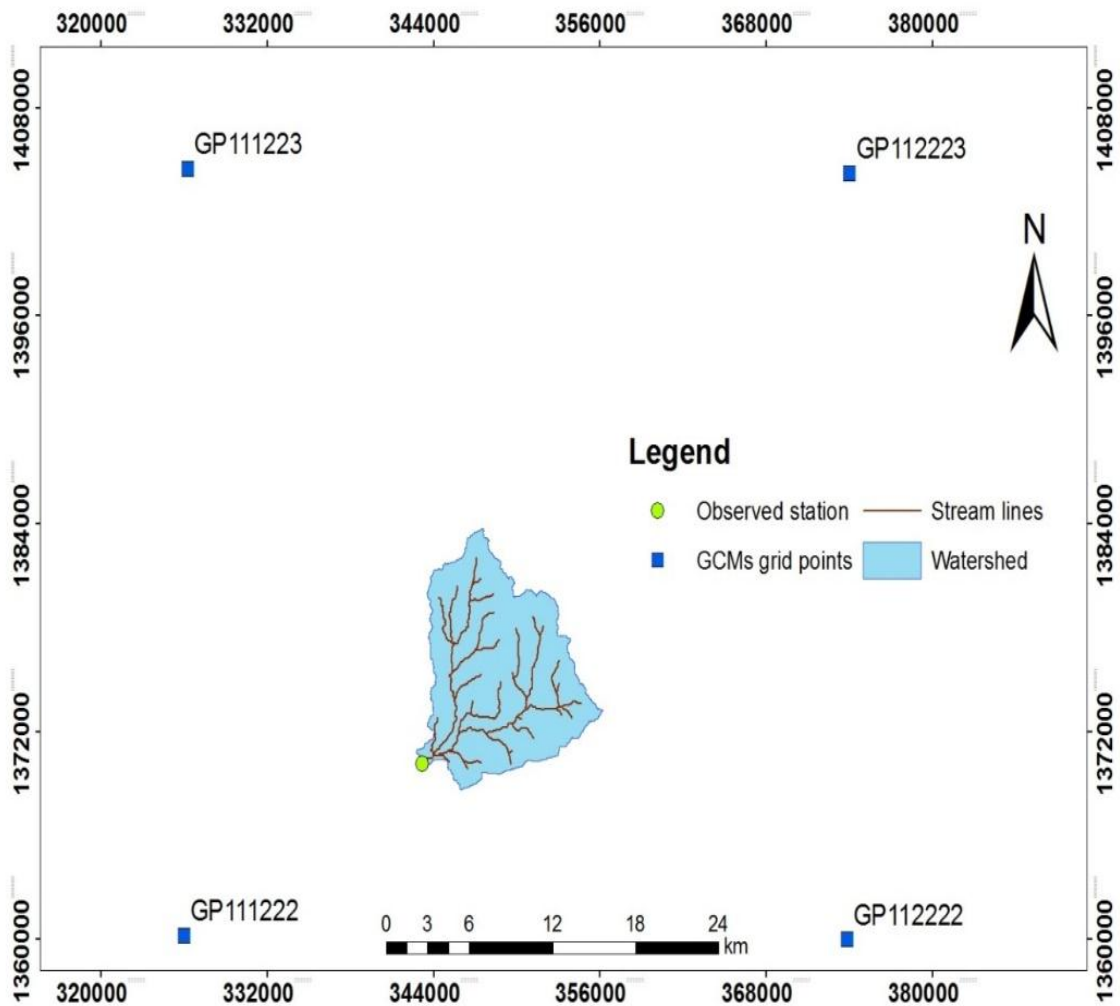


Figure 12. Grid point daily climate variable value representing and observed station

As shown from the figure 12 GP111222 grid point has near to the observed station and has good coefficient of determination (R^2). Hence GP 111222 was selected as predictor variable for station to perform biased correction in order to evaluate the potential impact of climate change on sediment yield.

3.6.2 Bias Correction

It is very often the process of downscaling data produces a fine resolution dataset that equivalent to the observed data, but has a slightly different distribution, mean or standard deviation. The reasons for some of these differences come from biases found in the GCMs used to produce the dataset. Removing or correcting these biases is useful in climate change studies because the purpose of the study was to evaluate changes in variability and spatial patterns of climate variables of interest (Johnson and Sharma, 2011). The precipitation and temperature outputs from the model data were bias corrected before doing the analyses. The bias correction procedure used in this study was quite simple, and aimed to readjust the model data to match the monthly mean and monthly standard deviation of the future period to baseline period. The Linear-scaling approach biased correction method of downscaling was used for this study. The selection of this method was based on its suitability for bias correction at daily basis of time scale. Observed data from 1976 to 2005 was calculated at daily mean basis. The future daily bias corrected temperature (T daily future) and daily precipitation (P future) time series was done by using equations 3.7 and 3.8 respectively. The estimation were performed on daily values (precipitation, maximum and minimum temperature) to produce a daily bias corrected dataset which could be compared to other climate datasets and could be analyzed using established hydrology techniques to detect trend.

$$P'_{GCM, fut} = P_{meas} * (\bar{P}_{GCM, fut} \div \bar{P}_{GCM, his}) \quad 3.7$$

$$T'_{GCM, fut} = T_{meas} + (\bar{T}_{GCM, fut} - \bar{T}_{GCM, his}) \quad 3.8$$

Where $P'_{GCM, fut}$ is precipitation for future global climate data, P_{meas} is precipitation for measured data, $\bar{P}_{GCM, fut}$ is mean precipitation for future global climate data $\bar{P}_{GCM, his}$ is

mean precipitation for historical global climate data, $T'_{GCM, fut}$ is mean temperature for future global climate data, T_{meas} is temperature for measured data $\bar{T}_{GCM, fut}$ is mean temperature for future global climate data and $\bar{T}_{GCM, his}$ is mean temperature for historical global climate data

3.7 Potential evapotranspiration

Potential evapotranspiration was a measure of the ability of the atmosphere to remove water from the surface through the processes of evaporation and transpiration. It is one parameter that use as an input for PED-W model to simulate the future discharge and sediment yield and it can be calculated using (enku and melese 2014).

$$ET_o = \frac{(T_{max})^n}{k} \quad 3.9$$

Where $K=48 * T_{mm}-330$ for combined wet and dry condition, $K=73 * T_{mm}-1015$ for dry seasons, and $K=38 * T_{mm}-63$ for wet season and T_{mm} ($^{\circ}C$) is the long term daily mean maximum temperature for the seasons under condition and $n=0.25$ mass constant

3.8 Trend test for meteorological data

Trend refer to any population characteristic changing in some predictable manner with another variable. Detecting and assessing temporal and spatial trends was important for many climate studies. Trend tests were generally important as a comparison measurement to monitoring the change of time series data over time alternative to prediction limits. For this study Mann (1945) and Kendall (1970) statistical trend test was used to assess whether a set of data values is increasing over time or decreasing over time, and whether the trend in either direction is statistically significant. Subsequent calculation of Kendall's Tau permits a comparison of the strength of correlation between two data series. Software used for performing the statistical Mann-Kendall test is Addinsoft's XLSTAT 2017. The null hypothesis is tested at 95% confidence level for precipitation, both maximum and minimum temperature.

3.9 PED-W water balance module

The water balance module in PED-WM is a semi-distributed module, capable of predicting discharge at a daily time step by considering saturation excess runoff (Moges et al., 2016). Within the module the watershed is divided into three zones: two surface runoff zones, the valley bottoms which become saturated during the main rainy season, and the degraded hillsides with a slowly permeable sub-horizon within 10-20 cm from the soil surface. The remaining part of the watershed are the hillsides where the rainwater infiltrates and either contributes to interflow (zero order reservoirs) or base flow (first order reservoir). The model computes the water balance (Eq.3.10) using Thornthwaite Mather (Steenhuis and Van der Molen, 1986) for defining the actual evapotranspiration. The water balance for each of the three zones can be written as”:

$$S_t = S_{t-\Delta t} + [P - AET - Q_{sf} - Perc]\Delta t \quad 3.10$$

Where S_t is the moisture storage (mm/day), $S_{t-\Delta t}$ is previous time step storage (mm/day), P is precipitation (mm/day), AET is actual evapotranspiration (mm/day), Q_{sf} is runoff from excess of saturation in zones 1 (periodically saturated bottom lands) and zone 2 (degraded hill sides), Δt is the time step which is one day in our application. Finally $Perc$ is percolation to the sub soil (mm/day) in permeable hillside (zone 3) and equals the sum of the interflow, Q_{sf} and the base flow, Q_{sf} . The model has nine main parameters including the area fraction (A) and the maximum storage capacity (S_{max}) for the three zones and three subsurface parameters: the half-life ($t_{1/2}$) to describe the exponential decay in time and maximum storage capacity (B_{Smax}) of the first order reservoir and the drainage time of the zero order reservoirs (τ^*) describing a linear decrease in time for the interflow. Detailed description about the model can be found from (Tilahun et al., 2013).

3.10 PED-W sediment module

The sediment module was developed by (Tilahun et al., 2013) and assumes that there are predominantly two runoff producing areas of saturated bottom slope and degraded areas of watershed. The sediment concentration from these two areas are transport limited during the beginning of the rainy period and source limited towards the end of

the rainy period. The module considers that sediment concentrations are decreasing for the same discharge throughout the rainy season. The sediment concentration in the runoff water C_s is found by using the calculated flow components from the water balance module (Eq.3.11) and assuming that only the surface runoff from degraded areas and the valey bottoms contain sediment. Sediment concentrations are transport limited after the fields are plowed and source limited at the end of the rain phase. The sediment module of PED-W model could be written as:

$$C_s = \frac{[(A_1 Q_1^{1.4} (a_{s1} + (a_{t1} - a_{s1}) M_s)) + A_2 Q_2^{1.4} (a_{s2} + (a_{t2} - a_{s2}) M_s)] + A_3 (Q_{bf} + Q_{if}) a_{t3}}{A_1 Q_1 + A_2 Q_2 + A_3 (Q_{bf} + Q_{if})} \quad 3.11$$

The sediment module has five parameters that require calibration. This includes transport limiting and source limiting factors for both the saturated and degraded areas and the maximum or threshold cumulative effective precipitation (P_T). The sediment concentrations in both the baseflow and the interflow can be assumed zero in small watersheds like the gumero watershed.

3.11 PED-W model calibration and validation

A sensitivity analysis was performed on the model to select the most sensitive parameters, out of the total of 9 input parameters that are included in PED-W, for calibration which was used for the sensitivity analysis of the parameters following the initial parameterization in the previous default model. The most sensitive parameters of the model have been selected by using manual calibration technique. Hence both the discharge and sediment model parameters were calibrated on daily basis for (2014-2015) and validated for (2016) days. The parameters were first determined by maximizing the efficiency criterion of the Nash–Sutcliffe efficiency coefficient (eq 3.13) then the coefficient of determination (R^2) (eq 3.12) and finally minimizing the Root Mean Square Error (RMSE) (eq 3.14). The initial values were based on the previous default model parameters by (Steenhuis et al, 2009). These initial values were changed systematically until the best goodness-of-fit was achieved between simulated and observed flows and sediment yield. In the sediment model, there were two calibration parameters for each of

the two surface runoff source areas A1 and A2 for transport limit a_t , in the beginning of the rainy phase, and source limit, a_s , in the end of the rainy phase.

$$R^2 = \frac{\left[\sum_{i=1}^n (q_{si} - \bar{q}_s)(q_{oi} - \bar{q}_o) \right]^2}{\sum_{i=1}^n (q_{si} - \bar{q}_s)^2 \sum_{i=1}^n (q_{oi} - \bar{q}_o)^2} \quad 3.12$$

$$NSE = 1 - \frac{\sum_{i=1}^n (q_{oi} - q_{si})^2}{\sum_{i=1}^n (q_{oi} - \bar{q}_o)^2} \quad 3.13$$

$$RMSE = \sqrt{\frac{\sum_{i=1}^n (q_{oi} - q_{si})^2}{\sum_{i=1}^n (q_{oi} - \bar{q}_o)^2 - 1}} \quad 3.14$$

3.12 Impact analysis

The impact of climate change on discharge and sediment yield of the catchment has also been evaluated. This assessment was really necessary to know the effect of climate change on discharge and sediment yield in the study area to the future time period of 2100 years based on baseline period. The biased correct future climate data downscaling from GCM based on watershed scale and observed baseline climate data apply into PED-W model to simulate the discharge and sediment yield. The observed baseline and future simulating discharge and sediment yield mean change difference, and trend data series were used to evaluate impact magnitude of climate change on sediment yield.

4 RESULT AND DISCUSSION

4.1 Climate change analysis

4.1.1 Baseline and observation data

In order to assess the implications of future climate changes on the environment, it was first necessary to have information about current or recent conditions as a reference point or baseline (Carter, 1999). The models generally had poor correlation for all observed variables (temperature and precipitation). For instance, the correlation for precipitation was 0.14 and 0.67 for daily and monthly basis respectively over the historical period of the emission scenario output of the watershed. The decision to bias correct the selected RCP data was made due to the significant differences in mean values.

Table 5. Grid point coefficient of correlation (R^2) without biases correction

		Daily		Monthly		
		Min	Max	Min	Max	
Grid point	Precipitation	temp	temp	Precipitation	temp	temp
Gp111222	0.14	0.13	0.33	0.67	0.39	0.55
Gp111223	0.13	0.13	0.32	0.68	0.38	0.41
Gp112222	0.1	0.14	0.27	0.67	0.41	0.32
Gp112223	0.11	0.13	0.27	0.68	0.4	0.33

The observed data indicated that mean annual precipitation over the basin was nearly 1120 mm/year, while the baseline GCM models output had varying spatial disagreements with observed value. The GCM of RCP 2.6 (low emission) and RCP 8.5 (high emission) scenario output baseline annual precipitations was 1865 mm/year. Their variation was due to spatial and temporal resolutions of observed data and relatively coarse GCM models cannot adequately capture this variability. Similarly the figure 13 below shows the variation of the GCM model output baseline data and future downscaled rainfall distribution data over the watershed. The reason behind the incompetence of the baseline rainfall data to the future was due to the spatial and temporal variation of socio-economic

impact of human activity to climate change. The baseline GCM model output data was based on previous time period socio-economic impact contribution to greenhouse gases of CO₂ emission to the atmosphere. However, the projected time period of GCM model output data was due to the future time period socio economic impact contribution to greenhouse gases of CO₂ emission to the atmosphere.

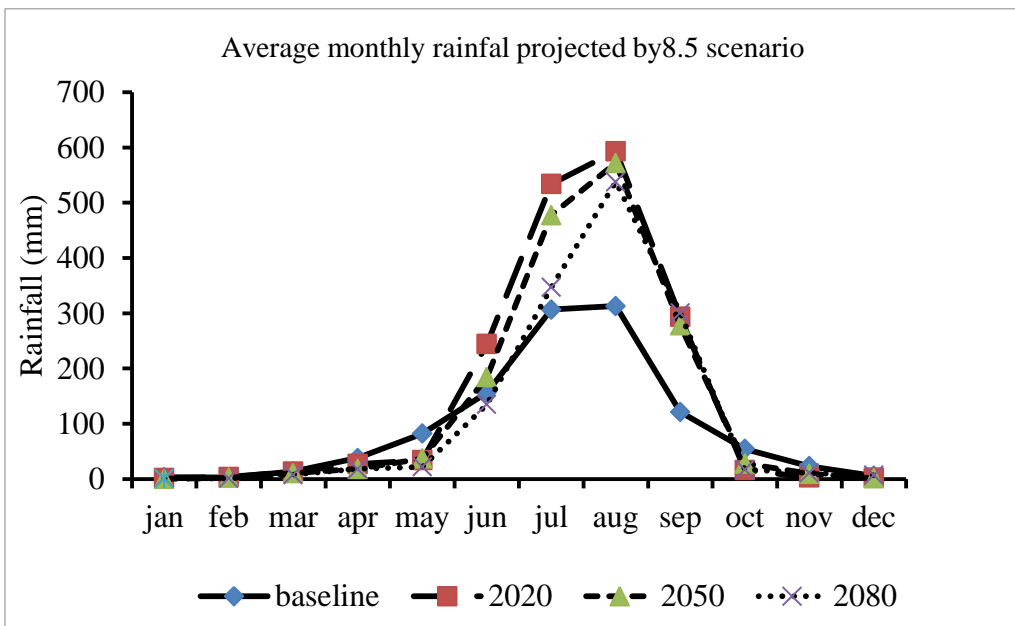
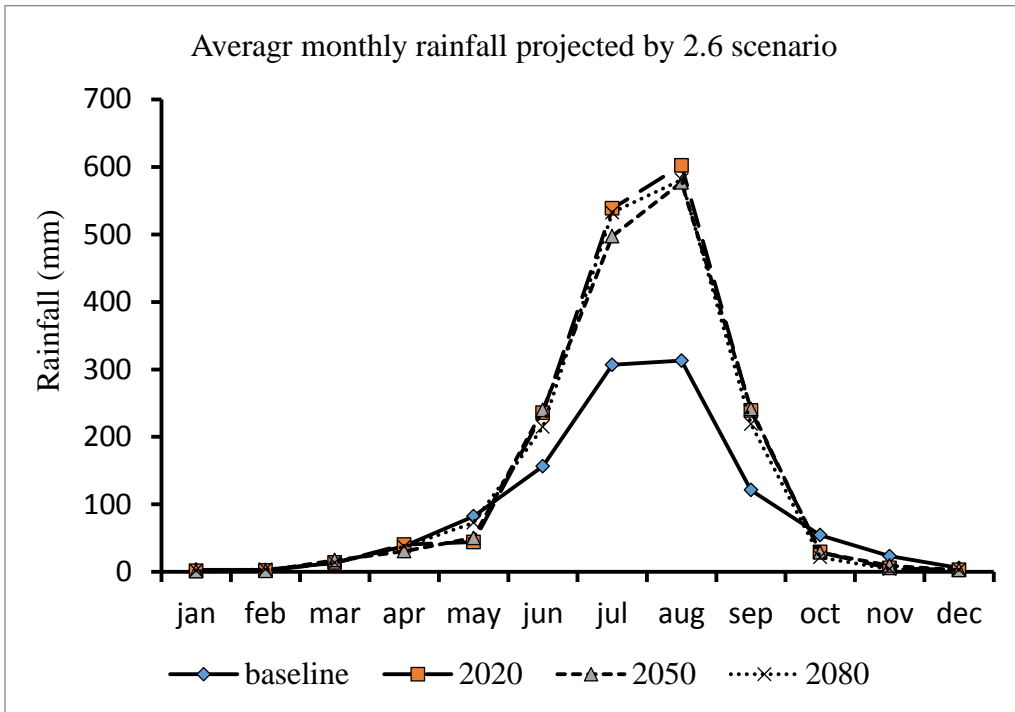
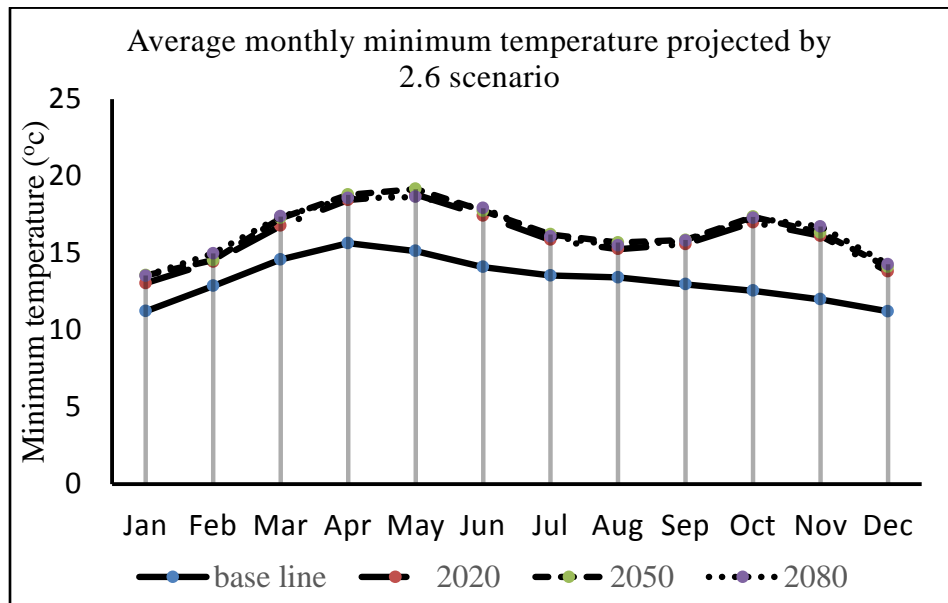
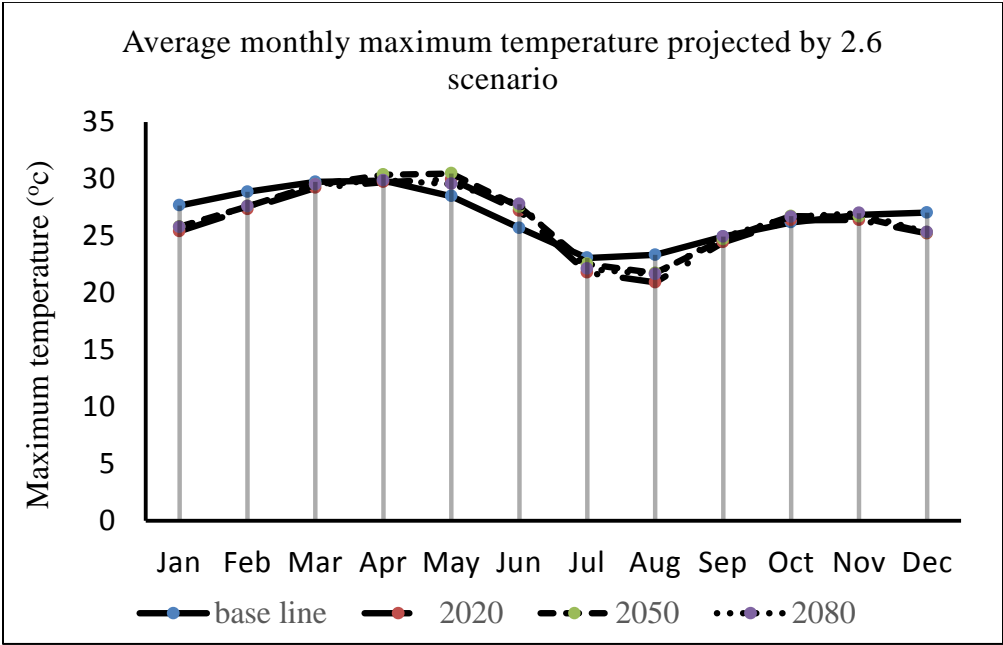
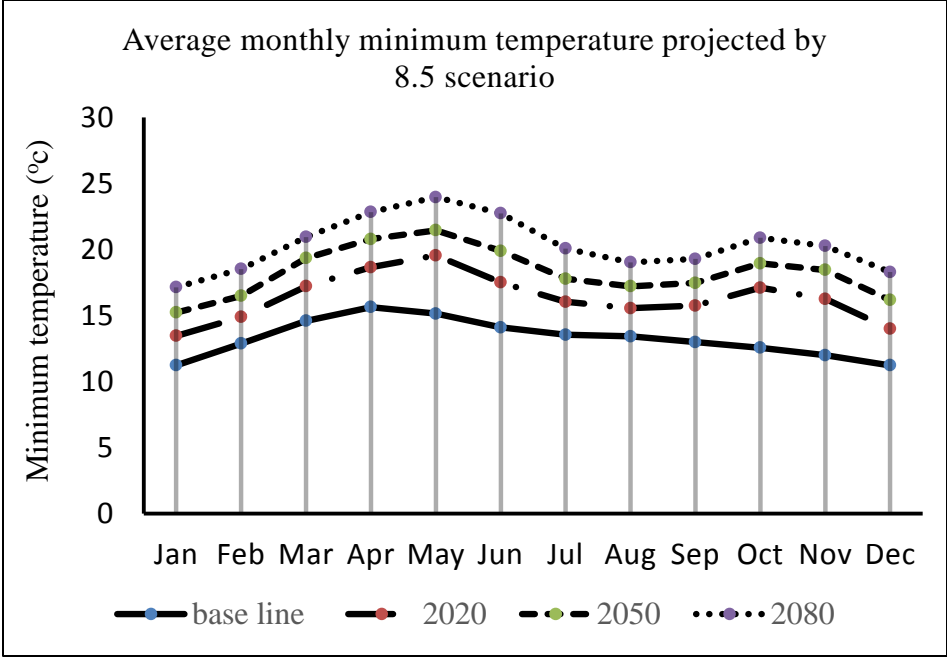


Figure 13. Projected average annual monthly rainfall distribution over 1970-2100 before biased correction

Like rainfall the observed maximum and minimum temperature data had poor correlations 0.13 and 0.55 daily and monthly respectively over the historical baseline period of GCM model output data of the watershed. The historical data records showed that average maximum and minimum temperature of 26.9°C and 13.3°C, while the baseline GCM models output maximum and minimum temperature had high variation from the observed annual mean maximum and minimum temperature. The GCM of RCP 2.6 (medium to low) and RCP 8.5 (high emission) output baseline annual mean maximum and minimum temperature was 25.7 and 14.9 °C respectively. Figures 14 below show the variations of GCM model output baseline data to future projected temperature distributions data over the watershed. The GCM model baseline output data show poor correlation with the observed data, however, a relatively simple bias correction was used to shift and adjust the data to correct the projected mean.





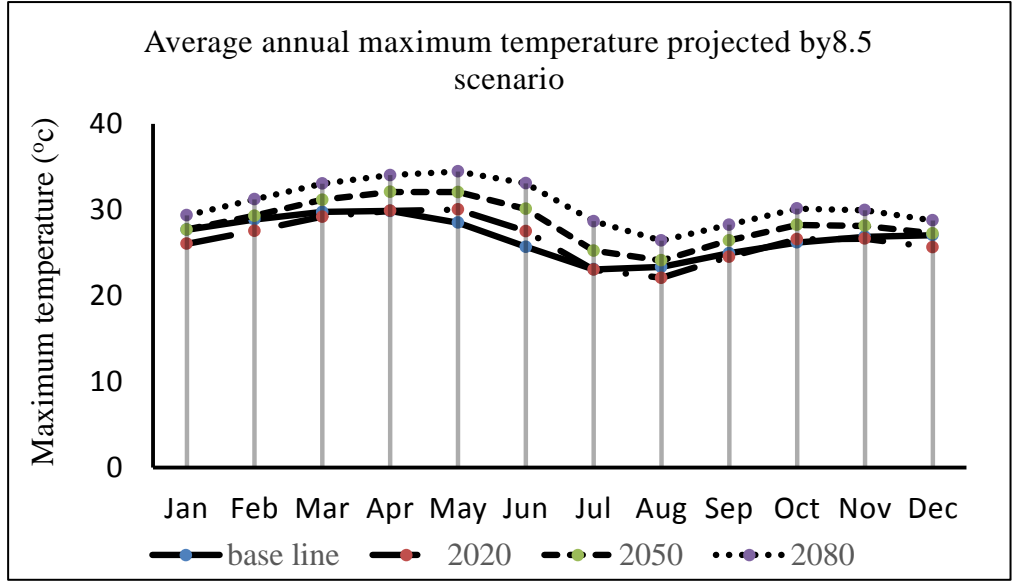


Figure 14. Projected average annual monthly maximum and minimum temperature distribution over 1970-2100 before biased correction

Generally, the historical baseline climate raw data with baseline observation has indicated large variations, as a result bias correction was needed.

4.2 Bias correction

As it can be seen in (figures 15, and 16) the bias corrected GCM model outputs of projected precipitation, maximum and minimum temperature result shows that better matched with the value and trend of the observed baseline data. After biases correction the projected mean annual participation, maximum and minimum temperature in RCP 2.6 emission scenario match acceptably with the observed mean annual precipitation, maximum and minimum temperature data than RCP 8.5 emission scenarios mean annual projected data. However, this variation was due to the doubling emission of CO₂ in RCP 8.5 (high emission) scenario than RCP 2.6 (low emission) scenario (IPCC, 2013).

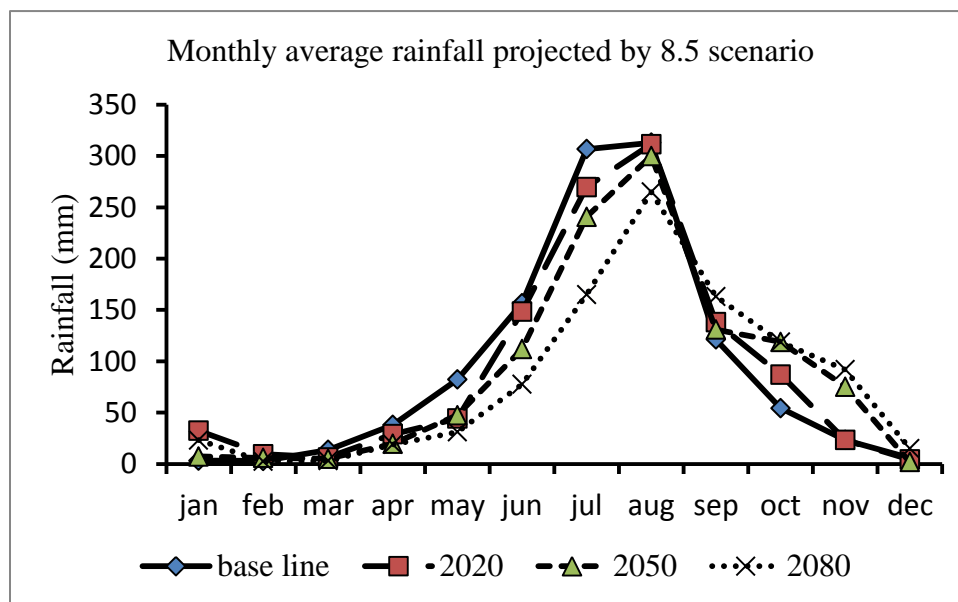
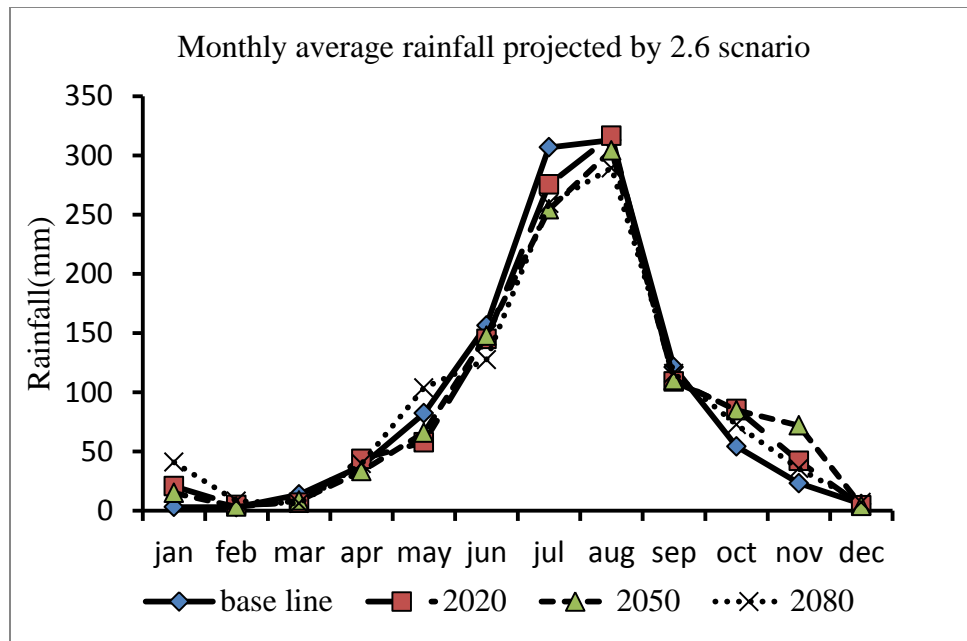
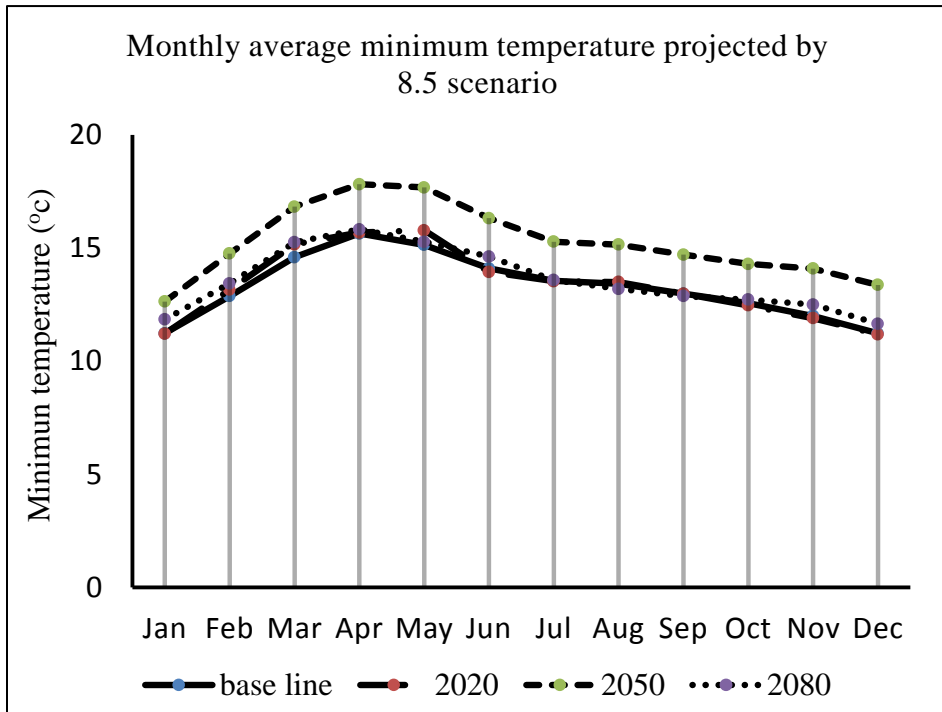
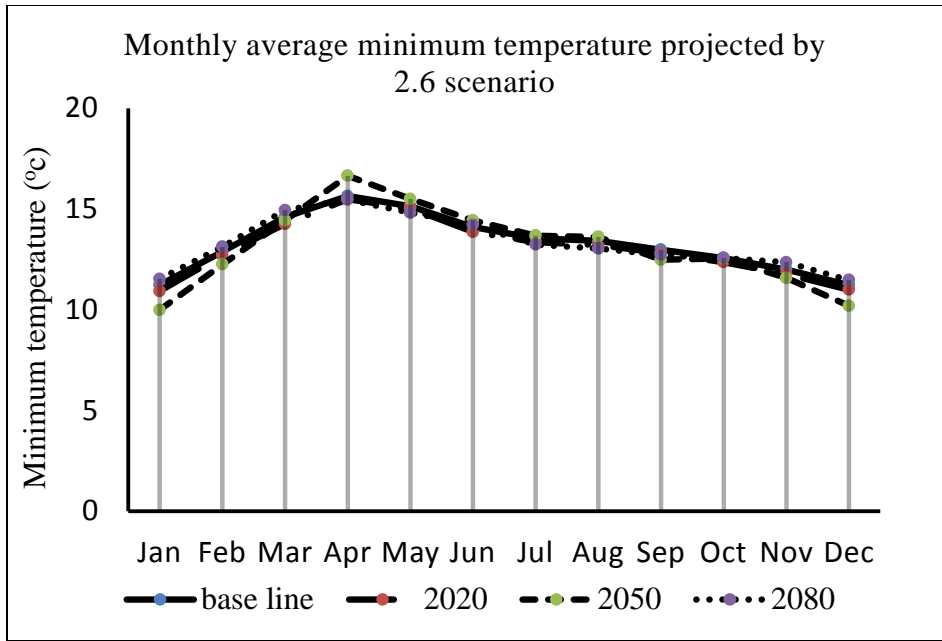


Figure 15. Projected average annual monthly rainfall distributions over 1970-2100 after biased correction



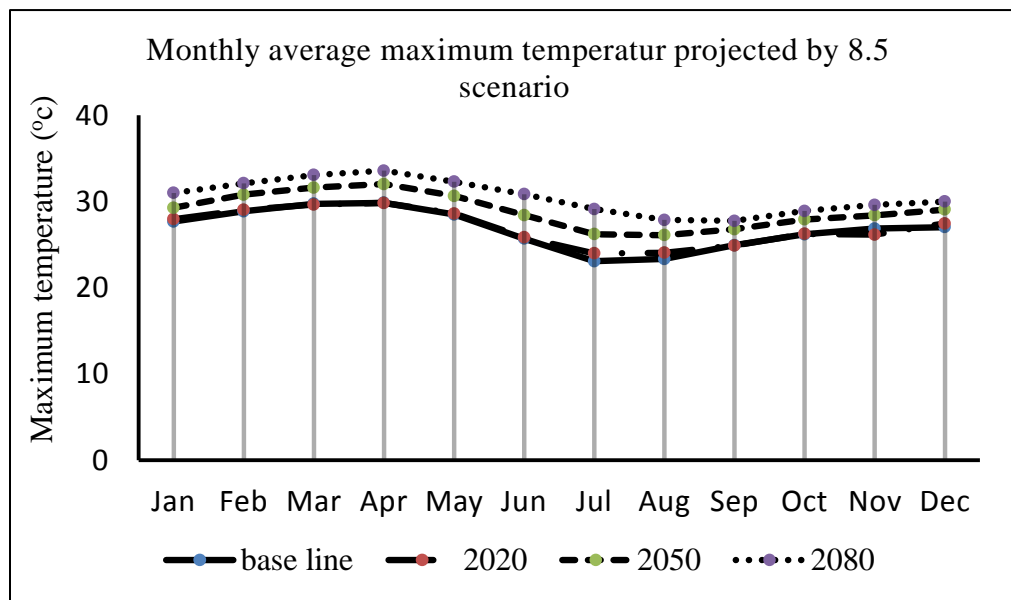
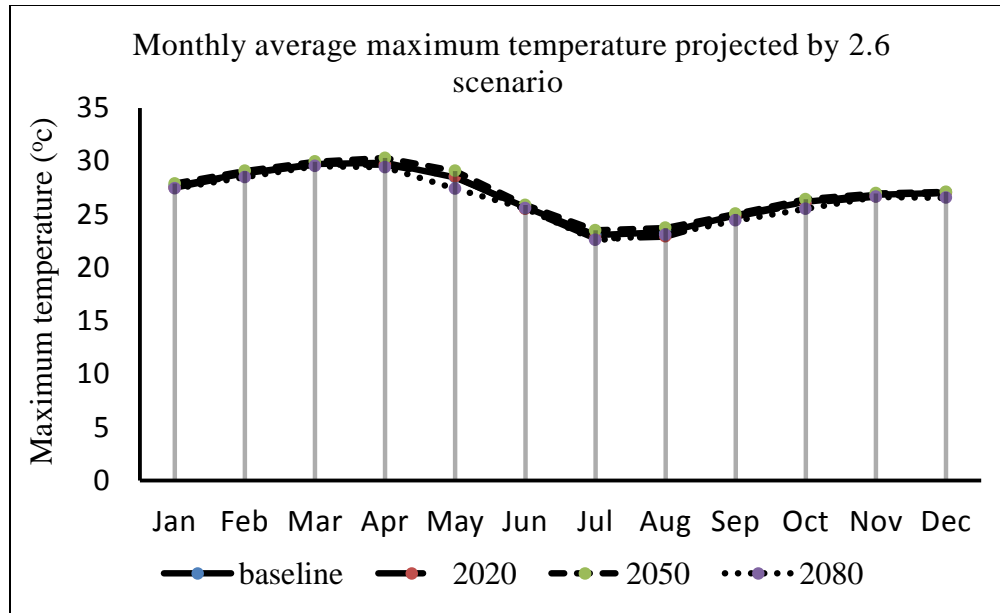


Figure 16. Projected average annual monthly maximum and minimum temperature distributions over 1970-2100 after biased correction

4.3 Trend Test of Climate data

4.3.1. Mean annual observed baseline rainfall trend analysis

The trend analysis of the observed baseline rainfall for Gumero watershed station from 1976-2005 year was evaluated by using Mann-Kendall trend test. This year was taken as

the observed baseline period which enables us to see the climate change value by comparing with the GCM model output baseline data year of 1976-2005. The historical datasets trends were also compared using the Mann-Kendall trend test statistic. The observed baseline and GCM output historical precipitation (figure 17 and figure 19) shows a slight decreasing trend over 1976-2005 and temperature (figure 18 and 20) shows a significant increasing trend over 1976-2005. The projected bias corrected GCM precipitation data (figure 21-23) also shows a decreasing trend and, the projected mean temperature data (figure 24-26) shows increasing trend.

Table 6. Annual observed baseline average rainfall statistics for Mann -Kendall trend test

Parameter	Baseline
Kendall's Tau	-0.205
S	-122
alpha	0.05
Var(S)	4957.33
p-value (two tailed test)	0.086

Based on the above result and interpretation, the average annual rainfall has shown the decreasing trend with in the past 30 years (1976-2005).

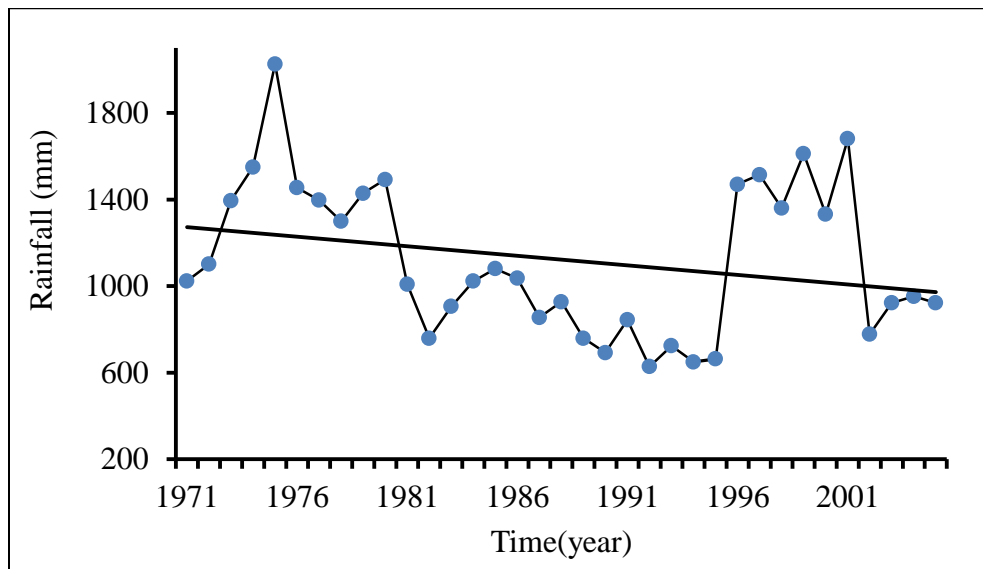


Figure 17. Mann-Kendall trend test of observed baseline average annual rainfall of the watershed

Figure 17 indicates the observed annual rainfall at the earlier time period was to seem an increasing trend but decrease in the late near time period. This indicates the change in rainfall over the past 30 years

4.3.2 Mean annual observed baseline temperature trend analysis

The trend of mean annual temperature for (1976-2005) years of data has been evaluated by Mann-Kendall trend test.

Table 7. Mean annual observed baseline temperature statistics for Mann Kendall trend test

Parameter	Baseline
Kendall's Tau	0.388
S	231
alpha	0.05
Var(S)	0
p-value (two tailed test)	0.001

Based on the above result and interpretation, the average annual temperature has shown increasing trend with in the past 30 years (1976-2005).

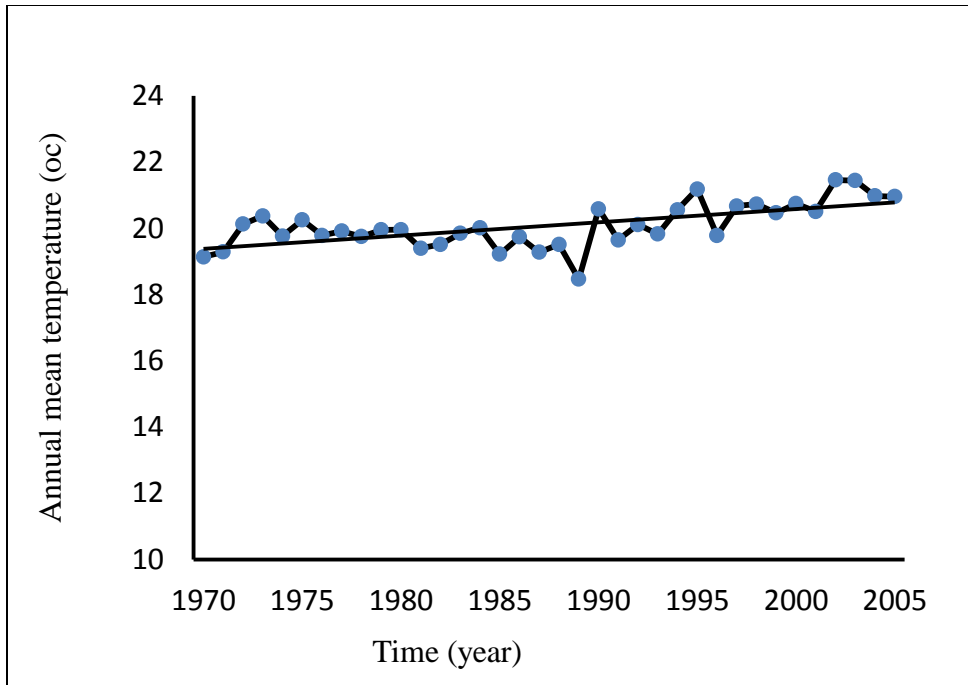


Figure 18. Mann-Kendall trend test of observed annual mean temperature for the watershed

Figure 18 above shows the observed average annual mean temperature at the earlier time period was indicated a decrease trend but increase in the late near time period. This shows there was significant change in temperature over the past 30 years in the watershed and it shows both temperature and rain fall indirect relation in change with time.

4.3.3 Mean annual baseline rainfall trend analysis

Downscaled the projected RCP scenario baseline rainfall data (1976-2005) time periods was analyzed by Mann-Kendall trend test. Figure 19 below indicates there no clear trend to the baseline rainfall for 30 time periods indicated insignificant variations.

Table 8. Mean annual baseline rain fall statistics for Mann Kendall trend test

Parameter	Baseline
Kendall's Tau	-0.039
S	-23

alpha	0.05
Var(S)	0
p-value (two tailed test)	0.757

Based on the above result and interpretation, the average annual rainfall has shown the decreasing trend with in the past 30 years (1976-2005).

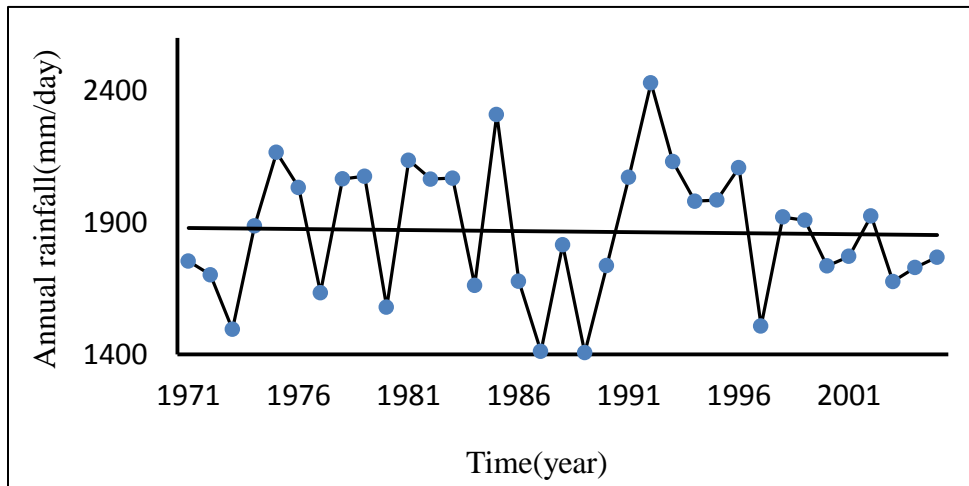


Figure 19 . Mann-Kendall Trend test of baseline precipitation for the watershed.

4.3.4 Mean annual baseline temperature trend analysis

Downscaled the projected RCP scenario baseline mean temperature data (1976-2005) time periods was analyzed by Mann-Kendall trend test. Figure 20 below indicates the baseline average annual mean temperature was indicated a significant increasing trend for 30 time period of the study area.

Table 9. Average annual baseline temperature statistics for Mann- Kendall trend test

Parameter	Baseline
Kendall's Tau	0.328
S	195.0
alpha	0.05
Var(S)	0
p-value (two tailed test)	0.005

The values of the above parameters indicate that the baseline average annual mean temperature for 30 time period of the study area shows an increasing trend (1976-2005).

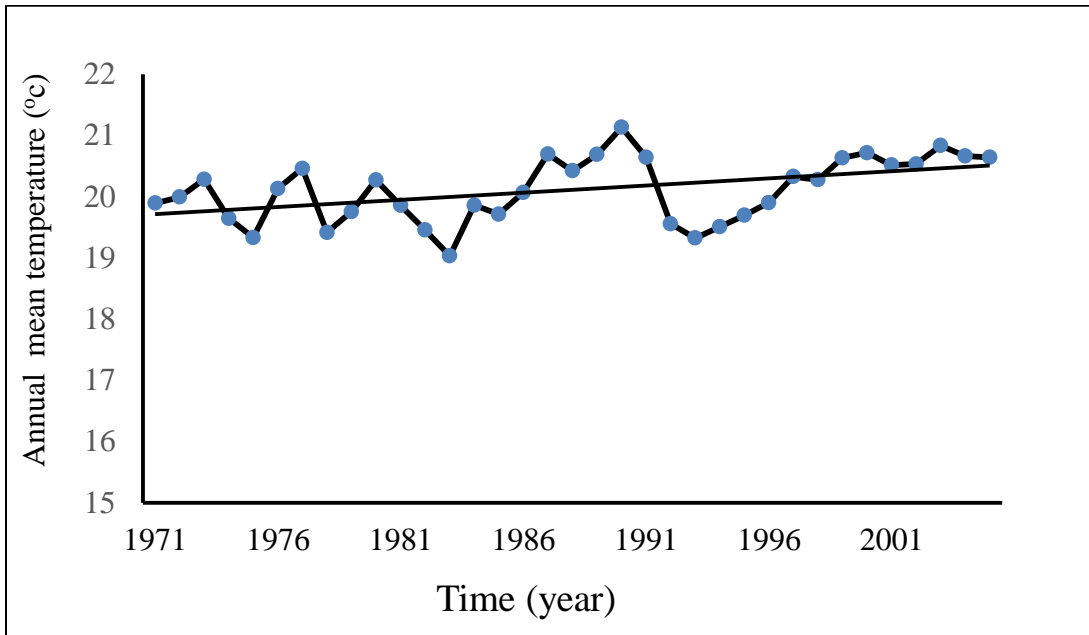


Figure 20. Mann-Kendall Trend test of baseline average annual mean temperature for the watershed

4.3.5 Mean annual projected rainfall trend analysis

Downscaled the projected RCP scenario average annual rainfall data of 2020s ,2050s and 2080s time periods trends was analyzed by Mann-Kendall test.

Table 10. 2020s average annual rainfall Mann-Kendall trend test value

Parameter	2.6	8.5
Kendall's Tau	-0.194	-0.032
S	-122	-20
alpha	0.05	0.05
Var(S)	0.1	0.797
p-value (two tailed test)	44	0

Based on Mann-Kendall interpretation, the values of the above statistical parameters indicated that the average annual rainfall of 2020s (2011-2040) future time period of the study area shows a decreasing trend.

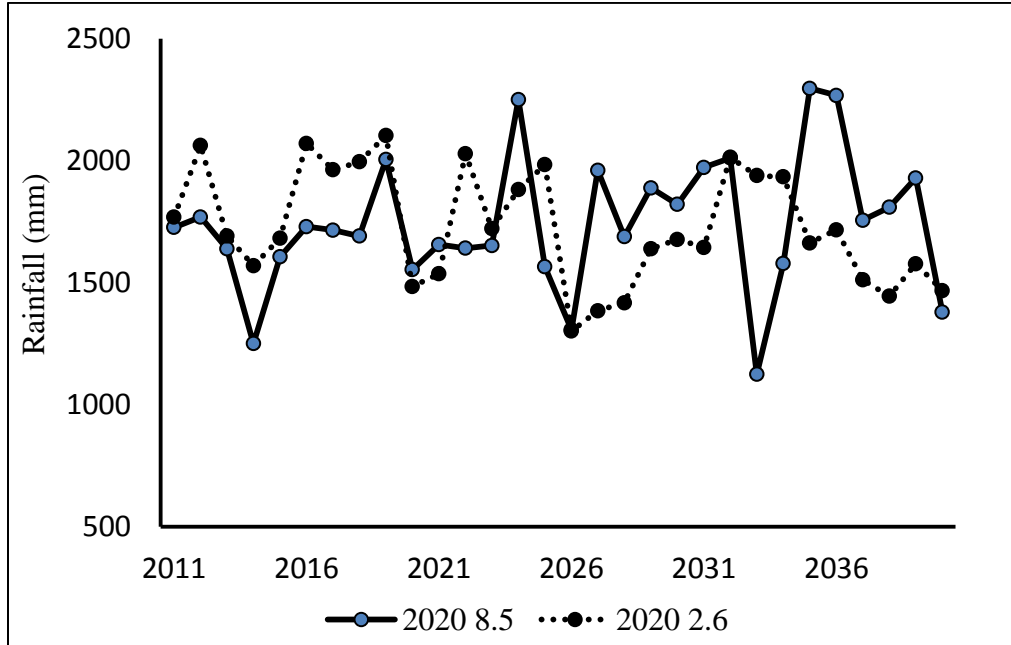


Figure 21. Mann-Kendall Trend test of projected average annual precipitation of the watershed for 2020s (2011-2040).

Based on Mann-Kendall interpretation, the figure 21 above shows that the average annual rainfall of the study area indicated a decreasing trend under both RCP scenarios for 2020s future time period.

Table 11. 2050s average annual rainfall Mann-Kendall trend test value

Parameter	2.6	8.5
Kendall's Tau	-0.016	-0.121
S	-10	-76
alpha	0.05	0.05
Var(S)	44	0
p-value (two tailed test)	0.903	0.31

Based on Mann-Kendall interpretation, the values of the above statistical parameters indicated that the average annual rainfall of 2050s (2041-2070) future time period of the study area shows a decreasing trend.

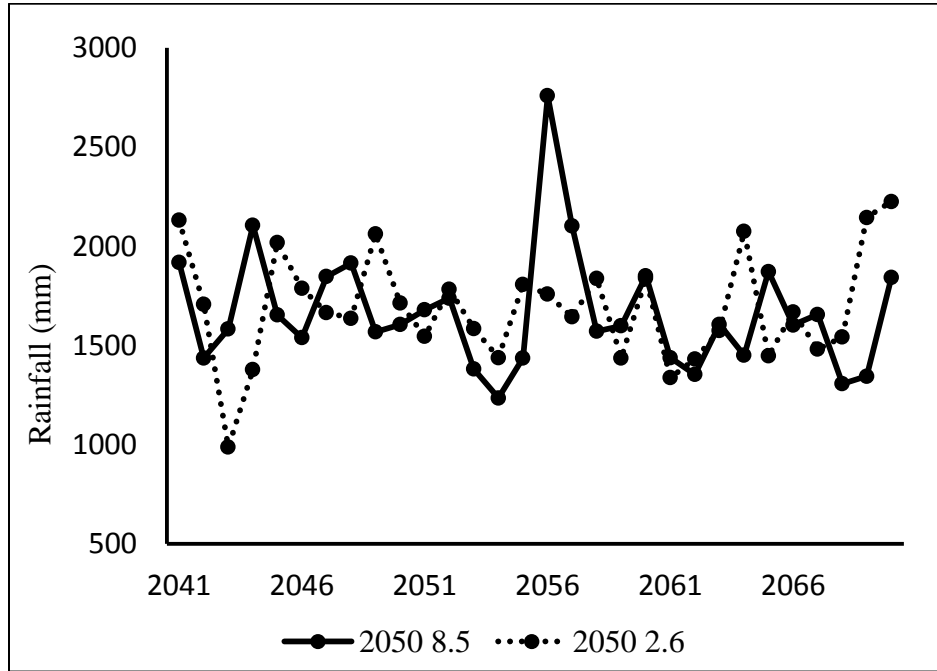


Figure 22. Mann-Kendall trend test of projected average annual precipitation of the watershed for 2050s (2041-2070)

Based on Mann-Kendall interpretation, the figure 22 above shows that the future average annual rainfall of the study area indicated a decreased trend under both RCP scenarios for 2050 future time period.

Table 12. 2080s average annual rainfall Mann-Kendall trend test value

Parameter	2.6	8.5
Kendall's Tau	-0.123	-0.059
S	-31	-15
Alpha	0.05	0.05
Var(S)	0	0
p-value (two tailed test)	0.434	0.715

Based on Mann-Kendall interpretation, the values of the above statistical parameters indicated that the average annual rainfall of 2080s (2071-2100) future time period of the study area shows a decreasing trend.

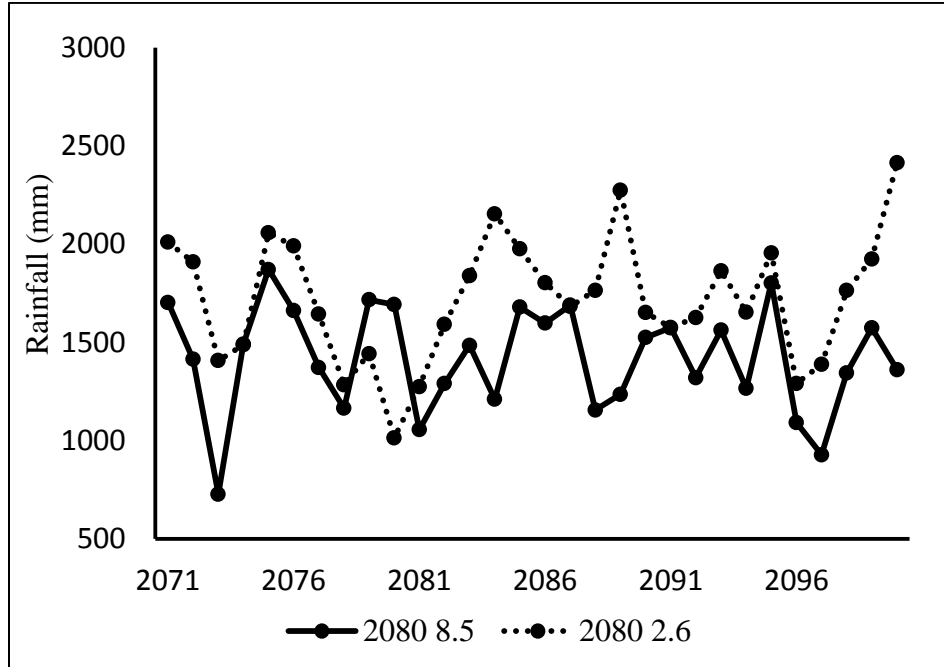


Figure 23. Mann-Kendall trend test of projected average annual precipitation of the watershed for 2080s (2071-2100)

Based on Mann-Kendall interpretation, the figure 23 above shows that the future rainfall of the study area indicates a decreased trend under both RCP scenarios for 2080 future time period.

4.3.6 Mean annual projected temperature trend analysis

Downscaled the projected RCP scenario mean temperature data of 2020s, 2050s and 2080s time periods trend was analyzed by Mann-Kendall test.

Table 13. 2020s average annual mean temperature Mann-Kendall trend test value

Parameter	2.6	8.5
Kendall's tau	0.333	0.500
S'	4.000	6.000
Var(S')	14.000	24.000
p-value (Two-tailed)	0.423	0.307
alpha	0.05	0.05

Based on Mann-Kendall interpretation, the values of the above parameters indicate that the average annual mean temperature of 2020s (2011-2040) future time period of the study area shows an increasing trend.

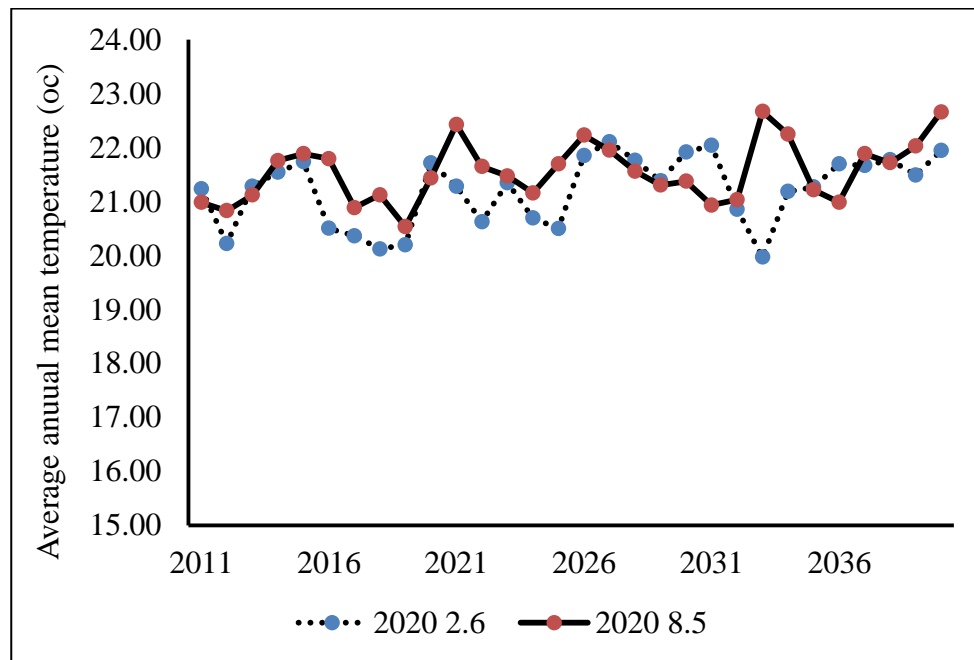


Figure 24. Mann-Kendall Trends test of projected mean annual temperature for the watershed (2011-2040)

Based on Mann-Kendall interpretation, the figure 24 above shows that the future average annual mean temperature of the study area indicated an increasing trend under both scenarios for 2020s future time period.

Table 14. 2050s average annual mean temperature Mann-Kendall trend test value

Parameter	2.6	8.5
Kendall's tau	0.333	0.833
S'	4.000	10.000
Var(S')	12.000	12.000
p-value (Two-tailed)	0.386	0.009
alpha	0.05	0.05

Based on Mann-Kendall interpretation, the values of the above parameters indicate that the average annual mean temperature of 2050s (2041-2070) future time period of the study area shows an increasing trend.

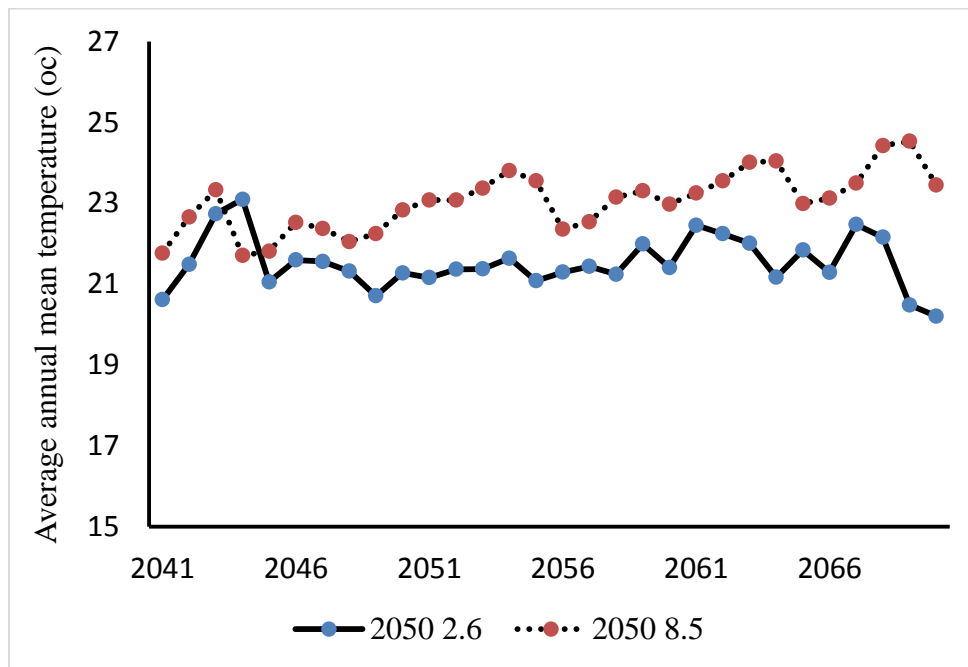


Figure 25. Mann-Kendall Trends test of projected mean annual temperature for the watershed (2041-2070)

Based on Mann-Kendall interpretation, the figure 25 above shows that the future average annual mean temperature of the study area indicated an increasing trend under both scenario for 2050s future time period.

Table 15. 2080s average annual mean temperature Mann-Kendall trend test value

Parameter	2.6	8.5
Kendall's tau	0.667	0.833
S'	8.000	10.000
Var(S')	12.000	12.000
p-value (Two-tailed)	0.043	0.009
alpha	0.05	0.05

Based on Mann-Kendall interpretation, the values of the above parameters indicate that the average annual mean temperature of 2080s (2070-2100) future time period of the study area shows an increasing trend.

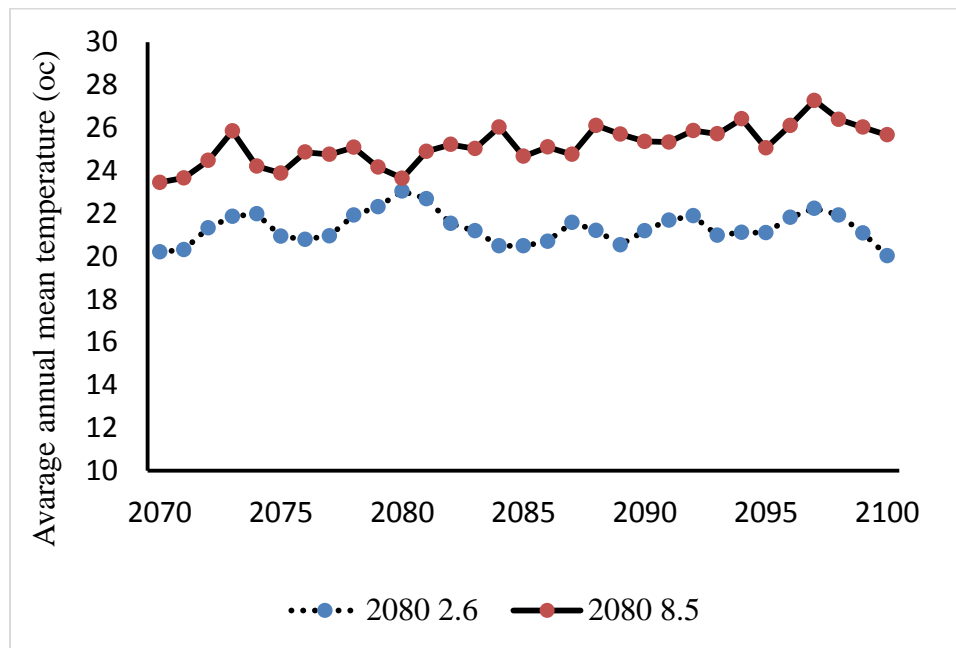


Figure 26. Mann-Kendall Trends test of projected mean annual temperature for the watershed (2071-2100)

Based on Mann-Kendall interpretation, the figure 26 above shows that the future average annual mean temperature of the study area indicated an increasing trend under both scenario for 2080s future time period. Consequently, variations in precipitation amounts would change flows more in all seasons. Another important finding from this research is

that temperature increases will have a greatly different impact on sediment yield depending upon season of the year. The timing of temperature increases with season of the year, as predicted by RCP emission scenario, will greatly influence the predicted sediment yield response on watershed. In addition an increasing temperature would result high evapotranspiration in the watershed it affecting water availability. Overall, climate change affected both flow and erosion rates. Precipitation increases would cause high flows in streams, while temperature increases caused bigger reductions in low flows. Because low flows and high flows commonly occur in summer and winter seasons, respectively.

4.4 PED-W model simulation

4.4.1 Sensitivity analysis

Model parameter Sensitivity analysis was carried out manually by increasing or decreasing each parameter by 10 % while others were kept constant. The watershed model performances were evaluated using common model efficiency measuring criteria, i.e. the Nash-Sutcliff efficiency, NSE (Nash and Sutcliff, 1970).

Table 16. Water balance module sensitive parameter (NSE) value

10%	-50	-40	-30	-20	-10	0	10	20	30	40	50	Rank
As	0.71	0.71	0.71	0.71	0.71	0.71	0.71	0.70	0.70	0.70	0.70	4
Smax s	0.71	0.71	0.71	0.71	0.71	0.71	0.71	0.71	0.71	0.71	0.71	5
Ad	0.71	0.71	0.71	0.71	0.71	0.71	0.71	0.71	0.71	0.71	0.71	5
Ah	0.49	0.56	0.62	0.67	0.69	0.71	0.71	0.7	0.63	0.53	0.4	1
Bsmax	0.68	0.73	0.71	0.71	0.71	0.71	0.71	0.71	0.71	0.71	0.71	3
t1/2	0.71	0.71	0.71	0.71	0.71	0.71	0.71	0.71	0.71	0.71	0.71	5
t*	0.71	0.71	0.71	0.71	0.71	0.71	0.71	0.71	0.71	0.71	0.71	5
Smax d	0.71	0.71	0.71	0.71	0.71	0.71	0.71	0.71	0.71	0.71	0.71	5
Smax,h	0.59	0.62	0.65	0.67	0.69	0.71	0.71	0.72	0.72	0.71	0.7	2

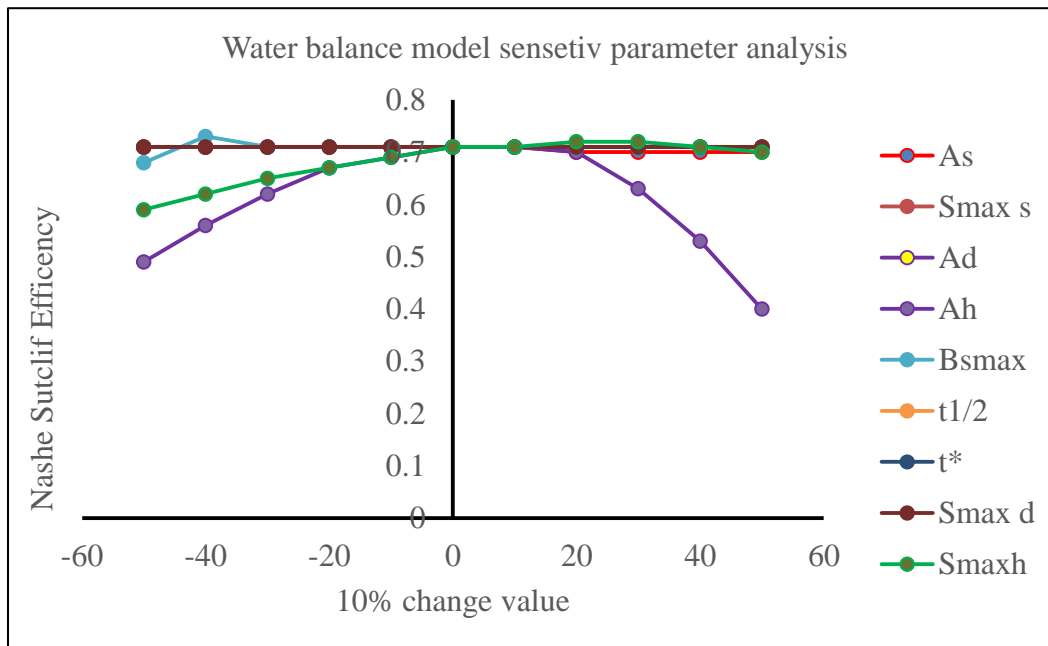


Figure 27. Water balance module sensitivity analysis Nash Sutcliffe Efficiency value

The water balance module sensitivity parameters analysis was done manually. The parameter having high Nash Sutcliffe Efficiency (NSE) variation was the most sensitive parameter and would take as first rank of sensitivity (figure 27, and table 16). Which indicate any value change on this parameter would was most significantly affecting the dynamics of flow compared with other parameters. Based on the analysis the most sensitive parameter was hill-side areal coverage (Ah), maximum storage capacity of hillside area coverage (Smax, h), saturated areal coverage (As) and maximum storage for base flow of the study watershed (Bsmax). The representative sensitive parameters identified in this study was similar with the research previously done in suitability of watershed models to predict distributed hydrologic response in the Awramba watershed in Lake Tana basin ,Ethiopia (Moges et al .,2016).

Table 17. Sediment module sensitive parameter analysis Nash Sutcliff Efficiency value

10%	-50	-40	-30	-20	-10	0	10	20	30	40	50	Rank
Saturated a_t	0.48	0.52	0.54	0.56	0.56	0.56	0.55	0.52	0.49	0.45	0.4	2
Degraded a_t	0.56	0.56	0.56	0.56	0.56	0.56	0.56	0.56	0.56	0.56	0.56	3
PT	0.25	0.36	0.45	0.51	0.56	0.56	0.56	0.56	0.55	0.54	0.53	1
Saturated a_s	0.56	0.56	0.56	0.56	0.56	0.56	0.56	0.56	0.56	0.56	0.56	3
Degraded a_s	0.56	0.56	0.56	0.56	0.56	0.56	0.56	0.56	0.56	0.56	0.56	3

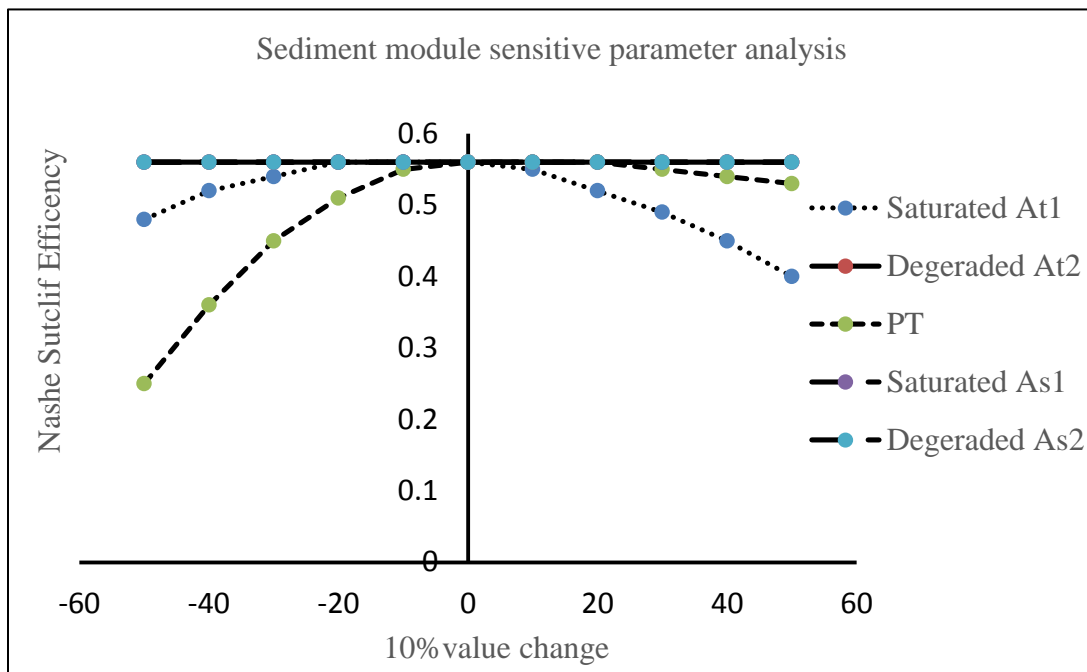


Figure 28 . Sediment module sensitivity analysis Nash Sutcliffe Efficiency

Like water balance PED-W module the sediment module was analysis the sensitivity parameter manually. The parameter having high NSE variation was the most sensitive parameter and would take as first rank of sensitivity (figure 28 and table 17). Which indicate any value change on this parameter would was most significantly affecting the dynamics of sediment yield in the watershed compared with other parameters. Based on the sensitivity analysis for the study watershed the most sensitive parameter was

cumulative effective precipitation and saturated areal coverage in the begging of monsoon time period. The result also indicated PED-WM (Tilahun et al., 2013).

4.4.2 PED –W Model calibration

The comparison between the observed and simulated discharge and sediment yield indicated a good agreement between the observed and simulated. Their agreement was verified by using the values of coefficient of determination (R^2), Nash Sutcliffe efficiency (NSE) and rot mean square error (RMSE) as shown below table 18 and the figure (31 and 32) shows there good agreements .

Table 18. Model calibration Statistical value

Water balance module of PED-W model			
Model performance statistics		Daily	Monthly
	R2	0.71	0.91
	NSE	0.71	0.92
	RMSE	0.54	0.28
Sediment module of PED-W model			
	R2	0.55	0.94
	NSE	0.56	0.83
	RMSE	0.66	0.41

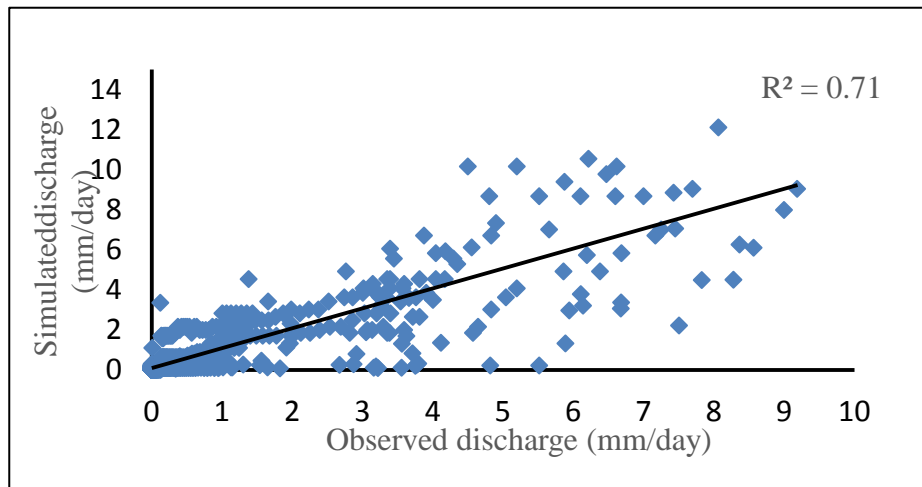


Figure 29. Coefficient of correlation (R^2) of Gumero daily discharge during calibration period (2014-2015)

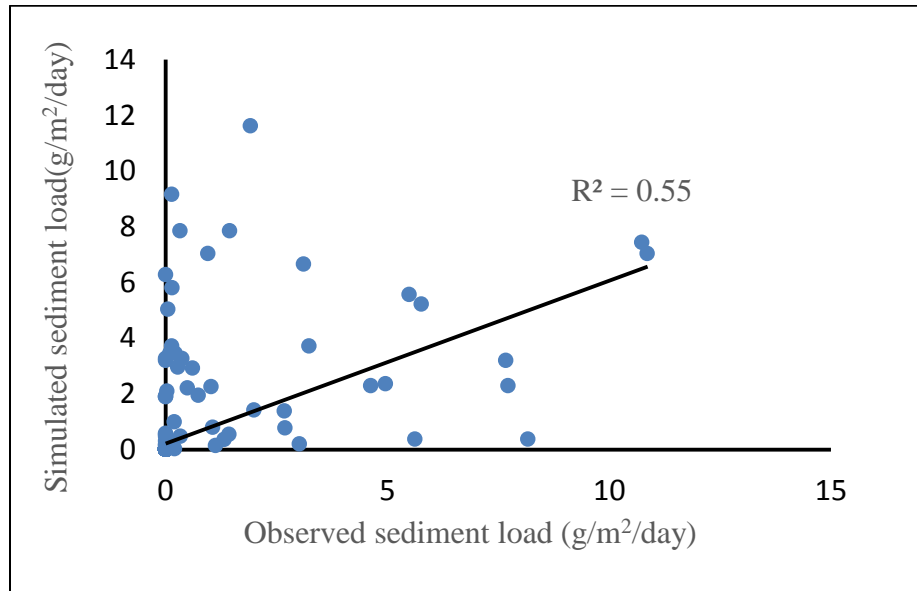


Figure 30. Coefficient of correlation (R^2) of Gumero daily sediment yield during calibration period (2014-2015).

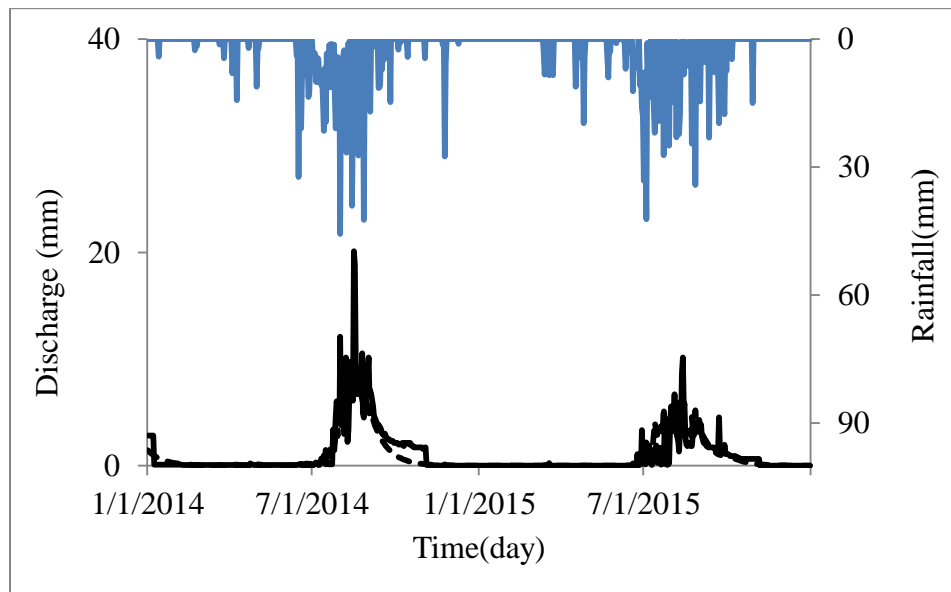


Figure 31. The daily predicted (dash line) and observed (solid line) discharge of Gumero during calibration period (2014-2015)

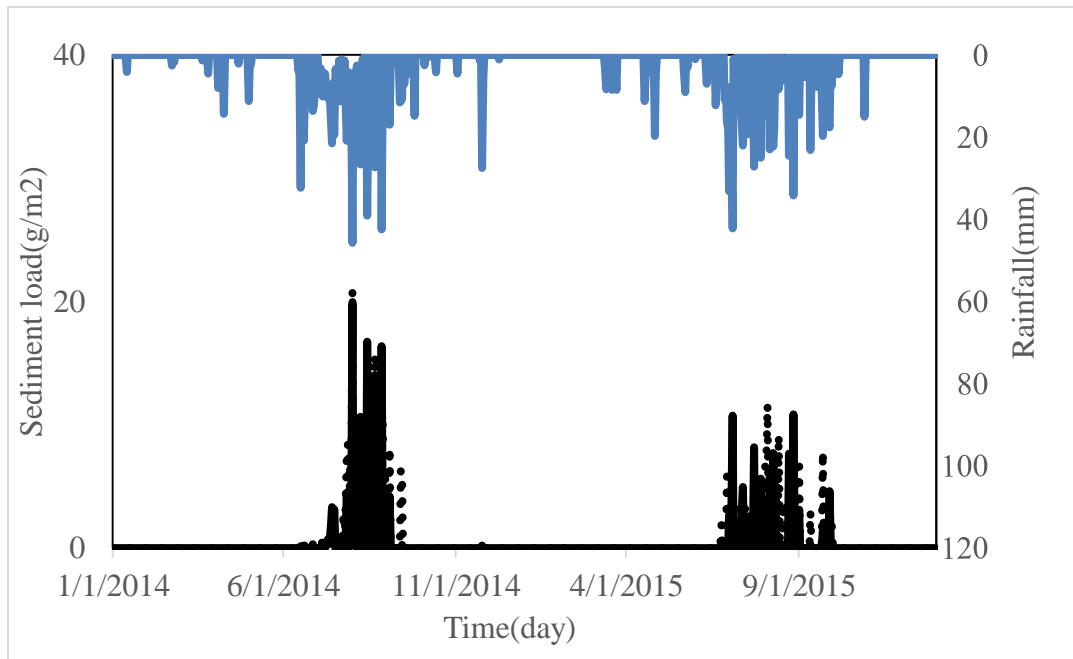


Figure 32. The daily predicted (solid line) and observed (dash line) sediment yield of Gumero during calibration period (2014-2015)

Table 19. Calibrated models parameters in Gumero watershed

No	Parameter	Description of the parameter	Optimum value
1	Ah	Portion of hillside area (%)	94
2	$S_{max,s}$	Maximum soil water storage(mm) in As	73
3	T^*	Interflow(days)	6
4	B_{smax}	Maximum storage for base flow(mm) linear reservoir	210
5	Ad	Portion of degraded area (%)	1
6	As	Portion of saturated area (%)	4.5

7	$t_{1/2}$	Base flow half life time(days)	12
8	$S_{max,d}$	Maximum soil water storage in Ad	15
9	$S_{max,h}$	Maximum soil water storage(mm) in Ah	150

In PED-W model parameters optimized value showed that direct runoff at the outlet originated from saturated area (constituting 4.5 % of the watershed) and degraded slopes (1.0%). In the remaining part of the watershed the rain infiltrated contributing to inter flow (zero order reservoirs) and base flow (first order reservoirs) (Table 19) .This study parameter optimized value rang seam consistent with other range of previous studies of PED-WM (Moges et al., 2016).

4.4.3 PED –W Model validation

The values of the objective functions have not showed significant difference when they were compared with the efficiency values in calibration. The model (PED-W) efficiency in validation process had also been determined by R^2 , NSE and RMSE. Based on the result the model had been showing its consistency with those optimized values of parameters on the study area. These parameter values are representative for Gumero watershed. The agreement of simulated against observed flow of the catchment was illustrated under table 20 and figure 34. Due to the scarcity of data validation was carried out for water balance model.

Table 20. Model validation statistical value

Water balance module PED-W model			
Model performance statistics	Daily	Monthly	
R^2	0.70	0.87	
NSE	0.69	0.78	
RMSE	4.66	0.1	

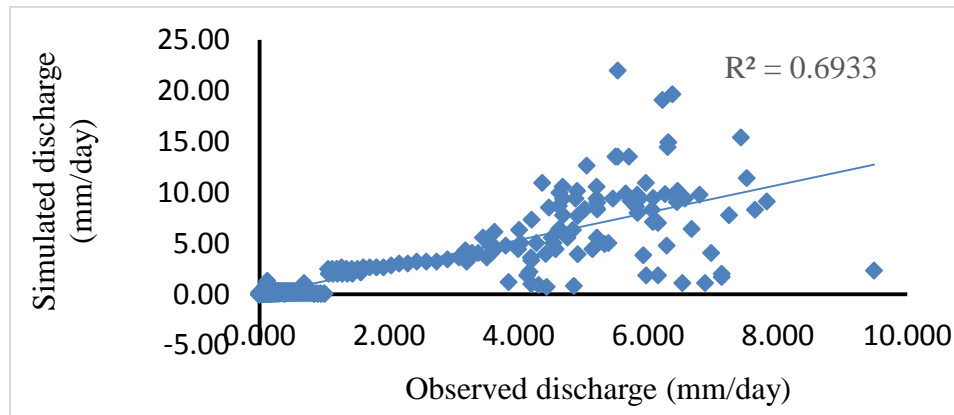


Figure 33. Coefficient of correlation (R^2) of Gумero daily discharge during validation period (2016).

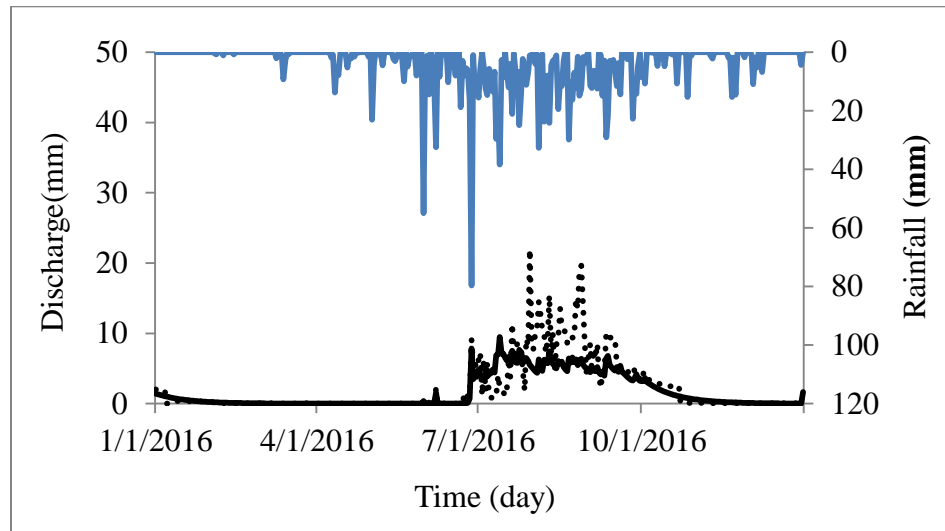


Figure 34. The daily predicted (solid line) and observed (dash line) discharge of Gумero during validation period (2016)

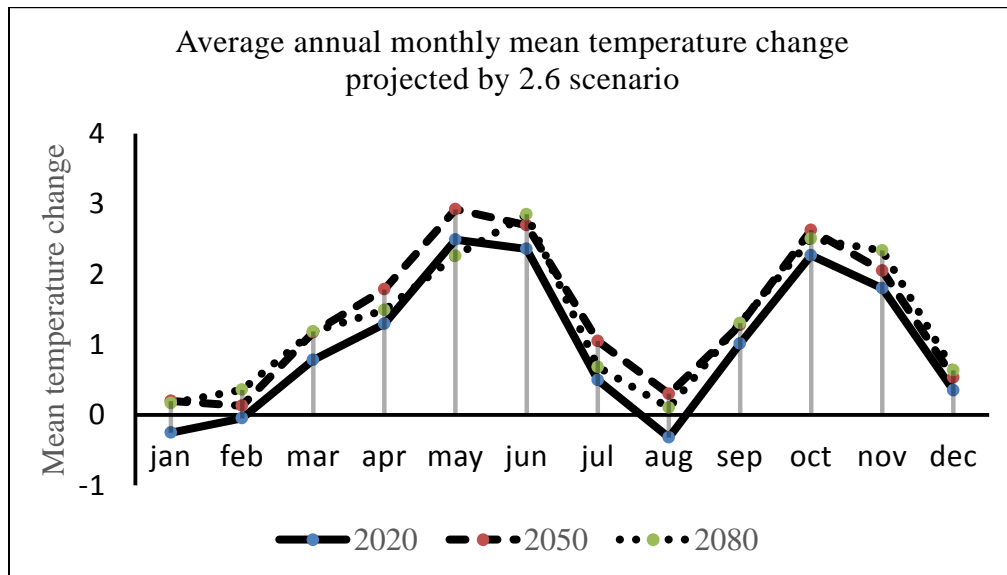
Overall during calibration and validation periods, respectively (Figure 31, 32 and 34, Table 18 & 20) model performance at daily and monthly time step showed that similar results within the range of previous studies of PED-WM (Tilahun et al., 2013)

4.7 Changes in future meteorological variables

The graphical comparison between observed average long term mean monthly precipitation, and mean temperature with corresponding simulations indicated the result of the downscaled biased corrected projected data replicated the basic pattern of observations in (figures 35, 36) below. The RCP emissions scenarios output was downscaled into watershed scale with a daily time step to force on precipitation and temperature changes in winter (DJF) and summer (JJA), as these are the main rainy and dry season of the watershed.

4.7.1. Projected downscaled average mean temperature change

The projected average temperature generally shows an increasing trend in the watershed for three future time period of the two emission scenarios when compared to baseline temperature. But these projections vary by magnitude depending on the scenario.



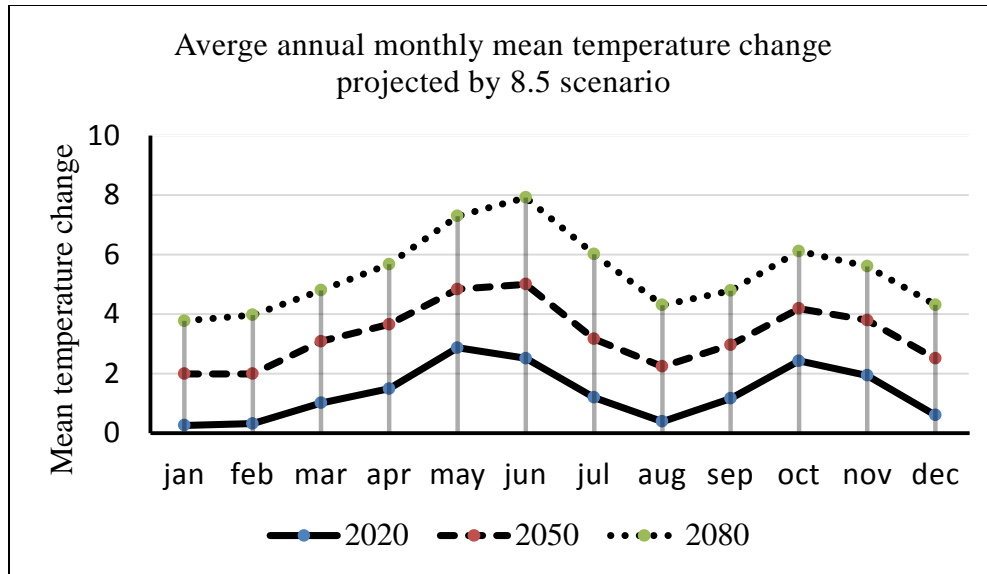


Figure 35. Projected average annual monthly mean temperature change difference

The mean temperature scenario showed that there would be an increasing trend in average mean annual temperature for three future time period of the 2020s, 2050s and 2080s under both emission scenarios when compare to baseline period and also compare to each scenario time period 2080 show increasing trend than 2020s and 2050s time period under 8.5 scenario but under 2.6 scenario 2050s future time period show more increment than 2020s and 2080s future time period. For those scenarios the average mean annual temperature shows clear slight increasing trends for dry season of (December - February) under 8.5 scenario but decreasing under 2.6 scenario and high increment (march-may) and (September - November) and decreasing trend in rainy season of (Jun - August) months of the year for three future time periods of 2020s 2050s and 2080s under both emission scenarios.

Table 21. Average annual mean temperature change difference in (%)

RCP	Average annual mean temperature (°c)			change in temperature (%)			
	Base line	2020	2050	2080	2020	2050	2080
2.6	20.09116	21.02728	21.59533	21.37055	+4.65%	+7.48%	+6.36%
8.5	20.09116	21.44123	23.37532	25.47054	+6.71%	+16.34%	+26.77%

This investigation of average mean annual temperature projections indicate that warming will continue in the watershed through the intermediate and late 21st century to a level of (+4.65% to 26.77%). The estimated result of projected average mean annual temperature would changes from 2006 to 2100 is +1.4 to +5.8°C according to scenarios developed by the (IPCC, 2007).It is also constant with Upper Blue Nile River Basin results indicate average mean annual temperature increase from a range of 1.4°C to 2.6 °C with a change of 2.3°C from the weighted average scenario (Kim and Kalurachchi, 2009). Yates and Strzepek (1998a) used 3 GCMs and the result revealed that the change in temperature range from 2.2°C to 3.5°C. Yates and Strzepek (1998b) also used 6 GCMs and the result showed that mean annual future temperature increased from 2.2°C to 3.7 °C. Generally the ensemble mean of all models showed that similar change in the mean annual future temperature increase between 2°C and 5°C. This study result sown that similar to those of authors means that under RCP 2.6 emission scenario, +0.94°C, +1.51 °C and +1.28°C of shows average mean temperature increment for future three time period of 2020s, 2050s and 2080s respectively and under RCP 8.5emission scenario +1.34°C, +3.28°C, and +5.37°C of shows average mean temperature increment for future three time period 2020s, 2050s, and 2080s respectively. In this study the average mean annual temperature maximum change increasing +5.37°C (26.77%) under 8.5 emission scenario of 2080s future time period and average mean annual minimum temperature change increasing +0.94°C (4.65%) under 2.6 emission scenario of 2020s future time period (table21). For the study watershed area the projected average mean annual temperature increasing with relative to the baseline average mean annual temperature for two scenarios of three future time periods (figure 35). As predictable, Scenario 8.5 is relatively warmer than Scenario 2.6. The reason is related to the level of radiation emission forcing, the higher GHG emission scenario has large effect on climate than the lowest GHG emission scenario.

4.7.2. Projected downscaled average precipitation change

Precipitation projections generally show a deceasing trend in the watershed for future time period of the two emission scenarios when compared to baseline rainfall. But these

projections vary by magnitude depending on the scenario, unlike the projections for temperature.

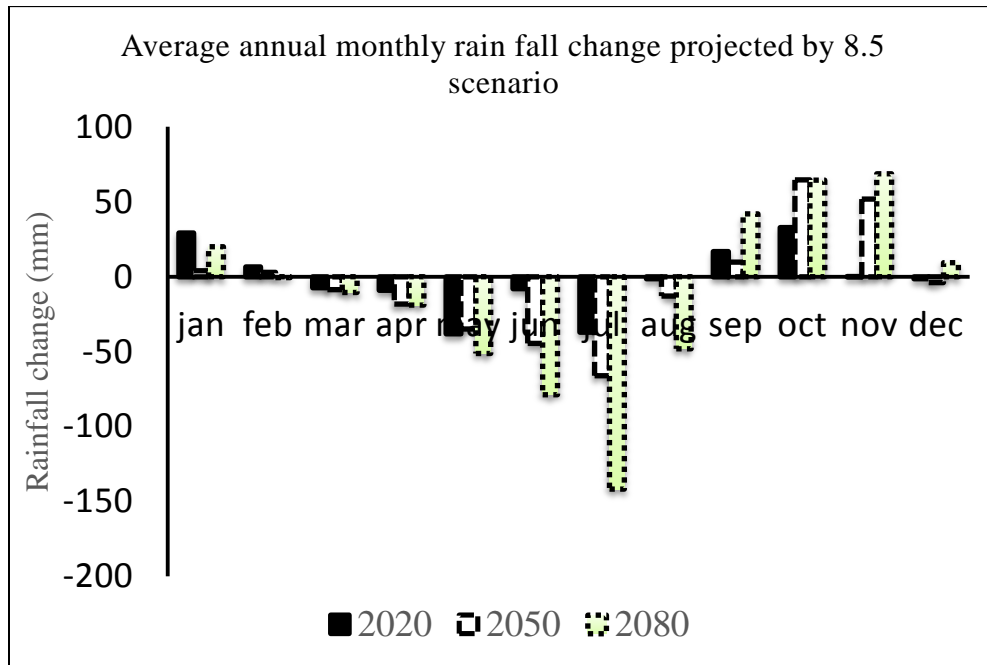
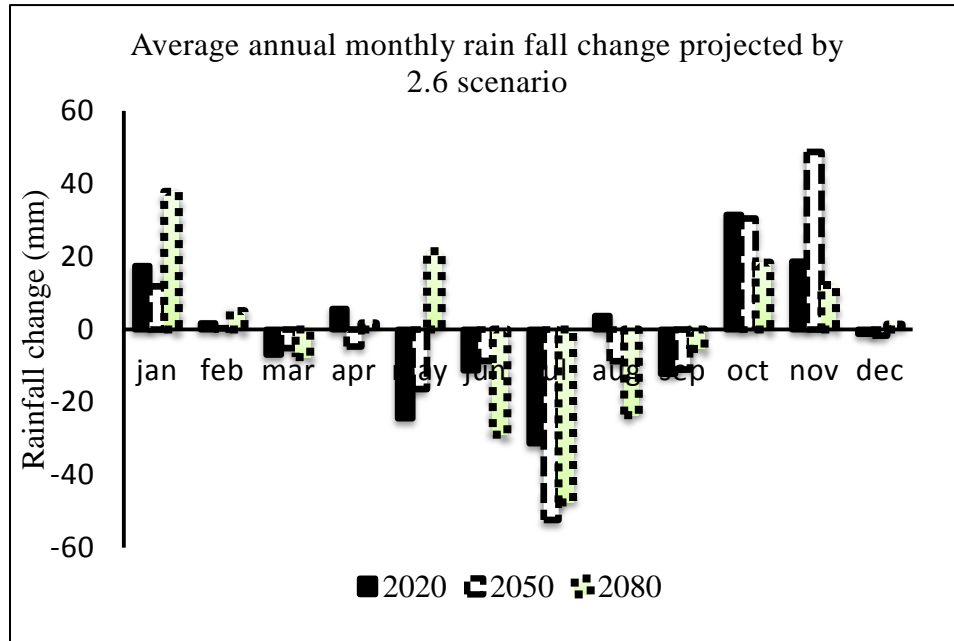


Figure 36. Projected average annual monthly rainfall change difference

The figure above show that relative change in average annual precipitation at watershed stations. The average precipitation in the watershed will decrease under both scenarios

for future time period. The simulation projected an average change in precipitation of -0.75%, -1.52% and -1.32% in the 2020s, 2050s and 2080s future time period respectively under 2.6 emission scenario. For the watershed similarly, an average change in precipitation -1.52%, -4.98% and -12.9% under 8.5 emission scenarios in the 2020s, 2050s and 2080s future time period respectively will be observed at the watershed. Both scenarios show similar decreasing trend in projected average precipitation. The predicted average precipitation at station is likely to decrease during rainy season of (Jun - July) in 2020s, 2050s and 2080 future time period but increase during August in 2020s and decrease in 2050s, and 2080s for future time period under 2.6 emission scenario and decrease during rainy season of (Jun-August) under 8.5 emission scenarios of 2020s, 2050s and 2080s future time period respectively. The average precipitation will show more decrease trend during September under 2.6 emission scenarios than 8.5 emission scenario for all future time period. On the other hand, predicted average precipitation will increase during (October-November) under both emission scenarios of 2020s, 2050s and 2080s future time period respectively. Similarly, under both emission scenarios the average precipitation is expected to decrease during the dry season of December for all future time period and will increase during dry season of (January - February) and (March and May) for all future time period. Similarly, in April under 8.5 emission scenario the average precipitation will increase for all future time period but under 2.6 emission scenario the average precipitation will increase for 2020s and 2080s and decrease for 2050 future time period. In this study average annual precipitation maximum will decrease to (145.46 mm/year) -12.9% under 8.5 scenario for 2080s future time period and minimum decreasing to (8.36 mm/year) -0.75% under 2.6 scenarios of 2020s future time period.

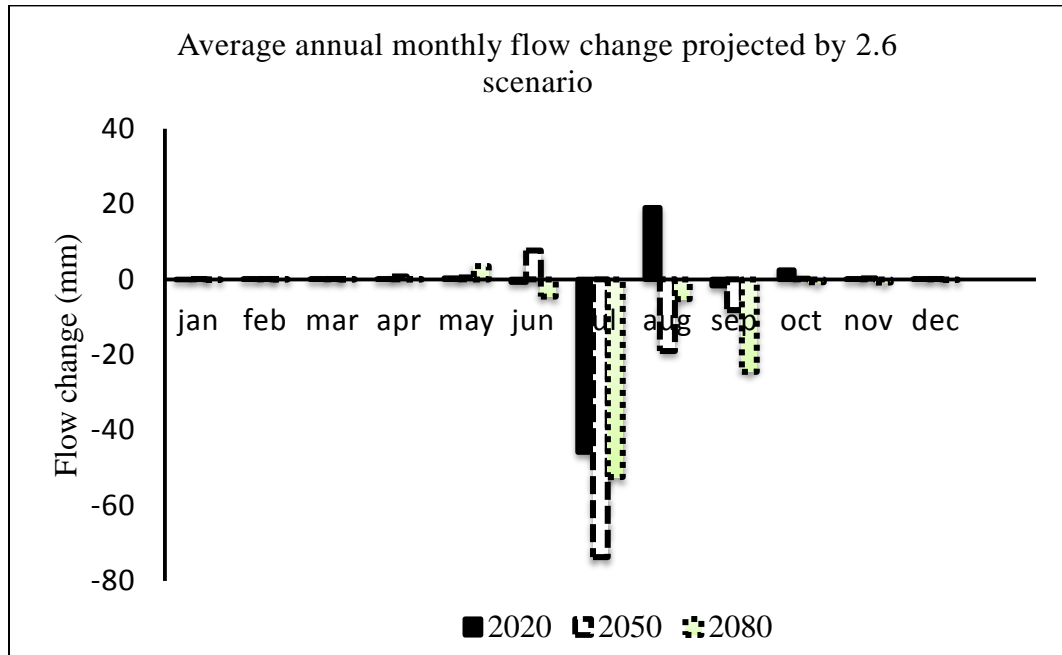
Table 22. Average annual mean rain fall changes differences in (mm)

RCP	Average annual rainfall (mm)				Change in (%)		
	baseline	2020	2050	2080	2020	2050	2080
2.6	1120.739	1112.387	1103.737	1105.902	-0.75%	-1.52%	-1.32%
8.5	1120.739	1103.815	1064.89	975.2878	-1.51%	-4.98%	-12.9%

In both emissions scenario the average precipitation will decreasing for future time periods. The directions of precipitation changes are highly variable from scenarios to scenarios and from period to period. Generally table 22 shows that a decreasing trend in average annual precipitation under both emission scenario. However, the magnitude is different among the scenarios, which is larger variability change in magnitude under RCP 8.5 emission scenario and small under RCP 2.6 climate emission scenarios. Particularly, RCP 8.5 emission scenario reveals with higher magnitude and large change range. However, under RCP 2.6 climate emission scenarios show more else reasonable result and relatively small difference in their future prediction. The reason is related to the level of radiation emission forcing, the higher GHG emission has large effect on the wet/dry days in the watershed. According to IPCC (2007), between 75 and 250 million people are projected to be exposed to increased water stress due to climate change in Africa. Several individual researches have been done to study the impacts of climate change on the water resources of Upper Blue Nile River Basin. Taye et al. (2011) reviewed some of the research outputs and concluded that clear discrepancies were observed. Kim (2008) used the outputs of six GCMs to project future precipitations and temperature, the result suggested that the changes in average annual precipitation from the six GCMs range from -11% to 44% with a change of 11% from the weighted average scenario at 2050s future time period. Likewise, Yates and Strzepek (1998a) used 3 GCMs and the result revealed that the changes in average precipitation range from -5% to 30%. Yates and Strzepek (1998b) also used 6 GCMs and the result showed in the range from -9% to 55% for precipitation. Generally the ensemble mean of all models showed that almost similar change in the average annual precipitation. This study result has shown that similar decreasing trend of precipitation to those of authors for the future three time period under both scenarios. These results indicate that precipitation will decrease during the future season. As rainy seasons are crop growing times in Ethiopia, climate change will have negative implications for the rain fed agricultural sector even if the increase in the maximum and minimum temperature has an effect by increasing evapotranspiration.

4.8 The impacts of future climate change on discharge

Climate change over the next century will be expected to severely impact water resources; arid and semi-arid areas are particularly more vulnerable to that change and are projected to suffer from water shortage due to precipitation reduction (Setegn et al., 2011). Alteration in hydrologic conditions will affect almost every aspect of natural resources and human well-being (Xu, 1999).



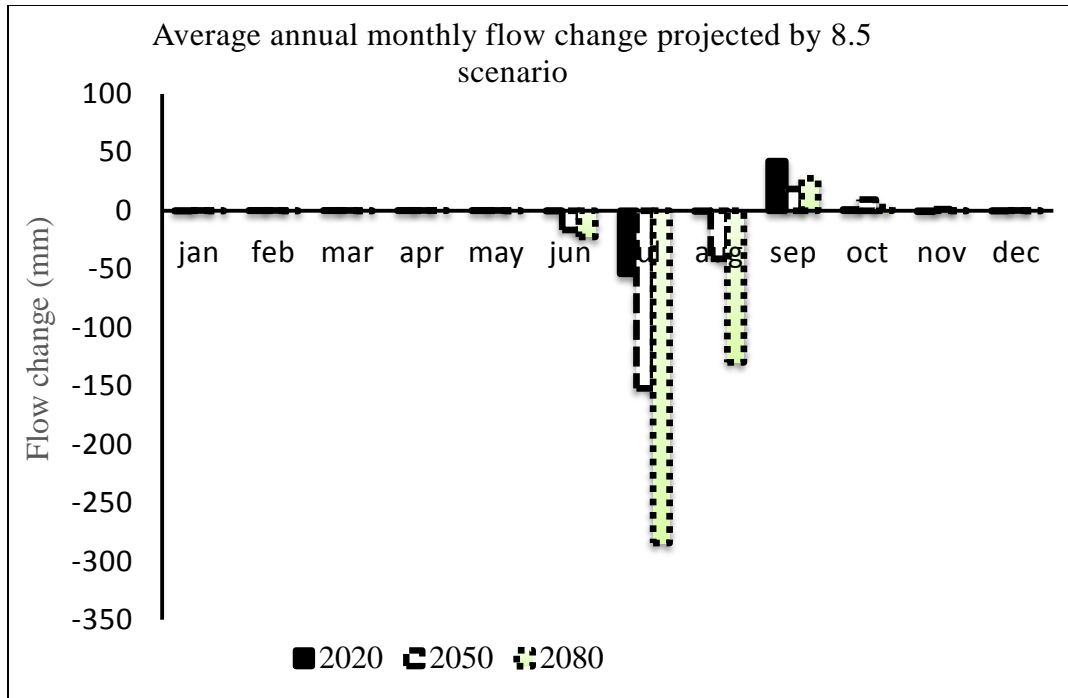


Figure 37. Projected average annual monthly mean flow change difference

Figure 37 show the relative change in average annual discharge at watershed stations. The average discharge in the watershed will decrease under both scenarios. The simulation projected an average change in discharge of -2.19%, -7.68% and -7.123% in the 2020s, 2050s and 2080s future time period under 2.6 RCP scenarios respectively. For the watershed similarly, annual average change in discharge -1.05%, -15.61% and -34.15% under 8.5 RCP scenarios in the 2020s, 2050s and 2080s future time period respectively will observed for the watershed. Both scenarios show similar decreasing trend in projected discharge for future time period. The predicted discharge at station is likely to decrease during rainy season of Jun for 2080s future time period under both scenario but in 2020s future time period in both scenario no clear change in predicted discharge will observe with baseline period but 2050s future time period show more increase under 2.6 and more decrease in 2080s future time period under 8.5scenario. In July month of year the predicted discharge will show decreasing trend for 2020s, 2050, and 2080s future time period under both emission scenario but in this month 2050s and 2080s future time period show more decreeing trend under 2.6 and 8.5 emission scenario respectively and 8.5 emission show more decreasing trend than 2.6 scenario. The

predicted discharge will increase during August in 2020s future time period and decrease in 2050s and 2080s under 2.6 emission scenario. Similarly, under 8.5 emission scenario the predicted discharge will decrease for all future time period during rainy season of August. The maximum predicted discharge decrease up to 0.39 - 0.20 mm/month for rain season under 2.6 and 8.5 emission scenario at the station in the 2050s and 2080s future time period respectively. The discharge will likely increase during September in the future time period of 2020s, 2050s and 2080s under 8.5 emission scenario and also in this scenario the more increasing in discharge will observe under 2020s future time period of September but in this month of year under 2.6 emission scenario the predicted discharge will show decreasing trend for all future time period. On the other hand, the discharge will increase during October for the future period of 2020s and 2050s under 2.6 and 8.5 scenarios respectively. The maximum increasing projected discharge in September will be 0.059, 0.026, and 0.039 mm/month for 2020s, 2050s, and 2080s future time period respectively. Similarly, under both scenarios the discharge is expected to decrease during the dry season (December-January) which could have a negative impact on the river.

Table 23. Average annual mean flow differences in (%)

RCP	Average annual flow (mm)				Change flow (%)		
	baseline	2020	2050	2080	2020	2050	2080
2.6	1188.56	1162.44	1097.39	1103.87	-2.2%	-7.6%	-7.1%
8.5	1188.56	1176.05	1009.01	782.614	-1.1%	-15.1%	-34.2%

In this study the average annual discharge minimum change decreasing up to 9.51mm/year (-1.1%) under 8.5 emission scenario of 2020s future time period and average annual maximum discharge change decreasing up to 402.95 mm/year (-34.2%) under 8.5 emission scenario of 2080s future time period.

4.9 The impacts of future climate change on sediment yield

Average annual percentage change of sediment yield has a similar pattern to that of stream flow. The average annual sediment yield decrease follows the trend of the average annual stream flow decrease. Sediment yield decrease more than linearly with a decrease

in stream flow (Naik and Jay 2011). Therefore, the impact of climate change on sediment yield is greater than on stream flow.

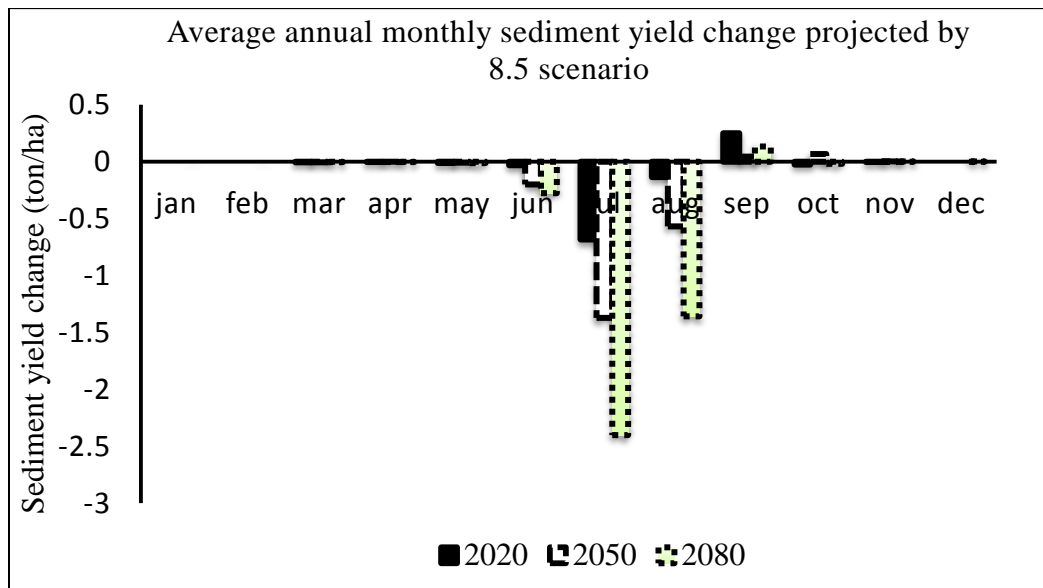
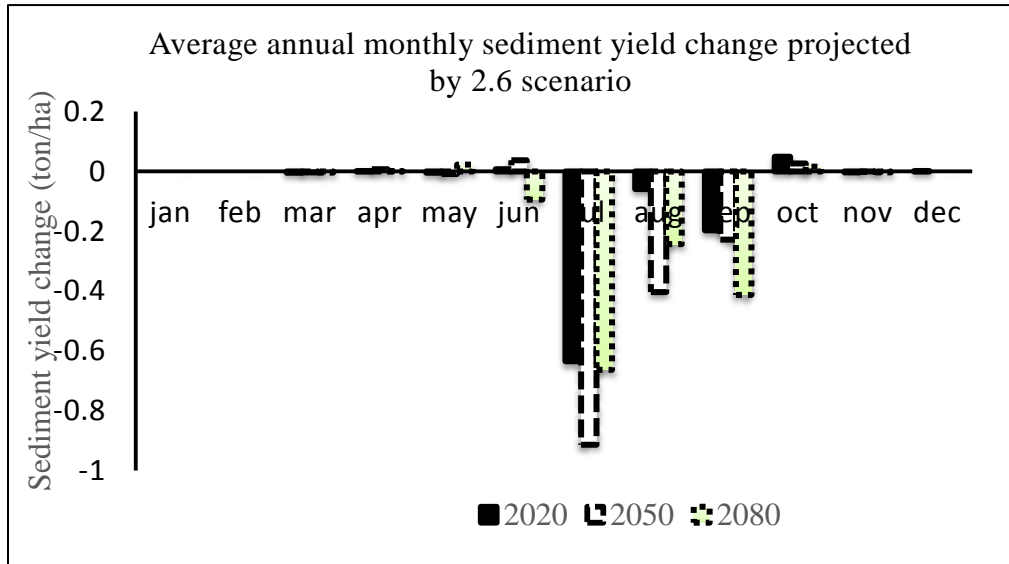


Figure 38. Projected average annual monthly sediment yield change difference

Figure 38 show the relative change in mean annual sediment yield at watershed stations. The sediment yield in the watershed will decrease under both scenarios for future time period. The simulation projected an average change in sediment yield of -9.4%, -16.7% and -15.5 in the 2020s, 2050s and 2080s future time period respectively under 2.6 emission scenario. For the watershed Similarly, an average change in sediment yield -

7.2%, -22.8% and -44.3% under 8.5 emission scenarios in the 2020s, 2050s and 2080s future time period respectively will be observed at the watershed. Both scenarios show a similar decreasing trend in projected sediment yield. The predicted sediment yield at station is likely to decrease during the rainy season of June for the 2080s future time period, under both scenarios but increase for the 2050s under the 2.6 scenario and decrease for the 8.5 scenario and no clear sediment yield change for the 2020 future time period under both emission scenarios but the predicted sediment yield from (July–August) will decrease for all future time periods of the 2020s, 2050s and 2080s under both emission scenarios respectively. Similarly, the predicted sediment yield in this rainy season of the 2050s under the 2.6 emission scenario and the 2080s under the 8.5 emission scenarios will show a more decreasing trend. The sediment yield will likely increase during September in the future time period of the 2020s, 2050s and 2080s under the 8.5 emission scenario but decrease for all future time periods of the 2.6 emission scenario. On the other hand, predicted sediment yield will increase during October for the periods of the 2020s and 2050s under the 2.6 and 8.5 emission scenarios respectively. Similarly, under both scenarios the sediment yield will be expected to decrease during the dry season (December-February). (Table 24) shows sediment transport provides highly uncertain results ranging from a decrease in rainfall.

Table 24. Average annual mean sediment yield change differences in (%)

RCP	Average annual sediment yield (ton/ha)				Change (%)		
	Baseline	2020	2050	2080	2020	2050	2080
2.6	8.884167	8.041667	7.400278	7.504783	-9.4%	-16.7%	-15.5%
8.5	8.884167	8.241389	6.850556	4.949565	-7.2%	-22.8%	-44.3%

In this study the predicted average annual minimum sediment yield change decreasing up to 0.64 ton/ha/year (-7.2%) under the 8.5 emission scenario of the 2020s future time period and average annual maximum sediment yield change decreasing up to 3.94 ton/ha/year (-44.3%) under the 8.5 emission scenario of the 2080s future time period.

Table 25. Percentage change comparison of projected hydro-meteorological variable based on baseline period

RCP		base	2020	2050	2080	2020	2050	2080
2.6	temperature	20.091	21.027	21.595	21.3705	+4.65%	+7.48%	+6.36%
	rain fall	1120.7	1112.3	1103.7	1105.9	-0.75%	-1.52%	-1.32%
	flow	1188.5	1162.4	1097.3	1103.8	-1.05%	-7.67%	-7.13%
	sed_yelid	8.8841	8.0416	7.4002	7.5047	-7.24%	-16.70%	-15.53%
8.5	temperature	20.096	21.443	23.372	25.474	+6.71%	+16.34%	+26.77%
	rainfall	1120.9	1103.5	1064.9	975.28	-1.51%	-4.98%	-12.98%
	flow	1188.6	1176.5	1009.1	782.61	-2.20%	-15.11%	-34.15%
	sed_yelid	8.8847	8.2419	6.8506	4.9495	-9.48%	-22.89%	-44.29%

Overall, the result indicted mean temperature increases and precipitation decrease for three future time period under both emission scenario. High increment in mean annual temperature and high decrement in mean annual precipitation in RCP 8.5 than RCP 2.6 scenarios (table 25) indicated. The reason is because due to high radiation concentration projection in RCP 8.5 scenario than RCP 2.6. As a result the predicted discharge and sediment yield shows a decrease trend for three future time period under both emission scenarios. Like similar reason to temperature and precipitation the predicted discharge and sediment yield show high decrement in RCP 8.5 than RCP 2.6 scenario. The decrement in future precipitation was the first predominant factor for decrement of predicted discharge and sediment yield in the watershed. The mean annual sediment cycle follows the trend of the mean annual discharge cycle. The change will be more significant for the wet season than dry season. Interestingly, the changes in sediment yields are higher than the corresponding changes in discharge. This implies that the impact of climate changes on sediment yield is greater than on stream flow, because sediment yield decrease more than linearly with a decrease inflow (Naik and Jay, 2011). While a decrease in the flow discharge will decrease the sediment loads for all scenarios. This study result is similar to the findings of the climate change impact study conducted by (Kim and Kalurachchi, 2009), and (Elshamy et al, 2009) in Upper Blue Nile Baseline Ethiopia.

5. CONCLUSION AND RECOMMENDATION

5.1. Conclusion

This study attempts to evaluate the impacts of climate change on sediment yield using the downscaled biased corrected output and Hydrological modeling approach of PED_W model. In doing this study reached to the following conclusions.

- The findings of this study has indicated an increasing in mean annual temperature was in the range expected changes temperature predicated by IPCC for Africa ranges from 2°c (low scenario) to 5°c (high scenario) by 2100.
- Rainfall for future scenarios change indicated decreased in all climate model scenario. The results obtained from the future climate of rainfall lies all most within the range expected changes of rainfall predicated by IPCC (IPCC, 2001) concluded that the Nile basin will decreases in rainfall ranging from zero to 20% by the end of the 21st century.
- The result of hydrological model calibration and validation indicates that the PED_W model simulates the discharge and sediment yield reasonable for the study area based on the model performance criterion.
- The predicted average annual discharge under 2.6 and 8.5 emission scenario will decrease from 1. 10% up to 7.13 % and 2.20% up to 34.15% for three future time period respectively and the predicted average annual sediment yield under 2.6 and 8.5 emission scenario will decrease from 7.24% up to 16.70% and 9.48% up to 44.29% for three future time period respectively.
- Sediment yield decrease more than linearly with a decrease in stream flow, therefore, the impact of climate change on sediment yield is greater than on stream flow.
- The simulated mean sediment yield and stream flow in the watershed indicated a decreasing trend due to climate change. So water resources in the watershed will be less reliable in the future. As result a new water resource management and planning strategies by integrating climate change effect should be done.

5.2. Recommendation

- Sediment yield and Stream flow projection made from this analysis can be further enhanced by taking relatively a high resolution and large number of climate model scenarios in order to reduce the uncertainty.
- The annual change and seasonal variation of hydrologic component due to future temperature increase and precipitation decrease should be evaluated and integrated into water resources planning and management in order to maintain more sustainable water demand and water availability in the watershed.

REFERENCE

- ASCHALEW, ASSEFA. (2007). Climate change detection and attribution in tropical Africa.
- Bates, Bryson, Kundzewicz, Zbigniew, & Wu, Shaohong. (2008). *Climate change and water*: Intergovernmental Panel on Climate Change Secretariat.
- Chen, Hua, Xu, Chong-Yu, & Guo, Shenglian. (2012). Comparison and evaluation of multiple GCMs, statistical downscaling and hydrological models in the study of climate change impacts on runoff. *Journal of hydrology*, 434, 36-45.
- Conway, Declan, Krol, Maarten, Alcamo, Joe, & Hulme, Mike. (1996). Future availability of water in Egypt: The interaction of global, regional, and basin scale driving forces in the Nile Basin. *Ambio*, 336-342.
- Easton, ZM, Fuka, DR, White, ED, Collick, AS, Biruk Ashagre, B, McCartney, M, . . . Steenhuis, TS. (2010). A multi basin SWAT model analysis of runoff and sedimentation in the Blue Nile, Ethiopia. *Hydrology and earth system sciences*, 14(10), 1827-1841.
- Gregory, Jonathan M, Stouffer, RJ, Raper, SCB, Stott, PA, & Rayner, NA. (2002). An observationally based estimate of the climate sensitivity. *Journal of Climate*, 15(22), 3117-3121.
- Grotch, Stanley L, & MacCracken, Michael C. (1991). The use of general circulation models to predict regional climatic change. *Journal of Climate*, 4(3), 286-303.
- Kim, Ungtae, & Kaluarachchi, Jagath J. (2009). Climate change impacts on water resources in the upper Blue Nile river basin, Ethiopia. *JAWRA Journal of the American Water Resources Association*, 45(6), 1361-1378.
- Meehl, Gerald A, Washington, Warren M, Arblaster, Julie M, Hu, Aixue, Teng, Haiyan, Tebaldi, Claudia, . . . Strand, Warren G. (2012). Climate system response to external forcings and climate change projections in CCSM4. *Journal of Climate*, 25(11), 3661-3683.
- Mitchell, Timothy D, Carter, Timothy R, Jones, Philip D, Hulme, Mike, & New, Mark. (2004). A comprehensive set of high-resolution grids of monthly climate for

- Europe and the globe: the observed record (1901–2000) and 16 scenarios (2001–2100). *Tyndall centre for climate change research working paper*, 55(0), 25.
- Moss, Richard H, Edmonds, Jae A, Hibbard, Kathy A, Manning, Martin R, Rose, Steven K, Van Vuuren, Detlef P, . . . Kram, Tom. (2010). The next generation of scenarios for climate change research and assessment. *Nature*, 463(7282), 747-756.
- Olmos, Santiago. (2001). Vulnerability and adaptation to climate change: concepts, issues, assessment methods: Climate Change Knowledge Network (CCKN).
- Parry, Martin, Canziani, Osvaldo, Palutikof, Jean, van der Linden, Paul J, & Hanson, Clair E. (2007). *Climate change 2007: impacts, adaptation and vulnerability* (Vol. 4): Cambridge University Press Cambridge.
- Parry, Martin L, Canziani, Osvaldo F, Palutikof, Jean P, van der Linden, Paul J, & Hanson, Clair E. (2007). IPCC, 2007: climate change 2007: impacts, adaptation and vulnerability. Contribution of working group II to the fourth assessment report of the intergovernmental panel on climate change: Cambridge University Press, Cambridge.
- Pell, Cardinal George. (2011). One Christian perspective on climate change. *The Global Warming Policy Foundation 2011 Annual GWPF Lecture*, 26.
- Sánchez, E, Gallardo, C, Gaertner, MA, Arribas, A, & Castro, M. (2004). Future climate extreme events in the Mediterranean simulated by a regional climate model: a first approach. *Global and Planetary Change*, 44(1), 163-180.
- Sillmann, J, Kharin, VV, Zwiers, FW, Zhang, X, & Bronaugh, D. (2013). Climate extremes indices in the CMIP5 multimodel ensemble: Part 2. Future climate projections. *Journal of Geophysical Research: Atmospheres*, 118(6), 2473-2493.
- Solomon, Susan. (2007). *Climate change 2007-the physical science basis: Working group I contribution to the fourth assessment report of the IPCC* (Vol. 4): Cambridge University Press.
- Stocker, Thomas F, Qin, Dahe, Plattner, G-K, Alexander, Lisa V, Allen, Simon K, Bindoff, Nathaniel L, . . . Emori, Seita. (2013). Technical summary *Climate change 2013: the physical science basis. Contribution of Working Group I to the*

- Fifth Assessment Report of the Intergovernmental Panel on Climate Change* (pp. 33-115): Cambridge University Press.
- Taye, Meron Teferi, Ntegeka, Victor, Ogiramoi, NP, & Willems, Patrick. (2011). Assessment of climate change impact on hydrological extremes in two source regions of the Nile River Basin. *Hydrology and Earth System Sciences*, 15(1), 209.
- Te Chow, Ven. (1988). *Applied hydrology*: Tata McGraw-Hill Education.
- Van Vuuren, Detlef P, Edmonds, Jae, Kainuma, Mikiko, Riahi, Keywan, Thomson, Allison, Hibbard, Kathy, . . . Lamarque, Jean-Francois. (2011). The representative concentration pathways: an overview. *Climatic change*, 109(1-2), 5.
- Vörösmarty, Charles J, Green, Pamela, Salisbury, Joseph, & Lammers, Richard B. (2000). Global water resources: vulnerability from climate change and population growth. *science*, 289(5477), 284-288.
- Wass, Paul D, & Leeks, Graham JL. (1999). Suspended sediment fluxes in the Humber catchment, UK. *Hydrological Processes*, 13(7), 935-953.
- Yates, David N, & Strzepek, Kenneth M. (1998). Modeling the Nile Basin under climatic change. *Journal of Hydrologic Engineering*, 3(2), 98-108.
- Zakieldeen, Sumaya Ahmed. (2009). Adaptation to climate change: a vulnerability assessment for Sudan.
- Zelege, Gete, & Hurni, Hans. (2001). Implications of land use and land cover dynamics for mountain resource degradation in the Northwestern Ethiopian highlands. *Mountain research and development*, 21(2), 184-191.
- Zhu, Yun-Mei, Lu, XX, & Zhou, Yue. (2008). Sediment flux sensitivity to climate change: A case study in the Longchuanjiang catchment of the upper Yangtze River, China. *Global and Planetary Change*, 60(3), 429-442.

- ABDO, K., FISEHA, B., RIENTJES, T., GIESKE, A. & HAILE, A. 2009. Assessment of climate change impacts on the hydrology of Gilgel Abay catchment in Lake Tana basin, Ethiopia. *Hydrological Processes*, 23, 3661-3669.
- ASCHALEW, A. 2007. Climate change detection and attribution in tropical Africa.
- BATES, B., KUNDZEWICZ, Z. & WU, S. 2008. *Climate change and water*, Intergovernmental Panel on Climate Change Secretariat.
- BEYENE, T., LETTENMAIER, D. P. & KABAT, P. 2010. Hydrologic impacts of climate change on the Nile River Basin: implications of the 2007 IPCC scenarios. *Climatic change*, 100, 433-461.
- CARTER, T. R. 1999. *Representing Uncertainty in Climate Change Scenarios and Impact Studies: Proceedings of the ECLAT Helsinki Workshop, 14-16, 1999*, Climatic Research Unit.
- CHERIE, N. & KOCH, M. Mono-and multi-model statistical downscaling of GCM-climate predictors for the Upper Blue Nile River basin, Ethiopia. Proceedings of the 6th International Conference on Water Resources and Environment Research, ICWRER, 2013. 3-7.
- CONWAY, D. 2005. From headwater tributaries to international river: observing and adapting to climate variability and change in the Nile basin. *Global Environmental Change*, 15, 99-114.
- CONWAY, D., KROL, M., ALCAMO, J. & HULME, M. 1996. Future availability of water in Egypt: The interaction of global, regional, and basin scale driving forces in the Nile Basin. *Ambio*, 336-342.
- EASTON, Z., FUKA, D., WHITE, E., COLLICK, A., BIRUK ASHAGRE, B., MCCARTNEY, M., AWULACHEW, S., AHMED, A. & STEENHUIS, T. 2010. A multi basin SWAT model analysis of runoff and sedimentation in the Blue Nile, Ethiopia. *Hydrology and earth system sciences*, 14, 1827-1841.
- ELSHAMY, M. E., SEIERSTAD, I. A. & SORTEBERG, A. 2009. Impacts of climate change on Blue Nile flows using bias-corrected GCM scenarios. *Hydrology and Earth System Sciences*, 13, 551-565.

- GREGORY, J. M., STOUFFER, R., RAPER, S., STOTT, P. & RAYNER, N. 2002. An observationally based estimate of the climate sensitivity. *Journal of Climate*, 15, 3117-3121.
- GROTCH, S. L. & MACCRACKEN, M. C. 1991. The use of general circulation models to predict regional climatic change. *Journal of Climate*, 4, 286-303.
- KIM, U. & KALUARACHCHI, J. J. 2009. Climate change impacts on water resources in the upper Blue Nile river basin, Ethiopia. *JAWRA Journal of the American Water Resources Association*, 45, 1361-1378.
- MEEHL, G. A., WASHINGTON, W. M., ARBLASTER, J. M., HU, A., TENG, H., TEBALDI, C., SANDERSON, B. N., LAMARQUE, J.-F., CONLEY, A. & STRAND, W. G. 2012. Climate system response to external forcings and climate change projections in CCSM4. *Journal of Climate*, 25, 3661-3683.
- MITCHELL, T. D., CARTER, T. R., JONES, P. D., HULME, M. & NEW, M. 2004. A comprehensive set of high-resolution grids of monthly climate for Europe and the globe: the observed record (1901–2000) and 16 scenarios (2001–2100). *Tyndall centre for climate change research working paper*, 55, 25.
- MOGES, M. A., SCHMITTER, P., TILAHUN, S. A., LANGAN, S., DAGNEW, D. C., AKALE, A. T. & STEENHUIS, T. S. 2017. Suitability of Watershed Models to Predict Distributed Hydrologic Response in the Awramba Watershed in Lake Tana Basin. *Land Degradation & Development*, 28, 1386-1397.
- MOSS, R. H., EDMONDS, J. A., HIBBARD, K. A., MANNING, M. R., ROSE, S. K., VAN VUUREN, D. P., CARTER, T. R., EMORI, S., KAINUMA, M. & KRAM, T. 2010. The next generation of scenarios for climate change research and assessment. *Nature*, 463, 747-756.
- OLMOS, S. 2001. Vulnerability and adaptation to climate change: concepts, issues, assessment methods. Climate Change Knowledge Network (CCKN).
- PARRY, M., CANZIANI, O., PALUTIKOF, J., VAN DER LINDEN, P. J. & HANSON, C. E. 2007a. *Climate change 2007: impacts, adaptation and vulnerability*, Cambridge University Press Cambridge.
- PARRY, M. L., CANZIANI, O. F., PALUTIKOF, J. P., VAN DER LINDEN, P. J. & HANSON, C. E. 2007b. IPCC, 2007: climate change 2007: impacts, adaptation

- and vulnerability. Contribution of working group II to the fourth assessment report of the intergovernmental panel on climate change. Cambridge University Press, Cambridge.
- PELL, G. 2011. One Christian perspective on Climate Change. Annual GWPF Lecture 26.10. 2011.
- SÁNCHEZ, E., GALLARDO, C., GAERTNER, M., ARRIBAS, A. & CASTRO, M. 2004. Future climate extreme events in the Mediterranean simulated by a regional climate model: a first approach. *Global and Planetary Change*, 44, 163-180.
- SILLMANN, J., KHARIN, V., ZWIERS, F., ZHANG, X. & BRONAUGH, D. 2013. Climate extremes indices in the CMIP5 multimodel ensemble: Part 2. Future climate projections. *Journal of Geophysical Research: Atmospheres*, 118, 2473-2493.
- SOLOMON, S. 2007. *Climate change 2007-the physical science basis: Working group I contribution to the fourth assessment report of the IPCC*, Cambridge University Press.
- STEENHUIS, T. & VAN DER MOLEN, W. 1986. The Thornthwaite-Mather procedure as a simple engineering method to predict recharge. *Journal of Hydrology*, 84, 221-229.
- STOCKER, T. F., QIN, D., PLATTNER, G.-K., ALEXANDER, L. V., ALLEN, S. K., BINDOFF, N. L., BRÉON, F.-M., CHURCH, J. A., CUBASCH, U. & EMORI, S. 2013. Technical summary. *Climate change 2013: the physical science basis. Contribution of Working Group I to the Fifth Assessment Report of the Intergovernmental Panel on Climate Change*. Cambridge University Press.
- TAYE, M. T., NTEGEKA, V., OGIRAMOI, N. & WILLEMS, P. 2011. Assessment of climate change impact on hydrological extremes in two source regions of the Nile River Basin. *Hydrology and Earth System Sciences*, 15, 209.
- TE CHOW, V. 1988. *Applied hydrology*, Tata McGraw-Hill Education.
- TILAHUN, S., GUZMAN, C., ZEGEYE, A., ENGDA, T., COLLICK, A., RIMMER, A. & STEENHUIS, T. 2013. An efficient semi-distributed hillslope erosion model for the subhumid Ethiopian Highlands. *Hydrology and Earth System Sciences*, 17, 1051-1063.

- VAN VUUREN, D. P., EDMONDS, J., KAINUMA, M., RIAHI, K., THOMSON, A., HIBBARD, K., HURTT, G. C., KRAM, T., KREY, V. & LAMARQUE, J.-F. 2011. The representative concentration pathways: an overview. *Climatic change*, 109, 5.
- VÖRÖSMARTY, C. J., GREEN, P., SALISBURY, J. & LAMMERS, R. B. 2000. Global water resources: vulnerability from climate change and population growth. *science*, 289, 284-288.
- WASS, P. D. & LEEKS, G. J. 1999. Suspended sediment fluxes in the Humber catchment, UK. *Hydrological Processes*, 13, 935-953.
- YATES, D. N. & STRZEPEK, K. M. 1998. Modeling the Nile Basin under climatic change. *Journal of Hydrologic Engineering*, 3, 98-108.
- ZAKIELDEEN, S. A. 2009. Adaptation to climate change: a vulnerability assessment for Sudan.
- ZELEKE, G. & HURNI, H. 2001. Implications of land use and land cover dynamics for mountain resource degradation in the Northwestern Ethiopian highlands. *Mountain research and development*, 21, 184-191.
- ZHU, Y.-M., LU, X. & ZHOU, Y. 2008. Sediment flux sensitivity to climate change: A case study in the Longchuanjiang catchment of the upper Yangtze River, China. *Global and Planetary Change*, 60, 429-442.

APEENDIX

Table1. Data use for fill the Missing value

station name	x-y co-ordinate	value	distance	weighting
Makesegnit	x1	342912	19.8479	2.53846E-09
	y1	1369928		
Gondar	x2	329624	56.2101	3.16499E-10
	y2	1384671		
Ayekel	x3	289788	40000.8	6.24974E-10
	y3	1388296		

Table2. Data use for Stationery test

Year	Max	Order	sort	rank	R	172
1976	1454.7	6	11.913	1	P	12
1977	1396.71	8	12.653	2	q	13
1978	1299.65	11	15.713	3	V	94
1979	1428.61	7	17.299	4	W	62
1980	1491.79	4	20.16	5	$\sum T$	0
1981	1008.78	15	22.051	6	Var(U)	403
1982	759.24	24	24.67	7	U	62
1983	906.3	20	25.29	8	Uav	78
1984	1022.7	14	26.393	9	u	-0.8386
1985	1080.27	12	29.311	10	$\sum T$	0
1986	1036.79	13	31.396	11	J	0
1987	855	21	31.907	12	N	30
1988	927.39	17	38.921	13		
1989	759.03	25	39.49	14		
1990	692.3	27	40.062	15		
1991	844.3	22	44.786	16		

1992	628.3	30	44.892	17
1993	724.6	26	51.706	18
1994	649.5	29	53.678	19
1995	663.5	28	60.517	20
1996	1469.91	5	67.73	21
1997	1514.61	3	69.258	22
1998	1360.7	9	87.639	23
1999	1611.8	2	71.78737	24
2000	1332.1	10	74.62677	25
2001	1680.8	1	77.46617	26
2002	777.4	23	80.30557	27
2003	922	18	83.14497	28
2004	952.3	16	85.98437	29
2005	922	18	88.82377	30

Table3. Double mas curve for consistency checking

Year	PCP.G	PCP.M	PCP.AY	AVR	CUM.	CUM.M	CUM.AY	COM.
ly	on	ak	KL	AG	Gn	ak	KL	AV
1976	1455	1455	1455	1455	9491	9626	9533	4424
1977	1156	1397	1855	1469	10648	11022	11388	5893
1978	1054	1300	1746	1367	11701	12322	13134	1049
1979	1011	1429	2331	1590	12713	13751	15465	2640
1980	1311	1492	2172	1658	14023	15243	17638	4298
1981	913	1009	1781	1234	14936	16251	19419	5532
1982	720	759	1075	851	15656	17011	20494	1050
1983	906	906	906	906	16562	17917	21400	1957
1984	1023	1023	1023	1023	17585	18940	22423	2979
1985	1050	1080	1326	1152	18635	20020	23748	4131
1986	999	1037	1341	1125	19633	21057	25089	1051

1987	1144	855	1133	1044	20777	21912	26222	2095
1988	1092	927	1276	1098	21869	22839	27497	3194
1989	1049	759	1189	999	22918	23598	28686	4193
1990	841	692	1005	846	23759	24290	29691	1052
1991	1040	844	1027	970	24799	25135	30718	2023
1992	920	628	804	784	25719	25763	31522	2807
1993	1172	725	1416	1104	26891	26488	32938	3911
1994	990	650	1115	918	27881	27137	34053	1053
1995	978	664	1150	930	28859	27801	35203	1984
1996	1164	1470	1076	1237	30023	29270	36279	3220
1997	1139	1515	1302	1318	31162	30785	37580	4539
1998	1515	1361	1230	1368	32677	32146	38810	1054
1999	1833	1612	1319	1588	34510	33758	40128	2642
2000	1766	1332	1287	1462	36276	35090	41415	4104
2001	1869	1681	1276	1609	38145	36770	42691	5712
2002	1004	777	1092	958	39148	37548	43783	1055
2003	1076	922	912	970	40224	38470	44695	2025
2004	1168	952	1031	1050	41392	39422	45726	3076
2005	1041	922	978	980	42433	40344	46704	4056

Table 4. Future mean annual temperature in oC projected by 2.6 & 8.5

	baseline	20202.6	20502.6	20802.6	20208.5	20508.5	20808.5
Jan	19.49	19.23	19.69	19.66	19.75	21.48	23.26
Feb	20.94	20.89	21.07	21.30	21.26	22.93	24.91
Mar	22.22	23.00	23.39	23.41	23.24	25.30	27.02
Apr	22.80	24.09	24.58	24.29	24.29	26.45	28.47
May	21.90	24.40	24.83	24.16	24.77	26.74	29.19
Jun	19.95	22.31	22.65	22.81	22.47	24.95	27.87
Jul	18.33	18.83	19.38	19.01	19.53	21.50	24.35
Aug	18.41	18.09	18.71	18.52	18.81	20.65	22.72
Sep	19.00	20.01	20.28	20.31	20.16	21.97	23.79
Oct	19.42	21.69	22.05	21.93	21.85	23.61	25.54
Nov	19.47	21.27	21.52	21.81	21.40	23.26	25.07
Dec	19.16	19.51	19.70	19.80	19.77	21.67	23.47

Table 5. Future mean annual rainfall in mm projected by 2.6 & 8.5

	baseline	20202.6	20502.6	20802.6	20208.5	20508.5	20808.5
Jan	3.17	20.64	15.02	41.00	32.34	7.23	23.17
Feb	2.99	4.77	3.35	8.06	9.47	5.89	2.39
Mar	13.66	6.70	8.56	6.08	6.33	5.10	3.15
Apr	37.97	43.71	33.31	39.66	29.01	19.67	19.04
May	82.30	57.86	65.95	103.81	44.22	47.49	31.07
Jun	156.40	145.15	147.75	127.50	148.36	111.93	77.65
Jul	306.73	275.42	254.43	259.23	269.79	240.76	165.00
Aug	312.94	316.73	304.21	289.40	311.56	300.01	264.84
Sep	121.23	109.02	110.25	115.88	138.05	130.88	163.16
Oct	54.33	85.91	84.79	72.71	87.09	118.89	118.76
Nov	23.29	42.00	72.04	35.51	23.33	75.19	91.98
Dec	5.72	4.48	4.07	7.08	4.29	1.85	15.07

Table 6. Future annual flow (mm/month) and sediment yield (ton/ha) projected by 2.6 & 8.5 scenario

	Jan	Feb	mar	Apr	may	Jun	Jul	Aug	seep	Oct	Nov	Dec
base line												
flow	0.25	0.04	0.00	0.00	0.04	25.3	357.10	489.80	252.38	52.80	9.26	1.58
2020 2.6flow	0.25	0.04	0.01	0.16	0.40	24.6	311.30	508.84	250.68	55.30	9.26	1.59
2050 2.6flow	0.26	0.04	0.04	0.82	0.56	33.0	283.40	470.83	244.23	53.03	9.53	1.63
2080 2.6flow	0.23	0.04	0.01	0.11	3.60	20.8	304.67	484.59	227.87	52.08	8.45	1.45
2020 8.5flow	0.22	0.04	0.00	0.06	0.05	25.1	303.03	489.21	294.65	53.91	8.36	1.43
2050 8.5flow	0.31	0.05	0.02	0.03	0.16	8.8	205.01	448.82	270.83	62.44	10.62	1.87
2080 8.5flow	0.24	0.04	0.00	0.02	0.02	2.9	72.77	360.05	280.10	55.92	9.02	1.55
baseline												
sediment												
yield	0.00	0.00	0.00	0.00	0.01	0.3	3.03	4.04	1.45	0.03	0.00	0.00
2020 8.5sed	0.00	0.00	0.00	0.00	0.00	0.3	2.35	3.91	1.70	0.01	0.00	0.00
2050 8.5sed	0.00	0.00	0.00	0.00	0.00	0.1	1.66	3.47	1.50	0.10	0.01	0.00
2080 8.5sed	0.00	0.00	0.00	0.00	0.00	0.0	0.63	2.68	1.59	0.01	0.00	0.00
2020 2.6 sed	0.00	0.00	0.00	0.00	0.01	0.3	2.40	3.98	1.26	0.08	0.00	0.00
2050 2.6sed	0.00	0.00	0.00	0.01	0.00	0.3	2.12	3.64	1.23	0.06	0.00	0.00
2080 2.6sed	0.00	0.00	0.00	0.00	0.04	0.2	2.37	3.80	1.04	0.05	0.00	0.00